Chapter III

Inhibition of KIX-targeting Activators

A. Abstract

Disrupting protein·protein interactions with small molecules has long been a goal in drug development. The design of such therapeutics, however, has been problematic due to the large surface area of protein·protein interfaces compared to the limited number of contacts available to small molecules, and the difficulty of targeting a protein landscape lacking native small molecule binding sites. We have developed a small molecule that interacts with the KIX domain of CBP in an overlapping region to that of natural transcriptions activators MLL and Jun. This molecule, iTAD **1**, competitively inhibits luciferase expression driven by Gal4-fused MLL and Jun minimal activation domains, suggesting that iTAD **1** prevents these activators from interacting with CBP. To further define the nature of the isoxazolidine·KIX interaction, several analogues of iTAD **1** were synthesized, appending functionality both to mimic side-chain residues found in natural activators and add non-native functionality, in an attempt to increase potency or specificity. We discovered, however, that most modifications greatly reduced efficacy and, in some cases, resulted in significantly increased toxicity. The ability of iTAD **1** to perturb endogenous signaling pathways was then examined by probing the effects of iTAD **1** on CCND1 (cyclin D1 gene), a gene whose expression is tightly regulated by Jun. iTAD **1** was found to decrease levels of cyclin D1 expression in MCF-7 breast cancer cells.

iTAD **1** thus successfully inhibits protein·protein interactions in the context of endogenous promoters, but additional work will be required to further optimize the activity of this molecular class.

B. Introduction

1) Protein·Protein Interactions

Protein·protein interactions are crucial for proper cell and tissue function, and the critical nature of these interactions makes them prime targets for therapeutic intervention. Blocking protein·protein interactions may occur through direct inhibition at the protein-binding interface, or through binding an allosteric site that changes the conformation of the interfacial region enough to preclude binding.[1-14]

This strategy is truly the exception to the current paradigm of blocking known small molecule binding sites in enzymes and receptors. There are few small molecules (*vide infra*) that target protein·protein interactions for several reasons: 1) protein interfaces are typically flat and featureless, 2) many proteins contain non-contiguous interfacial regions that are difficult to occlude with synthetic ligands, and 3) the propensity of small molecules to participate in non-productive interactions. Despite these issues, small molecules exhibit several favorable characteristics as potential modulators of protein·protein interactions. They are generally more stable and cell-permeable than peptides and are amenable to analog generation and structure-activity relationship (SAR) analysis.[1, 4, 5, 12] In addition, recent advances in high-throughput screening technology have enabled the testing of molecules in whole-cell assays, in addition to purified protein components, giving a better profile of the molecules tested with regard to cell permeability, stability, and toxicity.

2) Protein·Protein Interactions as Therapeutic Targets

The most well known examples of protein·protein interaction inhibitors (PPIs) are the compounds that block the interaction between p53 and MDM2. However, although there are several examples of compounds that inhibit this interaction (Figure III-1a-b), none have become clinically useful therapeutics. This is due in large part to inactivating mutations of p53 and other p53 inhibitor proteins such as MDMX that are not affected by these classes of compounds.[13, 15] Another advanced example of PPIs are compounds in development by Abbott Laboratories and Genentech that mimic an interaction between the anti-apoptotic proteins Bcl and the BH3-only proteins (Figure III-2).[16] These compounds, now 13 years in development, will likely be the first small molecule clinical therapeutics that target protein·protein interactions.
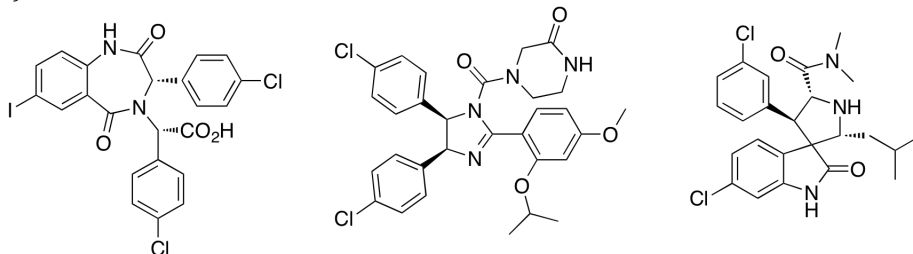
a)
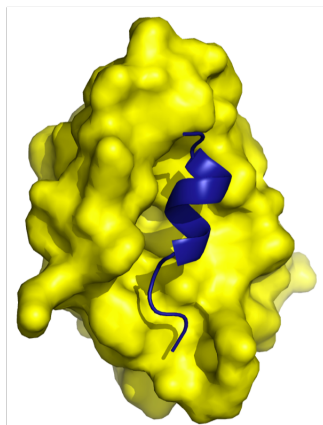
b)

Figure III-1. Structure of p53·MDM2 complex and its inhibitors. a) MDM2 is shown in yellow, p53 is in blue.[17] b) Benzodiazepine, cis-imidazoline, and nutlin inhibitors of p53·MDM2.[12] Structure adapted from 1ycr.

Bcl and p53 are important targets because impaired apoptosis is a characteristic of many malignant cells, enabling evasion of cell death signals and resistance to chemotherapy. p53 is a tumor suppressor that modulates cellular responses to stress by induction of cell-cycle arrest or apoptosis. MDM2 downregulates p53 activity, thus inhibition of the p53·MDM2 interaction results in increased levels of p53 in the cell, leading to growth arrest or cell death.[18, 19] Bcl proteins are pro-survival factors, overexpression of which overrides cell death signals leading to oncogenesis. The Bcl family is countered by the BH3-only proteins, members of the cell death machinery. Compounds that mimic the binding of these BH3-only proteins to the Bcl family will block interactions between the Bcl proteins and their targets, leading to induction of apoptosis.[16, 20-22] These examples, however, are not typical of most protein·protein interactions; both MDM2 and Bcl-2 contain deep hydrophobic binding clefts that are more amenable to small molecule targeting than other, more featureless, protein surfaces.
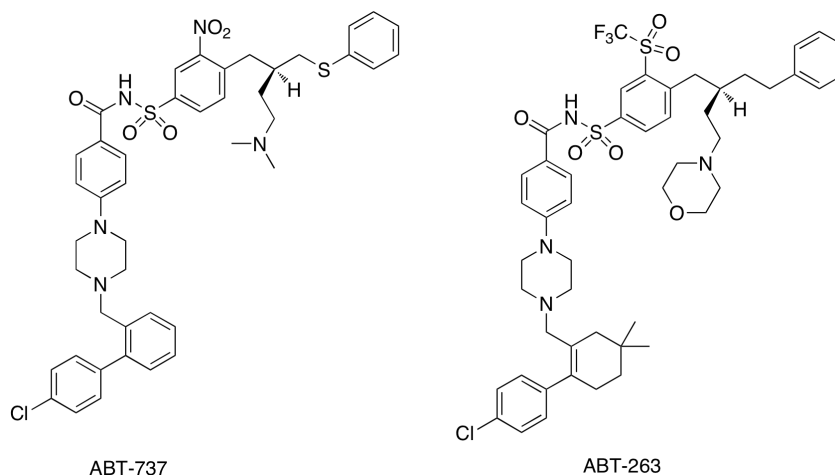

ABT-737   ABT-263

Figure III-2. Antagonists of Bcl proteins.[16] These compounds were developed by Abbott Laboratories in partnership with Genentech and mimic the BH3-only proteins.

3) iTAD·KIX Interaction

As outlined in Chapter 2, we have shown that iTAD **1** interacts with the MLL/Jun/Tat/Tax binding site within the KIX domain of CBP, and may thus function as a protein·protein interaction inhibitor. To exploit this binding site overlap,

however, the KIX·TAD interaction must be important for protein function; otherwise blocking that interaction would not have a downstream effect. Examination of the literature immediately revealed studies with Tat demonstrating that it retains full activity when its KIX-interacting region is deleted.[23-26] The molecular interactions of CBP and Tax are not well understood, though Tax is known to bind the KIX, CH1, and CH3 domains.[27-29] Thus our further studies focused on MLL and Jun, as their CBP contacts are well characterized and critical for activity. Both of these proteins are involved in oncogenesis, MLL primarily in hematopoietic defects, and Jun in several different solid tumors.[30, 31] Decreasing transcription of MLL and Jun target genes is a useful mechanism to further dissect the roles of these proteins in oncogenesis, and to probe the potential therapeutic value of decreased transcriptional output from these activators.

C. MLL

MLL is a 470 kDa protein that maintains expression of a number of developmental genes, most notably the Hox genes that are involved in hematopoiesis.[32-38] Not surprisingly, MLL has been implicated in ~10% of adult and infant primary and secondary leukemias, often arising from chromosomal translocations fusing MLL with another protein. There are over 40 proteins demonstrated to form oncogenic fusions with MLL, all of which result in aggressive leukemias that respond poorly to chemotherapy and exhibit a poor prognosis.[38-42] MLL has several epigenetic functions, including a SET domain (histone methyltransferase), and regions for binding the SWI/SNF complex and CBP (both containing HAT domains).[35, 43, 44] The MLL binding site on the KIX domain of CBP is also utilized by the viral activators Tat (Human Immunodeficiency Virus, HIV) and Tax (Human T-Cell Leukemia Virus, HTLV).[45, 46] These activators sequester CBP for use in activating transcription of the viral genome, and it is thought that competition of Tax and MLL for this binding site may account for some of the oncogenic properties of HTLV.[46-49] The KIX domain is thus an important region for the recruitment of CBP and the downstream effects that result. iTAD **1** will serve as a

useful small molecule probe of the molecular recognition events that occur during KIX binding.

D. Jun

c-Jun is a 39 kDa nuclear phosphoprotein involved in the regulation of cell growth, differentiation, and adhesion. c-Jun contains an N-terminal TAD and is regulated through phosphorylation at Ser63 and Ser73 by Jun-N-terminal kinases (JNKs), and is essential for embryonic viability past day twelve.[50] Jun is a component of the activator protein 1 (AP-1) complex that binds DNA at both tetradecanoylphorbolacetate response- (TRE) and cAMP response elements (CRE). AP-1 consists of homo- or heterodimers of the Jun, Fos, and ATF family of activators, though c-Jun is involved in the greatest number of AP-1 dimers.[31, 50-52] One mechanism by which Jun activates transcription is through recruitment of CBP to the promoter of target genes through direct binding of the KIX domain.[31, 51, 53]

An investigation of non-small cell lung primary and metastatic tumors showed that 31% of these tumors overexpress c-Jun. This is not surprising, considering the key role Jun plays in the regulation of the cell cycle. Jun decreases the expression of p53 (an important tumor suppressor), which in turn downregulates the expression of p21, a cyclin-dependent kinase inhibitor (Figure III-3a).[31, 51, 54-59] In addition, the expression of cyclin D1, a crucial component of the cell cycle control apparatus, is tightly controlled by c-Jun.[57, 58] Progression through the cell cycle is controlled by the periodic and phase-specific regulation of the activity and abundance of a defined cohort of proteins. Cyclin D1 is synthesized early in G1 phase and promotes the G1-S transition in a complex with Cdk4, by phosphorylating and inactivating the tumor suppressor Rb (Figure III-3b).[60-63] Due to its multiple roles in oncogenesis, modulation of Jun function is a powerful therapeutic target; small molecule inhibitors such as iTADs may provide a mechanism for such regulation.
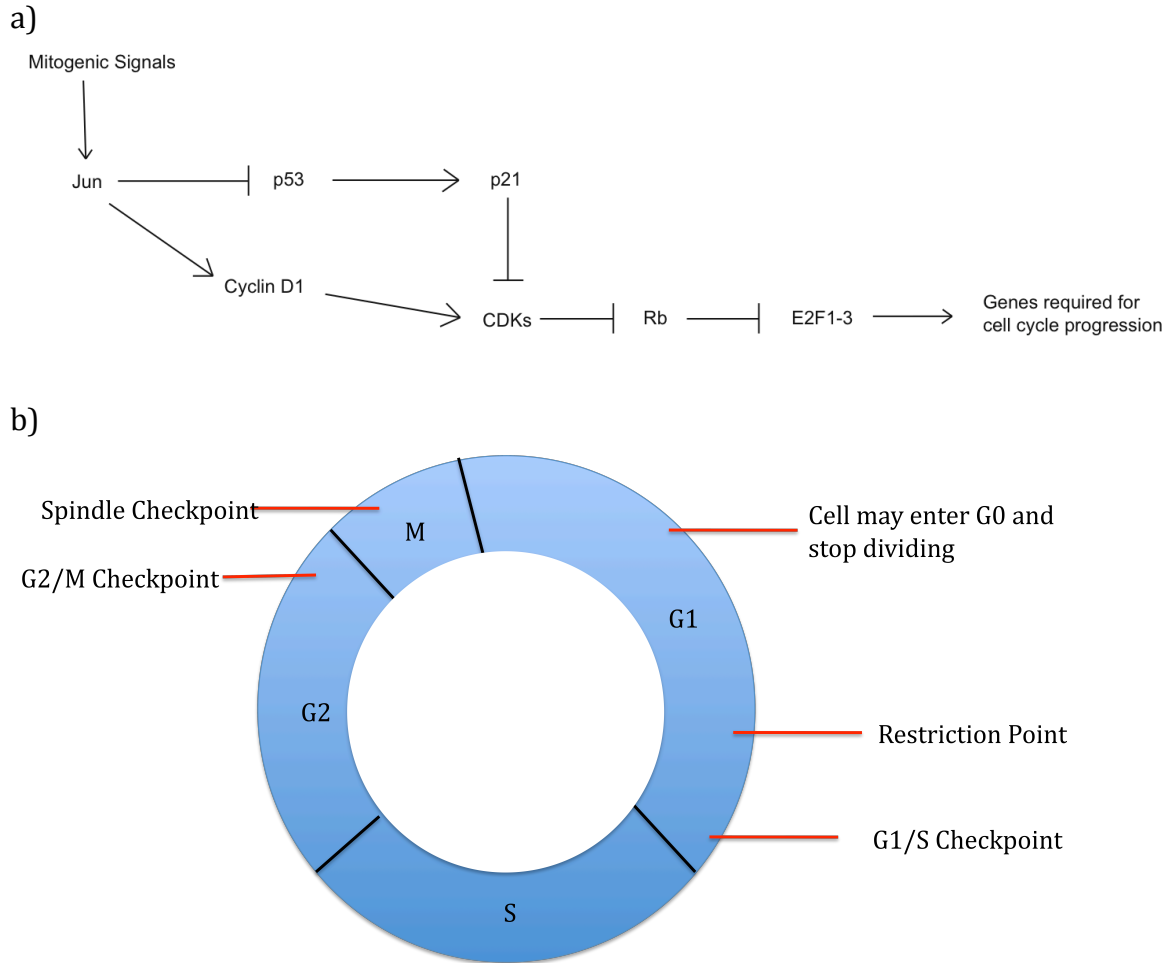
a)

b)

Figure III-3. The cell cycle. a) The role of cJun and cyclin D1 in the cell cycle. b) Schematic of the eukaryotic cell cycle.

E. Inhibition of KIX-Binding TADs in a Luciferase Assay

As we have previously demonstrated using NMR spectroscopy, iTAD **1** binds the KIX domain of CBP in an overlapping region to that of the natural activators MLL and Jun. A competitive inhibition experiment was conducted with MLL and Jun minimal activation domains and iTAD **1** to assess the functional effect, if any, of inhibiting this overlapping binding site in cells. The minimal activation domains, determined using gradual truncations of the full-length protein, had been determined for these TADs. The minimal TADs were fused to a Gal4-DBD facilitating localization of the TADs upstream of a reporter gene, and the cells were treated with iTAD **1**. In this case, the Gal4 fusion proteins were transfected into HeLa cells,

where, upon binding the reporter plasmid, the MLL or Jun TAD recruit their target proteins and upregulate transcription of the reporter gene. Inhibition of key protein·protein interactions by the small molecule would decrease reporter gene expression, quantified by luminescence of Firefly luciferase, compared to a Renilla luciferase control (Figure III-4a and b). Additional control experiments also showed that iTAD **1** does not inhibit Firefly or Renilla luciferase.
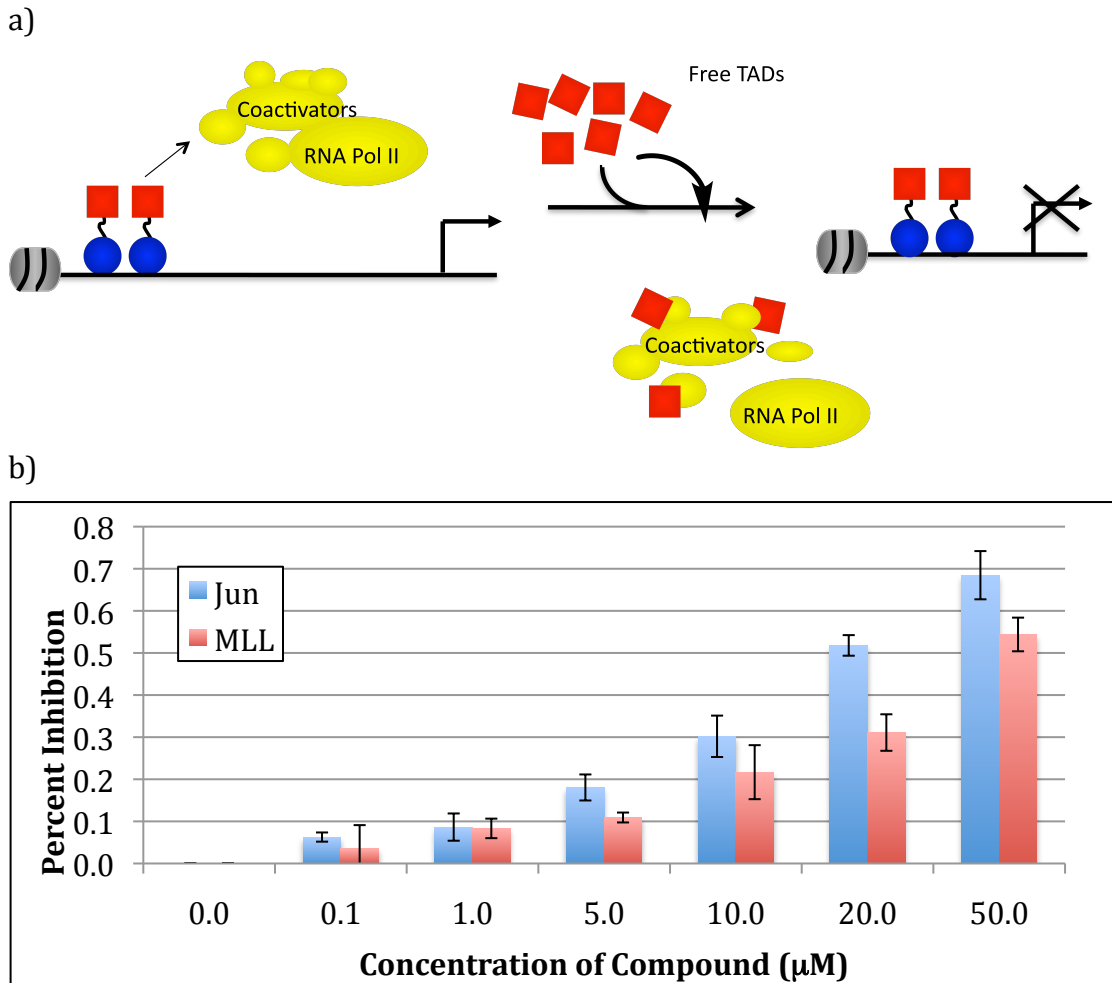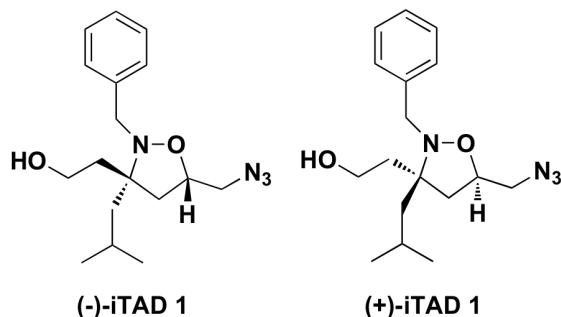
a)

b)

Figure III-4. Inhibition of KIX-binding TADs. a) Schematic of DNA-bound TAD inhibitor by free activation domain. b) Percent inhibition of Gal4-MLL- and Gal4-Jun-driven luciferase expression. Briefly, HeLa cells were transfected with a plasmid expressing the Gal4 DBD-MLL- or Jun-minimal TAD fusion protein, a reporter plasmid and transfection control, as has been previously described. Compound was added to the cells as a DMSO solution 6 h after transfection such that the final concentration of DMSO in all wells was 1% (vol/vol). Fold activation and error were calculated as previously described.

Previous work has shown that either enantiomer of iTAD **1** can activate transcription when tethered to a DBD.[64] To confirm that the absolute stereochemistry is not a critical factor in the interaction of iTAD **1** to the KIX domain, the two enantiomers of iTAD **1** were prepared by my colleagues Amy Danowitz and Dr. Will Pomerantz (Figure III-5a).
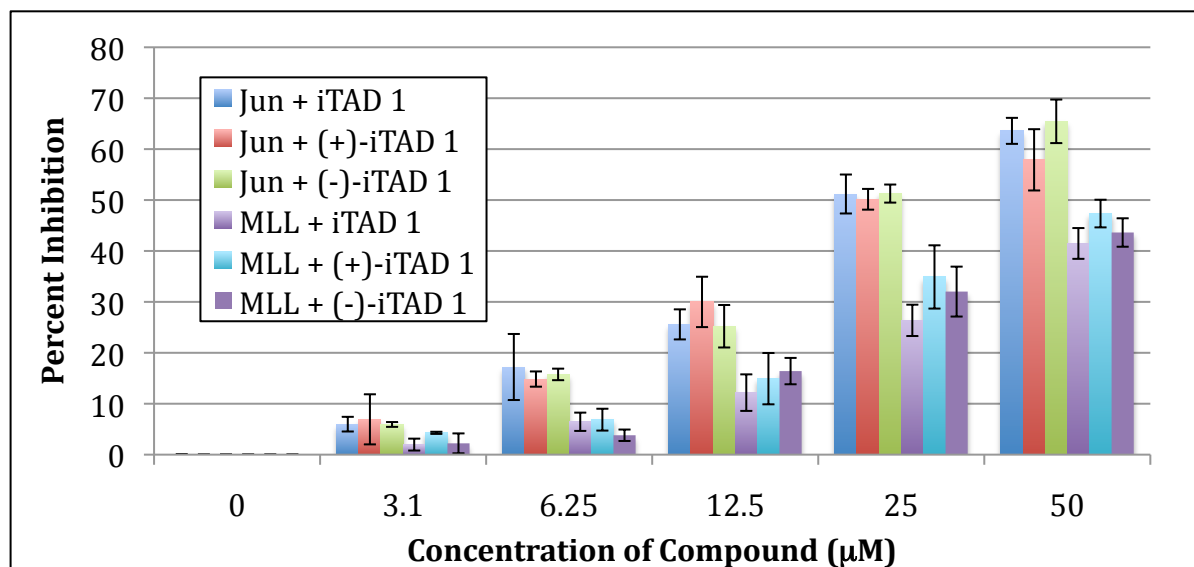
a)

(-)-iTAD 1   (+)-iTAD 1

b)

Figure III-5. Stereochemical configuration does not effect iTAD inhibiton of KIX-binding TADs. a) Structures of (+) and (-) iTAD 1. b) Inhibition of of Gal4-MLL- and Gal4-Jun-driven luciferase expression by (+), (-), and (±) iTAD **1**. Transfections and activity calculations were performed as previously described.

Both racemic and enantioenriched iTAD **1** inhibit luciferase expression driven by the MLL and Jun minimal TADs in a dose-dependent manner; therefore, stereochemical configuration is not an important determinant in these interactions

(Figure III-5b). Maximal inhibition was approximately 65% for Jun and 50% for MLL, both at the highest concentrations of iTAD **1** (50 μM). The different degrees of inhibition can be attributed, at least in part, to different levels of activity; MLL is a potent activator, while Jun is considerably weaker. It is not surprising that higher levels of inhibition were not observed; endogenous TADs contact multiple coactivators through different binding interactions.[65-67] Complete abrogation of activity would necessitate blocking each TAD·coactivator interacting surface, a highly unlikely event given the diversity of these interactions. At this time, it was unclear if iTAD **1** was selectively blocking the binding of these TADs to KIX or if it was indirectly inhibiting their function through a different, non-specific, mechanism.
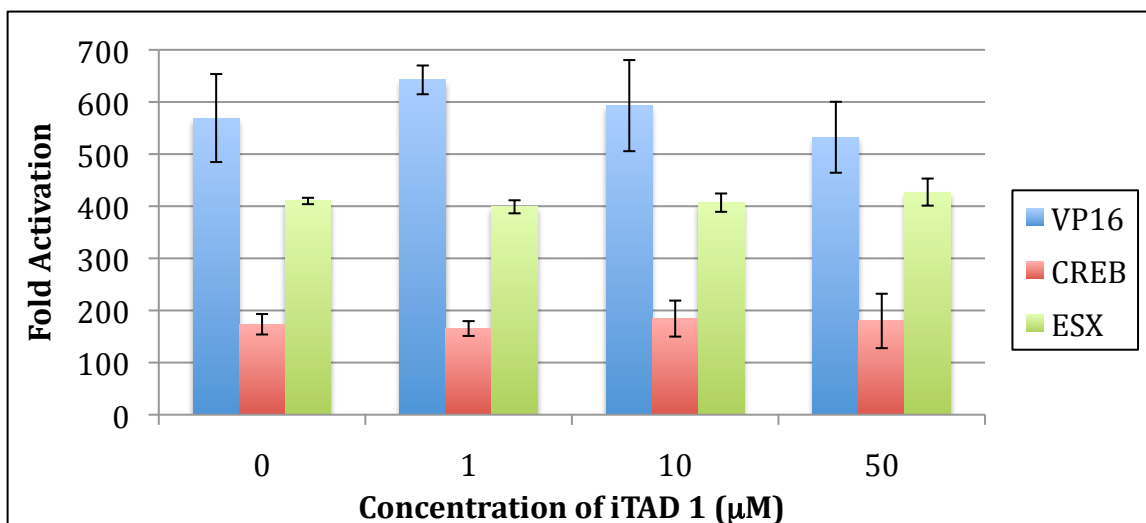

Figure III-6. Effect of iTAD **1** on non-KIX-binding TADs. Transfections and activity calculations were performed as previously described.

To examine this further, two additional activation domains, ESX and VP16, were tested in this assay. Neither VP16 nor ESX is known to bind the KIX domain of CBP; thus their activity should be unaffected by iTAD **1**. Indeed, neither protein is affected by addition of up to 50 μM iTAD **1** (Figure III-6). Furthermore, iTAD **1** does not affect the activity of CREB, which binds to another site on the KIX domain (Figure III-7). [43, 68, 69] These data show that iTAD **1** is not a general transcriptional inhibitor.
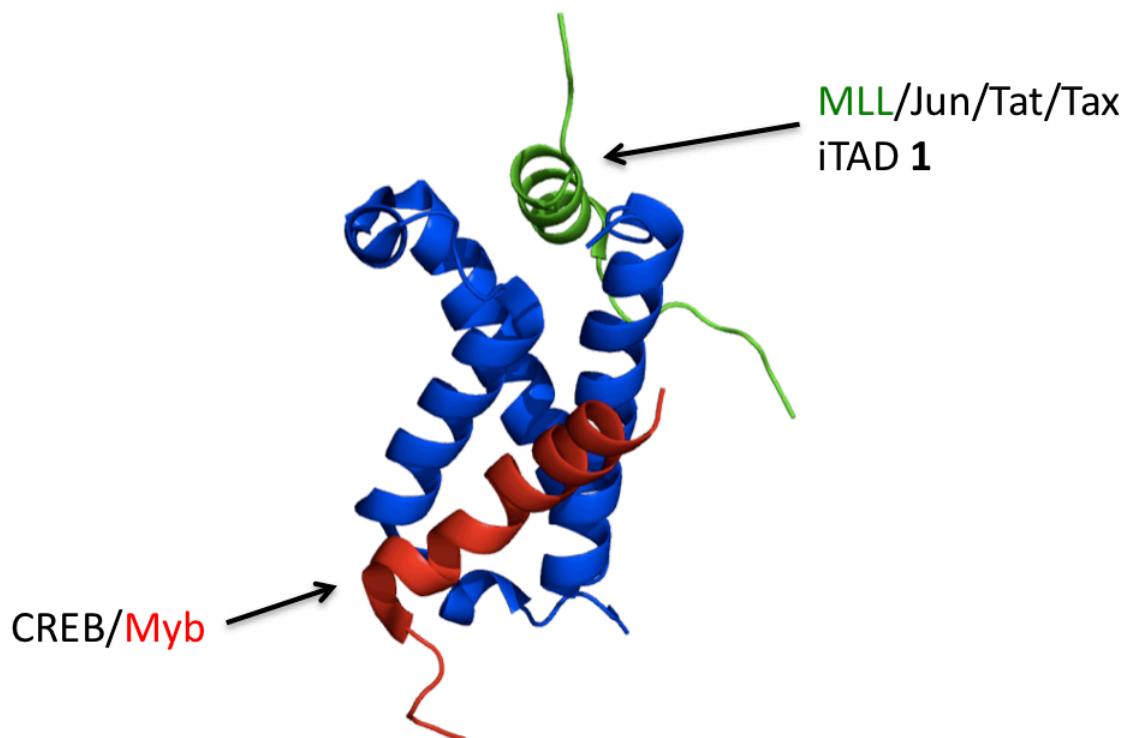
Figure III-7. KIX·Myb·MLL ternary complex. KIX is in blue, MLL in green, and Myb in red. Figure adapted from 2agh. iTAD **1** binds the MLL site and does not inhibit CREB binding to the CREB/Myb binding site.

F. Synthesis and Evaluation of iTAD Analogues

The sequence of the MLL and Jun KIX-binding regions are shown below in Figure III-8a; the putative residues mimicked/overlapped by iTAD **1** are highlighted in red. Due to the flexible nature of this binding site, it is likely that incorporation of different functionality on the iTAD framework will result in different small molecule binding modes. Other binding modes may, in turn, result in an increase in the potency of the compound, or alternatively, provide specificity for inhibiting a particular activator (i.e. significantly inhibit Jun without affecting MLL activity). Several compounds containing other functionality common to amphipathic TADs (acids, amines, alcohols) were synthesized in this endeavor, in addition to compounds containing "non-native" functionality. Figure III-8b shows representative examples of substitutions at four different positions around the isoxazolidine ring.

a)

MLL   DCGNILPSDIMDFVLKNTP

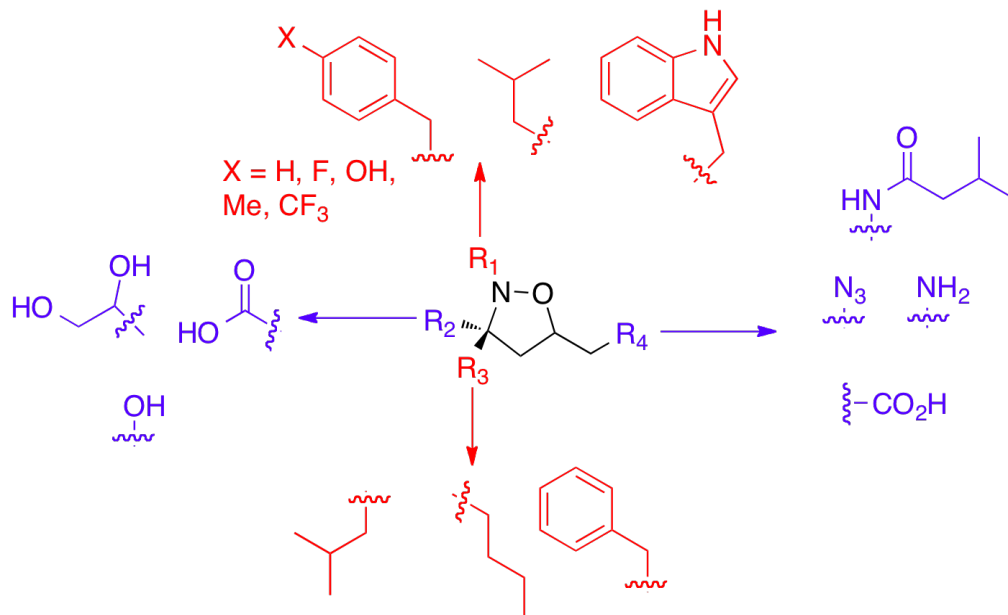Jun   LTSPDVGLLKLASPELERLIIQSSNGHIT

b)

Figure III-8. iTAD structural modifications. a) Putative residues on MLL and Jun mimicked by iTAD **1**. b) Examples of structural modifications made to the iTAD core architecture.

A series of alcohols and amines were generated starting from intermediate isoxazoline **4**: the benzyl group was appended under microwave conditions, followed by transformation of the alkene to a primary alcohol (*vide supra*) (Scheme III-1).[70]
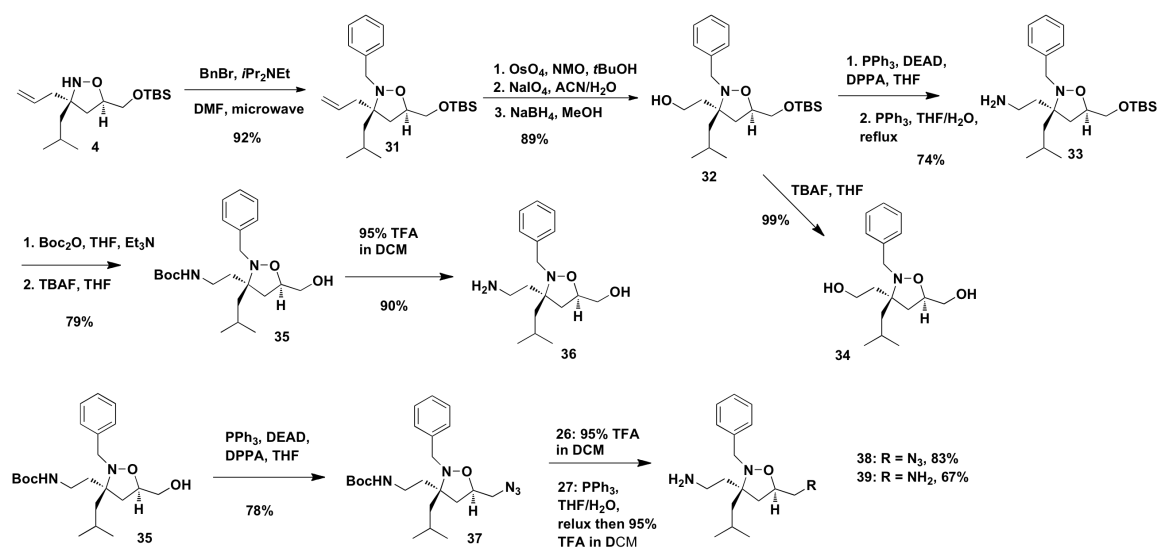
Scheme III-1. Synthesis of hydroxyl- and amine-functionalized iTADs.

Silyl ether **32** was then treated with tetrabutylammonium fluoride (TBAF) to generate diol **34** in excellent yield. Alternatively, **32** was treated with diphenylphosphoryl azide (DPPA) under Mitsunobu conditions to generate an azide at the C3 position. The azide was subsequently subjected to Staudinger reduction conditions with triphenylphosphine (PPh$_3$) to afford amine **33**. Treatment with Boc anhydride followed by cleavage of the TBS ether with TBAF afforded Boc protected alcohol **35**. Treatment with 95% trifluoroacetic acid removed the Boc group and afforded amine **36** in 90% yield. Treatment of compound **35** with DPPA under Mitsunobu conditions afforded azide **37**, followed by treatment with 95% TFA removed the Boc group providing amine **38**. Treatment of **37** with PPh$_3$ allowed access to diamine **39**, in moderate yield.

A series of carboxylic acids and esters were generated beginning with silyl ether **31** from the previous series (Scheme III-2). The *t*-butyldimethylsilyl (TBS) ether was removed using TBAF and the resulting alcohol underwent oxidation using the Jones reagent affording **41**. The resulting carboxylic acid was converted to methyl ester **42** using iodomethane. The alkene was subsequently converted to a primary alcohol through a three-step sequence as described previously to yield alcohol **43**. Treatment of **43** with lithium hydroxide afforded carboxylic acid **44**. Another carboxylic acid analogue was generated from **18** (iTAD **1**) by treatment

with Jones reagent to yield a C3 carboxylic acid (this was accomplished by Ryan Casey).[71] Azide and amine derivatives **45-47** were synthesized as previously described.
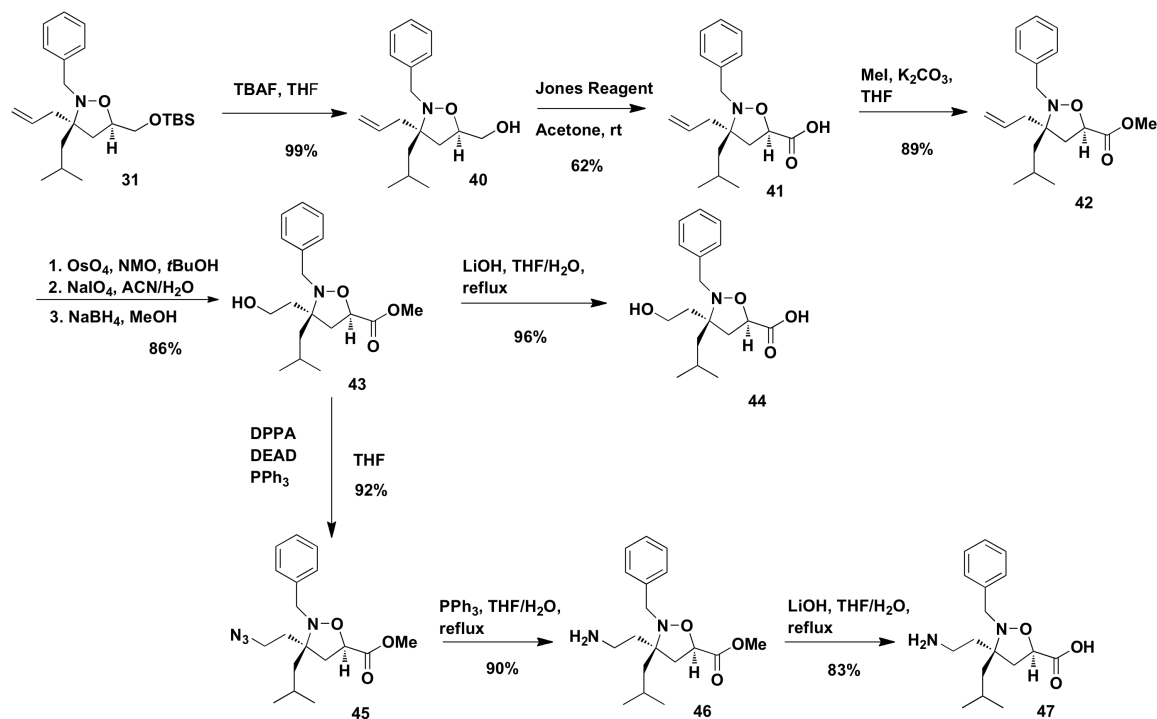
Scheme III-2. Synthesis of iTAD esters and carboxylic acids.

A final series of compounds was synthesized bearing a phenyl group at C3 in place of the isobutyl functionality. The synthesis began with benzaldehyde oxime, which underwent a 1, 3-dipolar cycloaddition with allyl alcohol, as previously described. The phenyl isoxazoline **49** was treated with $BF_3 \cdot OEt_2$ and allylmagnesium chloride to afford the hydroxy isoxazolidine **50**.[72, 73] The primary alcohol was treated with methanesulfonyl chloride followed by displacement with sodium azide to afford azide **51**, followed by alkylation as described previously to afford **52**. The alkene in **52** underwent subsequent oxidation, cleavage, and reduction as described previously to afford alcohol **59**. Reduction of the azide with PPh_3 proceeded in good yield to afford amine **64**.
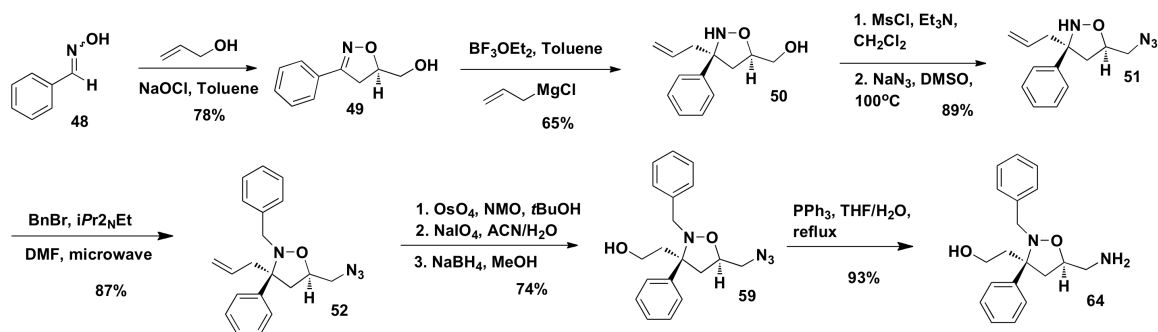
Scheme III-3. Synthesis of C3-phenyl-substituted iTADs.

These compounds possess diverse functionality around the isoxazolidine framework. Each compound was tested for inhibition of both MLL and Jun minimal TADs in the luciferase expression system described previously. For example, we had theorized that replacement of benzyl functionality with an aliphatic substituent would better mimic Jun (L67, L70) over MLL (F2852, L2854). In addition, there are several acidic and basic residues in these KIX-binding sequences (MLL: D2848, D2851, K2855, Jun: D64, K69, E74, E76) near the region that iTAD **1** is thought to mimic. It was hoped that addition of an acidic or basic group might advantageously affect binding to KIX.

MLL   DCGNILPSDIMDFVLKNTP

Jun   LLTSPDVGLLKLASPELERLIIQSSNGHIT

Figure III-9. Residues mimicked by iTAD analogues. Residues mimicked by iTAD **1** are in red, putative residues mimicked by analogues are in blue.

Figure III-9 (Residues mimicked by iTAD **1** in red, acidic/basic residues in blue). The inhibition data for these compounds is shown in Figures III-10 and 11, the structures of compounds tested are shown in Figure III-12.
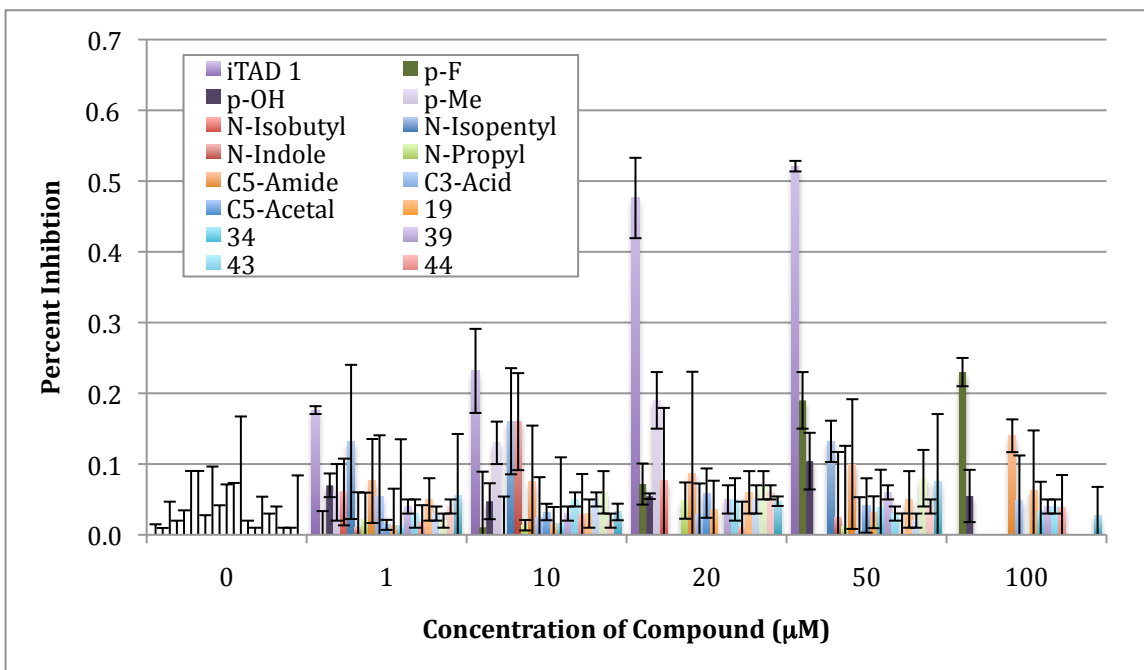
Figure III-10. Inhibition of Gal4-MLL-driven luciferase expression. Transfection conditions and activity and error calculations were performed as previously described.
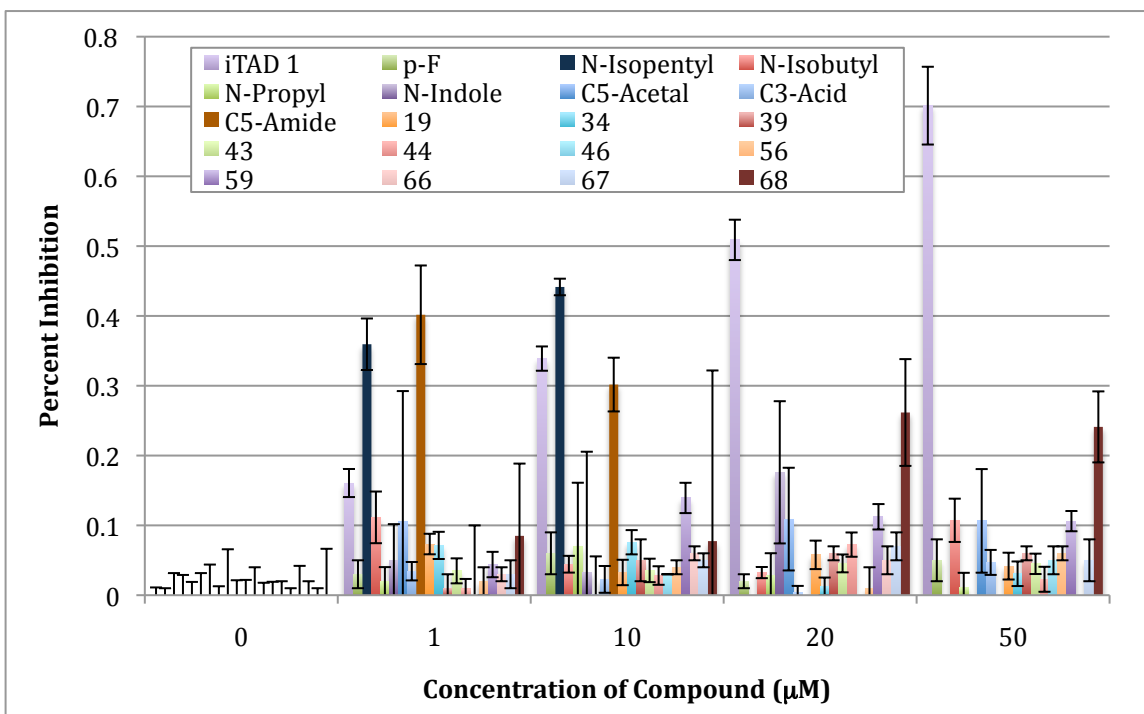

Figure III-11. Inhibition of Gal4-Jun-driven luciferase expression. Transfection conditions and activity and error calculations were performed as previously described.
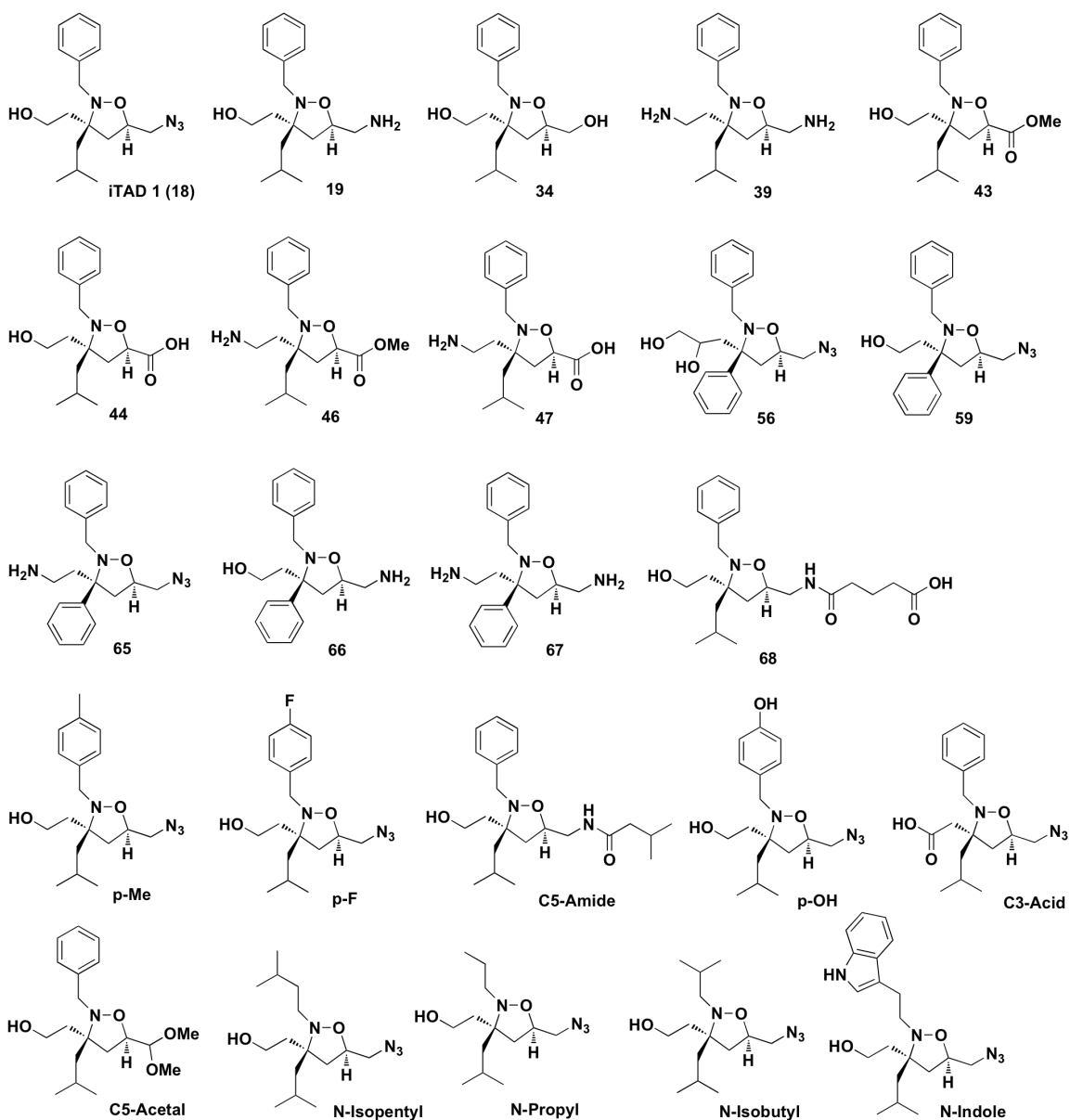
Figure III-12. Compounds tested for MLL and Jun Inhibition. (N2 derivatives and C5 amides were synthesized by Dr. Will Pomerantz)

The most active iTAD **1** analogues were the p-fluoro and p-methyl compounds, although p-Me was cytotoxic at concentrations over 20 μM. Two other relatively active compounds were the C5 amide and C5 dimethoxyacetal. Both molecules showed potent inhibition at low concentrations (relative to iTAD **1**), however, these molecules were also cytotoxic at concentrations approaching 20 μM.

iTAD **1** not only shows inhibition of MLL- and Jun-driven luciferase expression, it is not cytotoxic at concentrations up to 50 μM in Jun-transfected cells, and 100 μM in MLL-transfected cells.

Thus, we were unable to attain additional potency or specificity for MLL or Jun using the iTAD architecture. These results were not entirely surprising, for natural TADs are generally tolerant of mutagenesis; there are several examples where only mutation of many residues throughout the TAD completely abrogates TAD·coactivator binding and transcriptional activation. The N-terminal TAD of the viral activator VP16, for example, has four residues, F473, F475, E476, and F478 (out over 100), that all must be mutated to significantly impact activity.[74-80] Additionally, the Hinnebusch group has shown that there are seven clusters of hydrophobic residues in the yeast activator Gcn4; none of these clusters is essential for Gnc4 activity, suggesting these clusters perform redundant functions in activation.[81, 82]

The glucocorticoid receptor (GR) TAD has also been subjected to mutagenesis studies; mutation of E219, F220, and W234 in a 210 amino acid construct was enough to affect binding, though no other combination of mutations had significant impact.[83-85] These studies demonstrate the importance of hydrophobic amino acids for TAD function, and that certain hydrophobic residues are critical for coactivator binding and transcriptional activation. Interestingly, there is often one key polar residue amongst the hydrophobic amino acids, as is seen in above in GR and in the KIX-binding region of MLL. This provides additional evidence that alteration of the hydroxyl group (to an acid or amine) may significantly impact binding and function.

Thus, "mutation" of iTAD **1** functional groups leads to a reduction in the ability to block TAD·KIX interactions. Given the tolerance of natural TADs to mutagenesis, and the large difference in interacting surface area, it is not surprisingly that making minor structural changes to a small molecule would not improve potency. This also highlights the difference between designing small

molecule TADs and small molecule PPIs; TADs are localized to DNA, increasing their effective concentration and the relative concentration of their coactivator targets. Low binding affinity, in this case, is not detrimental to function; however, in the case of PPIs, low binding affinity and non-specific interactions may account for the loss in activity. Further investigation of the affinity and iTAD·coactivator co-complex lifetimes, possible metabolic modifications, and membrane permeability, for these molecules will aid in the elucidation of additional determinants for the design of iTAD-based PPIs.

G. Inhibition of Cyclin D1 Expression

The studies described above merited further investigation of iTAD **1**-mediated inhibition of MLL and Jun. However, these experiments were carried out using plasmid DNA in a competitive inhibition experiment. To assess the effect of iTAD **1** in an endogenous promoter context, the expression of a Jun-regulated gene, cyclin D1, was examined. Cyclins are allosteric regulators of cyclin-dependent kinases (CDKs), key regulators of cell-cycle progression. D-type cyclins (D1, D2, and D3) are G1 specific and associate with CDK4 and CDK6, promoting restriction point progression during the G1 phase of cell division (Figure III-13).[63] Unlike other cyclins, the expression of cyclin D1 is heavily influenced by mitogenic signals and thus not surprisingly is often overexpressed in cancers.[57, 58, 60-62]
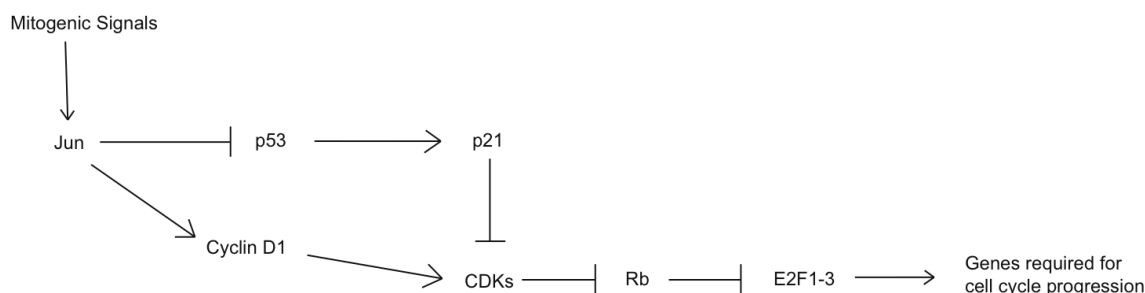

Figure III-13. Cyclin D1 and control of the cell cycle. Expression of cyclin D1 is influenced by mitogenic signals and results in activation of cyclin-dependent kinases, resulting in phosphorylation of Rb and an increase in expression of genes required for cell cycle progression.

The promoter region of CCND1 (cyclin D1 gene) contains an AP-1 binding site, where Jun (part of the AP-1 complex, *vide supra*) binds and recruits coactivators.[58] Due to limiting quantities of CBP in cells, perturbation of the Jun·CBP interaction may preclude activation of cyclin D1 gene transcription, slowing cell growth and stalling the cell cycle in the G1 phase.[86-89] Towards this end, MCF-7 breast cancer cells were treated with several concentrations of iTAD **1**, up to 100 μM, and Western blots were performed to assess the levels of cyclin D1 and Jun (Figure III-14a-b). MCF-7 cells express significant levels of both Jun and cyclin D1 and are therefore an excellent system in which to test the effects of iTAD **1** in an endogenous context.[54, 56, 59] The treatment of cells with 40 μM iTAD **1** resulted in the decrease of cyclin D1 expression with no changes in the expression of Jun or glyceraldehyde-3-phosphate dehydrogenase (GAPDH), a common indicator of cell viability. The compound appeared to have a deleterious effect on cells beginning at 50 μM concentration, evidenced by a decrease in the levels of GAPDH (Figure III-14c).
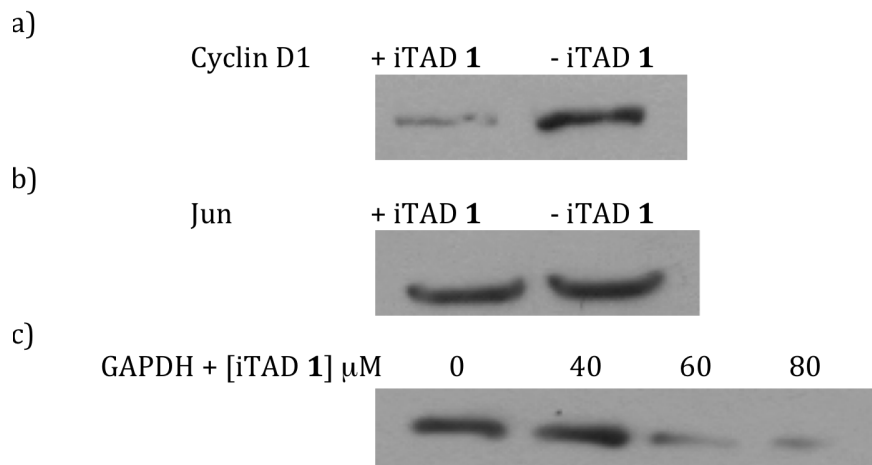
a)

Cyclin D1   + iTAD **1**   - iTAD **1**

b)

Jun   + iTAD **1**   - iTAD **1**

c)

GAPDH + [iTAD **1**] μM   0   40   60   80

Figure III-14. Effect of iTAD **1** on cyclin D1 expression. a) Western blot with anti-cyclin D1 antibody after 24h treatment of MCF-7 cells with 40 μM iTAD **1**. b) Jun expression is unaffected by treatment with 40 μM iTAD **1**. c) No toxicity is observed until treatment with > 40 μM iTAD **1**.

Further experiments were performed to investigate the effect of iTAD **1** on the growth of MCF-7 cells. Unfortunately, even at 40 μM, iTAD **1** had no significant

effect on the growth rate of treated cells, relative to control cells treated only with the DMSO vehicle (Figure III-15).
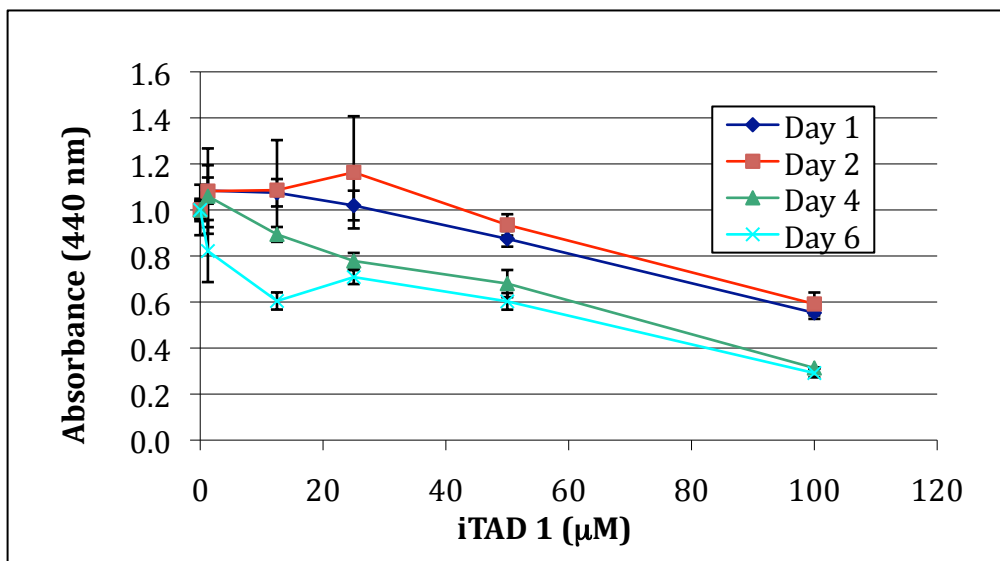

Figure III-15. Effects of iTAD **1** on growth of MCF-7 cells. Cells were treated with WST-1 dye for 1 hour prior to reading absorbance at 440 nm. Briefly, cells were plated and allowed to adhere for 12 h. Compound was added in 5 μL DMSO (final DMSO concentration 1% vol/vol) and the cells incubated for 24, 48, 96, or 144 h. Fresh media was added at day 4, absorbance readings were taken 1 h after addition of WST-1 dye.

This result was not particularly surprising since in c-Jun $^{-/-}$ cells, there is a 4.5 fold reduction in expression of cyclin D1, resulting in cell cycle arrest in the G1 phase after 3-4 days.[57] It is unlikely that iTAD **1** could so completely block c-Jun coactivator interactions as to approach the decrease in levels of cyclin D1 seen in c-Jun null cells. Additional compounds with the iTAD architecture may attain higher potency or specificity in this regime.

H. Conclusions

iTAD **1** has emerged as an inhibitor of the interaction between the CBP KIX domain and the TADs of endogenous activators MLL and Jun. Cell-based experiments have demonstrated that iTAD **1** can decrease production of a Jun-regulated gene, cyclin D1, in the context of an endogenous promoter. In addition, a

synthetic strategy has been implemented that allows for generation of iTAD analogues at four positions on the five-membered heterocycle, allowing for incorporation of diverse functionality around the ring. Most analogues were unsuccessful at inhibiting MLL or Jun driven transcription, showing intolerance for functional group alteration from iTAD **1**. These data, however, do provide an excellent starting point for further development of design criteria for small molecule inhibitors of TAD·coactivator interactions.

I. Experimental

General.

Unless otherwise noted, starting materials were obtained from commercial suppliers and used without further purification. Toluene, CH_2Cl_2, THF, and Et_2O were dried by passage through activated alumina columns. All reactions involving air- or moisture-sensitive compounds were performed under a dry N_2 atmosphere.[90] Unless otherwise noted, organic extracts were dried over Na_2SO_4, filtered, and concentrated under reduced pressure on a rotary evaporator. $BF_3 \cdot OEt_2$ and Et_3N were distilled from CaH_2. DMF was distilled under reduced pressure from P_2O_5. NBS was recrystallized from EtOH/water. Purification by column chromatography was carried out with E. Merck Silica Gel 60 (230-400 mesh) according to the procedure of Still, Kahn and Mitra.[91] Reverse-phase HPLC purification was performed on a Varian ProStar 210 equipped with Rainin Dynamix UV-D II detector using a C18 (8 x 100 mm) Radial PakTM cartridge using a gradient mixture of 0-80% 0.1% TFA/water and acetonitrile, unless otherwise specified. UV-Vis spectra were recorded in ethanol. ^1H and ^{13}C NMR spectra were recorded in $CDCl_3$ at 400 MHz and 125 MHz, respectively, unless otherwise specified. IR spectra were measured as thin films on NaCl plates using a Perkin Elmer Spectrum 1000 FT-IR. High-resolution mass spectra were measured on a VG-250-S Micromass, Inc., mass spectrometer at the University of Michigan Mass Spectrometry Laboratory. Compounds not directly referred to in the text are labeled **S**. The MLL plasmid was a generous gift from Dr. Jay Hess and the Jun plasmid was purchased from Promega.

Cell-based Activity Assay.

HeLa cells were purchased from the American Tissue Culture Center (ATCC) and plated onto treated polystyrene petri dishes (Corning) with 10 mL of D-MEM (+ 4.5 g/L d-glucose, + l-glutamine, - sodium pyruvate, + 10% FBS, + NEAA) (invitrogen). The cells were grown at 37°C 5% and 5% CO_2 to 80-90% confluence. Upon reaching the desired confluence, the D-MEM was removed and 4 mL 0.25% trypsin was added. The cells were incubated with the trypsin solution for 5 minutes at 37°C and 5% CO_2. Following the inubation, 10 mL of D-MEM were added and the resultant solution was pipetted up and down several times to ensure removal of all cells from the dish surface. The solution was centrifuged in a 15-mL Falcon tube at 1000 rpm for 2 minutes in a Fisher Centrific centrifuge. The supernatant was removed and the cell pellet was resuspended in 10 mL of D-MEM. The concentration of cells was calculated using a Hausser Scientific improved Neubauer phase counting chamber hemocytometer. Based on the determined concentration the cells were diluted to 100,000/mL in D-MEM. 100 μL of the cell solution was then added to each well of a Microtest flat-bottom, low-evaporation-lid 96-well plates (Becton-Dickinson) and the plated cells were incubated overnight at 37°C and 5% CO_2. The media was removed from the plated cells and they were washed once with Opti-MEM (+ HEPES, + 2.4 g/L sodium bicarbonate, + l-glutamine) (Invitrogen) and then transfected.

The transfection procedure consisted of first mixing appropriate plasmids and Lipofectamine 2000® together in Opti-MEM® media for each well being transfected. After a 20 minute incubation at room temperature 100 μL of the solution was placed in the appropriate wells and the cells were incubated for 5 hours at 37°C and 5% CO_2. At the end of the 5-hour incubation, the transfection solution was removed and 100 μL fresh D-MEM was added to each well. To the media was added 1 μL of either DMSO or the appropriate concentration of a molecule being tested dissolved in DMSO (the final concentration of DMSO in all the wells was 1%). The cells were then incubated for 24 hours at 37°C and 5% CO_2.

Following the 24-hour incubation, the media was removed from each well and the cells were washed once with PBS buffer. 20 μL of passive lysis buffer (Promega) was added to each well and the cells were incubated for 20 minutes at room temperature on an orbital shaker. Subsequently, the total volume of each well was added to a cuvette along with 25 μL of Luciferase Assay Reagent II (Promega) and the luminescence was recorded. Then 25 μL Stop & Glo reagent was added and the Renilla luminescence was recorded again on a Berthold FB12 single cuvette luminometer.[92]

Cyclin D1 expression.

MCF-7 cells were plated in 500 μL media (RPMI + 10% FBS) in a 24-well plate (40,000 cells per well) and allowed to adhere overnight (12h). Media was removed and 495 μL fresh media and 5 μL of DMSO alone or with compound (final concentation of DMSO = 1%). The cells were incubated with compound for 24 hours and then lysed using 50 μL passive lysis buffer per well (Promega) with a proEt3Nse inhibitor cocktail (Invitrogen) at rt on an orbital shaker for 20 minutes. The lysate was cleared by centrifugation at 14000 rpm for 10 minutes then mixed with loading dye and BME (final concentration of 1%) and heated at 95°C for 10 minutes. The lysates were separated by SDS-PAGE and detected by Western blot as previously described. Cyclin D1 (1:1000) and Jun (1:1000) antibodies were obtained from Santa Cruz Biotech.

MCF-7 cell proliferation.

MCF-7 cells were plated in 500 μL media (RPMI + 10% FBS) in a 24-well plate (40,000 cells per well) and allowed to adhere overnight (12h). Media was removed and 495 μL fresh media and 5 μL of DMSO alone or with compound (final concentration of DMSO = 1%). The cells were incubated overnight and the absorbance was read after 24 hrs (60 minutes after addition of WST-1 dye) and every 48h thereafter for 8 days (first reading is day 1). Media was changed and fresh compound added on Day 4.

**Small Molecule Synthesis and Characterization.**
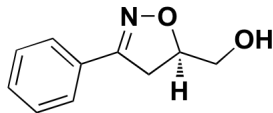
((*R*)-(3-phenyl-4,5-dihydroisoxazol-5-yl)methanol) (49): Allyl alcohol (2.8 mL, 41.3 mmol, 10 eq) was added to a solution of benzaldehyde oxime (**48**) (500 mg, 4.13 mmol, 1 eq) in toluene (42 mL). The mixture was stirred in an ice/water bath and aqueous NaOCl (15 mL of a 705 mM solution, 10.4 mmol, 2.5 eq) was added dropwise over 2h. The biphasic mixture was warmed to room temperature and stirred overnight. The aqueous layer was extracted with EtOAc (3 x 50 mL) and the combined organic extracts were washed with water (100 mL) and brine (100 mL) then dried over MgSO$_4$. The solvent was removed *in vacuo* and product was isolated by flash chromatography (9:1 Hex/EtOAc) providing 669 mg of **49** in 90% yield as a clear light yellow oil. ^{1}H NMR: δ 3.61-3.71 (m, 2H), 3.82-3.89 (m, 2H), 4.78-4.88 (m, 1H), 7.20-7.23 (m, 1H), 7.35-7.41 (m, 2H), 7.61-7.68 (m, 2H); ^{13}C NMR: 38.1, 64.0, 84.1, 129.0, 128.8, 130.6, 136.9, 157.7; HRMS (ESI) calcd for $[C_{10}H_{11}NO_2 + Na]^+$: 200.0687, found: 200.0689.
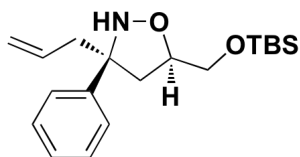

((3*S*,5*R*)-3-allyl-5-(((*tert*-butyldimethylsilyl)oxy)methyl)-3-phenylisoxazolidine) (53) To a solution of **49** (669 mg, 3.7 mmol, 1 eq) in CH$_2$Cl$_2$ (40 mL) cooled in an ice-water bath was added Et$_3$N (780 μL, 5.6 mmol, 1.5 eq), DMAP (46 mg, 0.4 mmol, 0.1 eq), and TBSCl (567 mg, 5.6 mmol, 1.5 eq). The reaction mixture was allowed to warm to rt and stir for 4h at which time the reaction was complete by TLC and MS analysis. Water (50 mL) was added and the aqueous layer was extracted with EtOAc (3 x 30 mL). The combined organic extracts were washed with brine (50 mL) and dried over MgSO$_4$. The solvent was removed *in vacuo* and carried directly through to the next step. To that end, the silyl ether was dissolved in

toluene (10 mL) and cooled in a dry ice/acetone bath. Freshly distilled BF$_3$·OEt$_2$ (320 μL, 2.5 mmol, 3 eq) was added drop wise over 10 min. The reaction mixture stirred for 45 minutes at which time allyl magnesium chloride (1.26 mL of a 2M solution in toluene, 2.5 mmol, 3 eq) was added dropwise over 15 minutes. The reaction stirred with continued cooling for 10h. The reaction was allowed to slowly warm to rt and sat. NH$_4$Cl (2 mL) was added followed by water (5 mL). The aqueous layer was extracted with EtOAc (3 x 10 mL) and the combined organic extracts were dried over MgSO$_4$ and the solvent removed *in vacuo*. The product was isolated by flash chromatography (95:5 Hex/EtOAc) to give 245 mg of **53** in 44% yield as a clear oil. ^{1}H NMR: δ 0.06 (s, 6H), 0.98 (s, 9H), 2.18-2.32 (dd, 2H, J = 12.0, 8.8), 3.61-3.71 (m, 2H), 3.82-3.89 (dd, 2H, J = 10.3, 5.9), 4.78-4.88 (m, 1H), 5.05-5.11 (m, 2H), 5.72-5.83 (m, 1H), 7.20-7.23 (m, 1H), 7.35-7.41 (m, 2H), 7.61-7.68 (m, 2H); ^{13}C NMR: -5.6, -5.5, 25.8, 38.1, 64.0, 76.4, 84.1, 117.5, 129.0, 128.8, 130.6, 136.9, 139.3; HRMS (ESI) calcd for [C$_{19}$H$_{31}$NO$_2$Si + Na]$^+$: 356.2022, found: 356.2029.
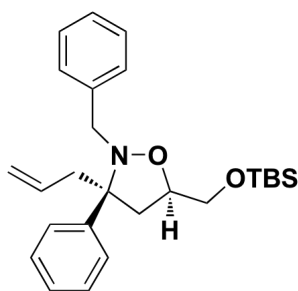

((3*S*,5*R*)-3-allyl-2-benzyl-5-(((*tert*-butyldimethylsilyl)oxy)methyl)-3-phenylisoxazolidine) (54): To a solution of **53** (150 mg, 450 μmol, 1 eq) in DMF (4.5 mL) were benzyl bromide (110 μL, 900 μmol, 2 eq) and *i*Pr$_2$NEt (170 μL, 940 μmol, 2.1 eq). The mixture was irradiated at 20% power for 15 seconds (x2) and allowed to cool to rt over 20 min. The procedure was repeated 10x, then the reaction mixture was partitioned between water (10mL) and Et$_2$O (10 mL) and the aqueous layer was extracted with Et$_2$O (3 x 10 mL). The combined organic extracts were dried over MgSO$_4$ and the solvent was removed *in vacuo*. The product was isolated by flash chromatography (99:1 Hex/EtOAc) to provide 179 mg of **54** in 98%

yield. ^{1}H NMR: δ 0.06 (s, 6H), 0.98 (s, 9H), 2.18-2.32 (dd, 2H, J = 12.0, 8.8), 3.61-3.71 (m, 2H), 3.78-3.93 (m, 4H), 4.78-4.88 (m, 1H), 5.05-5.11 (m, 2H), 5.85-5.93 (m, 1H), 7.22-7.41 (m, 8H), 7.61-7.68 (m, 2H); ^{13}C NMR: -5.5, -5.6, 25.8, 38.1, 63.4, 64.0, 76.4, 84.1, 117.5, 126.7, 128.1, 128.8, 129.0, 130.6, 135.4, 135.7, 136.9, 139.3; HRMS (ESI) calcd for $[C_{26}H_{37}NO_2Si + Na]^+$: 446.2491, found: 446.2502.
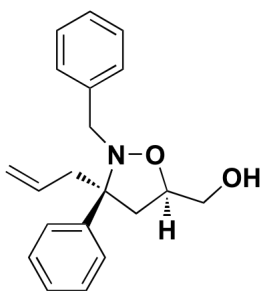
(((3S,5R)-3-allyl-2-benzyl-3-phenylisoxazolidin-5-yl)methanol) (55): To a solution of **54** (179 mg, 440 μmol, 1 eq) in THF (4.4 mL) cooled in an ice-water bath was added TBAF (1.8 mL of a 1.0 M solution in THF, 1.77 mmol, 4.0 eq) dropwise over 10 minutes and the reaction was allowed to warm to rt with stirring for 4h at which time the rxn appeared complete by TLC. Sat. NH_4Cl (2 mL) was added followed by H_2O (2 mL) and the aqueous layer was extracted with EtOAc (3 x 10 mL) and the combined organic extracts were dried over $MgSO_4$ and the solvent was removed *in vacuo*. The product was isolated by flash chromatography (95:5 Hex/EtOAc) to provide 135 mg of **55** in 99% yield as a clear oil. ^{1}H NMR: δ 2.18-2.32 (dd, 2H, J = 12.0, 8.8), 3.61-3.71 (m, 2H), 3.78-3.93 (m, 4H), 4.78-4.88 (m, 1H), 5.05-5.11 (m, 2H), 5.85-5.93 (m, 1H), 7.22-7.41 (m, 8H), 7.61-7.68 (m, 2H); ^{13}C NMR: 38.1, 64.0, 63.4, 76.4, 84.1, 117.5, 126.7, 128.1, 128.8, 129.0, 130.6, 135.4, 135.7, 136.9, 139.3; HRMS (ESI) calcd for $[C_{20}H_{23}NO_2Si + Na]^+$: 332.1626, found: 332.1634.
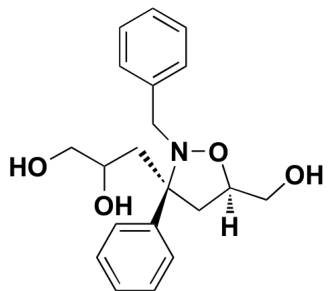
3-((3S,5R)-2-benzyl-5-(hydroxymethyl)-3-phenylisoxazolidin-3-yl)propane-1,2-diol) (57): To a solution of **55** (100 mg, 323 μmol, 1.0 eq) and NMO (57 mg, 485 μmol, 1.5 eq) in tBuOH/THF/H_2O (11 mL, 4:1:0.5) cooled in an ice-water bath was added OsO_4 (325 μL of a 2.5% wt solution in 2-propanol, 0.1 eq) dropwise over 5 minutes and the reaction was allowed to come to rt with stirring for 12h. To quench the reaction, saturated aqueous $Na_2S_2O_4$ (2 mL) was added in water and the mixture stirred at rt for 1h. Sat. NH_4Cl (2 mL) was added and the aqueous layer was extracted with EtOAc (3 x 15 mL) and the combined organic extracts were washed with brine (20 mL) and dried over $MgSO_4$. The product was isolated by flash chromatography (1:1 Hex/EtOAc) providing 96 mg of **57** as a clear oil in 86% yield. ^{1}H NMR: δ 1.94-2.39 (m, 6H), 3.40-3.81 (m, 5H),3.95-4.32 (m, 4H), 7.22-7.41 (m, 8H), 7.61-7.68 (m, 2H); HRMS (ESI) calcd for $[C_{20}H_{25}NO_4 + Na]^+$: 366.1681, found: 366.1685.
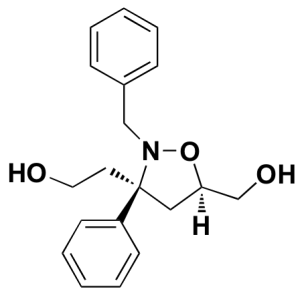

(2-((3S,5R)-2-benzyl-5-(hydroxymethyl)-3-phenylisoxazolidin-3-yl)ethanol) (58): To a solution of **57** (10 mg, 25 μmol, 1 eq) in ACN/H_2O (4 mL, 1:1) was added $NaIO_4$ (16 mg, 75 μmol, 3.0 eq). The reaction was stirred at rt for 3h at which point water (5 mL) was added and the aqueous layer was extracted with Et_2O (3 x 10 mL)

and the combined organic extracts were dried over MgSO$_4$ and the solvent removed *in vacuo*. The crude aldehyde was dissolved in MeOH (5 mL) and NaBH$_4$ (1.9 mg, 50 µmol, 2.0 eq) was added. The reaction stirred at rt for 1h at which point TLC analysis indicated the reaction was complete. Water (5 mL) was added to the reaction and the reaction mixture was extracted with Et$_2$O (3 x 10 mL). The organic extracts were dried over MgSO$_4$ and the solvent removed *in vacuo*. The product was isolated by flash chromatography (8:2 Hex/EtOAc) providing 6.5 mg of **58** in 83% yield as a clear oil. ^{1}H NMR: δ 1.70-1.79 (m, 3H), 1.91-2.01 (m, 1H), 2.06 (dd, 1H, *J* = 8.1, 12.7), 2.36 (dd, 1H, *J* = 8.0, 12.7), 3.41 (d, 2H, *J* = 4.7), 3.78-3.93 (m, 3H), 3.99 (d, 1H, *J* = 13.9), 4.19-4.28 (m, 1H), 7.22-7.49 (m, 8H) 7.61-7.68 (m, 2H); ^{13}C NMR: δ, 35.6, 40.8, 43.0, 53.7 54.5, 69.7, 70.4, 127.2, 128.4, 128.6, 135.4, 135.7, 136.9, 137.6, 139.3; HRMS (ESI) calcd for [C$_{19}$H$_{23}$NO$_3$ + Na]$^+$: 336.1576, found: 336.1588.
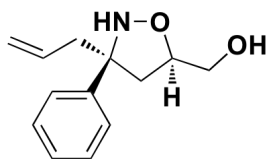
(((3*S*,5*R*)-3-allyl-3-phenylisoxazolidin-5-yl)methanol) (50): To a solution of **53** (200 mg, 0.6 mmol, 1.0 eq) in THF (5 mL) cooled in an ice-water bath was added TBAF (1.8 mL of a 1.0M soln in THF, 1.8 mmol, 3.0 eq) drop wise over 10 minutes and the reaction was allowed to warm to rt with stirring for 4h at which time the reaction appeared complete by TLC. Sat. NH$_4$Cl (2 mL) was added followed y water (5 mL) and the aqueous layer was extracted with EtOAc (3 x 10 mL) and the combined organic extracts were dried over MgSO$_4$ and the solvent was removed *in vacuo*. The product was isolated by flash chromatography (1:1 EtOAc/Hex) providing 129 mg of **50** in 98% yield as a clear oil. ^{1}H NMR: δ 2.05-2.14 (m, 1H), 2.50-2.68 (m, 3H), 3.54-3.63 (m, 1H), 4.01-4.09 (m, 1H), 4.96-5.05 (m, 2H), 5.48-5.61 (m, 1H), 7.27-7.35 (m, 5H); ^{13}C NMR: 41.9, 44.5, 69.4, 70.8, 86.0, 118.7, 126.1, 126.3, 127.3, 128.3, 133.5; HRMS (ESI) calcd for [C$_{13}$H$_{17}$NO$_2$ + Na]$^+$: 242.1157, found: 242.1161.
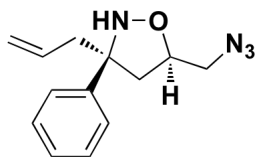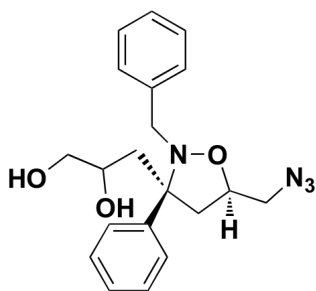
((3S,5R)-3-allyl-5-(azidomethyl)-3-phenylisoxazolidine) (51): To a solution of **50** (129 mg, .588 mmol, 1.0 eq) in CH_2Cl_2 (6 mL) cooled in an ice/water bath was added methanesulfonyl chloride (55 µL, .706 mmol, 1.2 eq) and Et_3N (98 µL, .706 mmol, 1.2 eq). The reaction mixture was allowed to warm to rt and was stirred for 3.5 h. Saturated NH_4Cl (10 mL) was added followed by water (10 mL). The aqueous layer was extracted with EtOAc (3x15 mL) and the combined organic layers were washed with brine, dried over $MgSO_4$ and the solvent removed under reduced pressure. The crude product was carried directly through to the azide. To that end, the crude product was dissolved in DMSO (5 mL) and NaN_3 (191 mg, 2.94 mmol, 5.0 eq) was added. The solution was heated to 100°C for 4 h and allowed to cool to rt. Water (50 mL) was added and the aqueous layer was extracted with Et_2O (3 x 20 mL) and the combined organic extracts were washed with brine, dried over $MgSO_4$ and the solvent evaporated *in vacuo*. The crude product was purified by flash chromatography (9:1 Hexanes/EtOAc) providing 126 mg of **51** as a clear, light yellow oil in 88% yield. ^{1}H NMR: δ 1.89-2.01 (m, 1H), 2.46-2.62 (m, 3H), 3.54-3.63 (m, 1H), 4.01-4.09 (m, 1H), 4.96-5.05 (m, 2H), 5.48-5.61 (m, 1H), 7.27-7.35 (m, 5H); ^{13}C NMR: 41.9, 44.5, 54.4, 69.4, 86.0, 118.7, 126.1, 126.3, 127.3, 128.3, 133.5; HRMS (ESI) calcd for $[C_{13}H_{16}N_4O + Na]^+$: 267.1222, found: 267.1230.
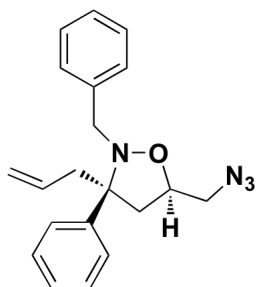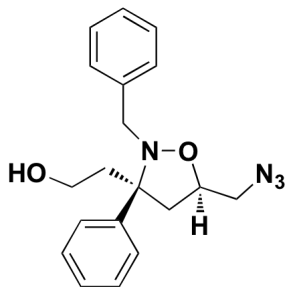

((3S,5R)-3-allyl-5-(azidomethyl)-2-benzyl-3-phenylisoxazolidine) (52): To a solution of **51** (100 mg, .41 mmol, 1.0 eq) in DMF (5 mL) was added benzyl bromide (107 µL,

0.9 mmol, 2.2 eq), and *i*Pr$_2$NEt (151 μL, 0.9 mmol, 2.2 eq). The reaction mixture was heated in a microwave at 20% power for 15 s and allowed to cool to rt. This was repeated 20 times. Water (15 mL) and ether (15 mL) were added followed by aqueous workup. The combined organic layers were washed with brine (20 mL) and purified by flash chromatography (99:1 Hexanes, EtOAc) providing 107 mg of **52** in 78% yield as a clear, light yellow oil. ^{1}H NMR: δ 2.38-2.45 (m, 2H), 2.64-2.73 (m, 1H), 2.77 (dd, 2H, *J* = 8.1, 12.7), 3.10-3.20 (m, 1H), 3.40-3.54 (m, 1H), 4.25-4.37 (m, 2H), 5.00-5.11 (m, 2H), 5.61-5.75 (m, 1H), 7.08-7.39 (m, 8H), 7.43-7.55 (m, 2H); ^{13}C NMR: 38.1, 41.0, 63.4, 76.4, 80.6, 84.1, 117.5, 126.7, 128.1, 128.8, 129.0, 130.6, 135.4, 135.7, 136.9, 139.3; HRMS (ESI) calcd for [C$_{20}$H$_{22}$N$_4$O+H]+: 335.1872, found: 335.1881.
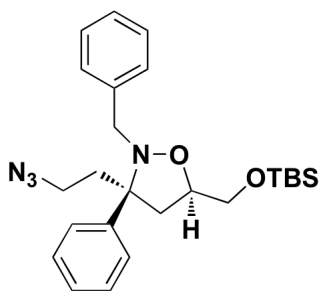

(3-((3*S*,5*R*)-5-(azidomethyl)-2-benzyl-3-phenylisoxazolidin-3-yl)propane-1,2-diol) (56): To a solution of **52** (670 mg, 2 mmol, 1 eq) and NMO (346 mg, 3 mmol, 1.5 eq) in *t*BuOH/THF/H$_2$O (22 mL, 4:1:0.5) and cooled in an ice-water bath was added OsO$_4$ (51 mg as 2.3 mL of a 2.5% solution in 2-propanol, 0.2 mmol, 0.1 eq) dropwise over 5 minutes and the reaction was allowed to come to rt with stirring for 12h. To quench the reaction, sat. aqueous Na$_2$S$_2$O$_4$ (5 mL) was added and the mixture stirred at rt for 1h. Sat. NH$_4$Cl (5 mL) was added and the aqueous layer was extracted with EtOAc (3 x 30 mL) and the combined organic extracts were washed with brine (50 mL) and dried over MgSO$_4$. The product was isolated by flash chromatography (7:3 Hex/EtOAc) providing 735 mg of **56** as a clear oil in 99% yield. ^{1}H NMR: δ 1.44-1.62 (m, 2H), 1.94-2.39 (m, 2H), 3.40-3.81 (m, 4H), 3.95-4.32 (m, 4H), 7.22-7.41 (m, 8H), 7.61-7.68 (m, 2H); HRMS (ESI) calcd for [C$_{20}$H$_{24}$N$_4$O$_3$ + Na]+: 391.1746, found: 391.1751.
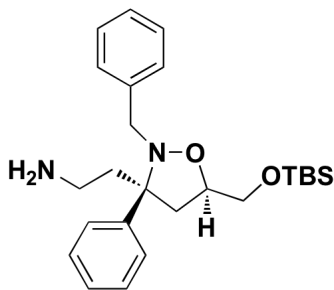
(2-((3S,5R)-5-(azidomethyl)-2-benzyl-3-phenylisoxazolidin-3-yl)ethanol)
(59): To a solution of **56** (735 mg, 2 mmol, 1 eq) in ACN/H_2O (40 mL, 1:1) was added $NaIO_4$ (1.28g, 6 mmol, 3 eq). The reaction was stirred at rt for 3h at which point water (20 mL) was added and the aqueous layer was extracted with Et_2O (3 x 20 mL) and the combined organic extracts were dried over $MgSO_4$ and the solvent removed *in vacuo*. The crude aldehyde was dissolved in MeOH (20 mL) and $NaBH_4$ (84 mg, 2.2 mmol, 1.1 eq) was added. The reaction stirred at rt for 1h at which point water (30 mL) was added to the reaction and the reaction mixture was extracted with Et_2O (3 x 50 mL). The organic extracts were dried over $MgSO_4$ and the solvent removed *in vacuo*. The product was isolated by flash chromatography (8:2 Hex/EtOAc) to provide 440 mg of **59** as a clear oil in 65% yield. ^1H NMR: δ 1.40-1.69 (m, 3H), 1.91-2.01 (m, 1H), 2.06 (dd, 1H, *J* = 8.1, 12.7), 2.36 (dd, 1H, *J* = 8.0, 12.7), 3.41 (d, 2H, *J* = 4.7), 3.64-3.83 (m, 3H), 3.99 (d, 1H, *J* = 13.9), 4.19-4.28 (m, 1H), 7.22-7.49 (m, 8H) 7.61-7.68 (m, 2H); ^{13}C NMR: δ, 35.6, 40.8, 43.0, 53.7 54.5, 56.3, 69.7, 127.2, 128.4, 128.6, 135.4, 135.7, 136.9, 137.6, 139.3; HRMS (ESI) calcd for $[C_{19}H_{22}N_4O_2 + Na]^+$: 361.1640, found: 361.1648.
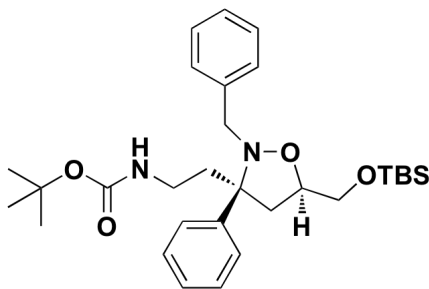

((3S,5R)-3-(2-azidoethyl)-2-benzyl-5-(((*tert*-butyldimethylsilyl)oxy)methyl)-3-phenylisoxazolidine) (66): **66** was prepared from the corresponding alcohol **17**
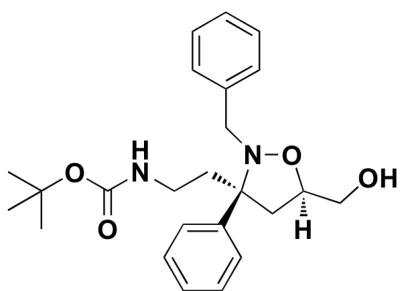
as previously described for **51**. Purification by flash chromatography (9:1 Hex/EtOAc) provided 55mg of **66** in 98% yield. ^{1}H NMR: δ 0.98 (s, 9H), 0.06 (s, 6H), 1.91-2.01 (m, 1H), 2.06 (dd, 1H, J = 8.1, 12.7), 2.12-2.30 (m, 4H), 2.36 (dd, 1H, J = 8.0, 12.7), 3.41 (d, 2H, J = 4.7), 3.94 (d, 1H, J = 13.9), 4.13-4.20 (m, 1H), 7.22-7.49 (m, 8H) 7.61-7.68 (m, 2H); ^{13}C NMR: δ -5.6, -5.5, 25.8, 38.1, 39.4, 40.8, 42.5, 43.0, 54.5, 69.7, 70.4, 127.2, 128.1, 128.2, 128.4, 128.6, 135.4, 135.7, 136.9, 137.6, 139.3; HRMS (ESI) calcd for $[C_{25}H_{36}N_4O_2Si + Na]^+$: 475.2505, found: 475.2513.


(2-((3*S*,5*R*)-2-benzyl-5-(((*tert*-butyldimethylsilyl)oxy)methyl)-3-phenylisoxazolidin-3-yl)ethanamine) (61): Reduction of azide **66** occurred as previously described for **12**. Acid, base, workup provided 24 mg of **61** in 49% yield. ^{1}H NMR: δ 0.98 (s, 9H), 0.06 (s, 6H), 1.70-1.79 (m, 2H), 1.91-2.01 (m, 1H), 2.06 (dd, 1H, J = 8.1, 12.7), 2.12-2.18 (m, 2H), 2.36 (dd, 1H, J = 8.0, 12.7), 3.41 (d, 2H, J = 4.7), 3.94 (d, 1H, J = 13.9), 4.13-4.20 (m, 1H), 5.04-5.10 (bs, 2H), 7.22-7.49 (m, 8H) 7.61-7.68 (m, 2H); ^{13}C NMR: δ -5.6, -5.5, 25.8, 35.6, 38.1, 39.4, 40.8, 43.0, 54.5, 69.7, 70.4, 127.2, 128.1, 128.2, 128.4, 128.6, 135.4, 135.7, 136.9, 137.6, 139.3; HRMS (ESI) calcd for $[C_{25}H_{38}N_2O_2Si + Na]^+$: 449.2600, found: 449.2611.

(*tert*-butyl (2-((3*S*,5*R*)-2-benzyl-5-(((*tert*-butyldimethylsilyl)oxy)methyl)-3-phenylisoxazolidin-3-yl)ethyl)carbamate) (62): To a solution of **61** (24 mg, 0.06 mmol, 1.0 eq) in MeOH (1.2 mL) and Et$_3$N (17 μL, 0.12 mmol, 2.0 eq) was added Boc$_2$O (26 mg, 0.12 mmol, 2.0 eq). The reaction was stirred for 4 h at rt. Water (3 mL) was added and the aqueous layer was extracted with EtOAc (3 x 10 mL). The combined organic extracts were dried over MgSO$_4$ and the solvent removed in vacuo. The residue was dissolved in MeOH and the product was isolated by flash chromatography (95:5 CH$_2$Cl$_2$/MeOH) to provide 19 mg of **62** in 81% yield. ^{1}H NMR: δ 0.06 (s, 6H), 0.98 (s, 9H), 1.45 (s, 9H), 1.70-1.78 (m, 2H), 1.92-2.01 (m, 1H), 2.06 (dd, 1H, *J* = 8.1, 12.7), 2.14-2.20 (m, 2H), 2.36 (dd, 1H, *J* = 8.0, 12.7), 3.41 (d, 2H, *J* = 4.7), 3.94 (d, 1H, *J* = 13.9), 4.13-4.20 (m, 1H), 7.22-7.49 (m, 8H) 7.61-7.68 (m, 2H); ^{13}C NMR: δ -5.6, -5.5, 25.8, 30.1, 35.6, 38.1, 39.4, 40.8, 43.0, 54.5, 69.7, 70.4, 79.7, 127.2, 128.1, 128.2, 128.4, 128.6, 135.4, 135.7, 136.9, 137.6, 139.3, 155.1; HRMS (ESI) calcd for [C$_{30}$H$_{46}$N$_2$O$_4$Si + Na]$^+$: 541.3125, found: 541.3146.


(*tert*-butyl (2-((3*S*,5*R*)-2-benzyl-5-(hydroxymethyl)-3-phenylisoxazolidin-3-yl)ethyl)carbamate) (63): Silyl deprotection occurred as was previously described for **50**. Purification by flash chromatography (9:1 CH$_2$Cl$_2$/MeOH) provided 14 mg of **63** in 99% yield. ^{1}H NMR: δ 1.45 (s, 9H), 1.70-1.78 (m, 2H), 1.92-2.01 (m, 1H), 2.06 (dd, 1H, *J* = 8.1, 12.7), 2.14-2.20 (m, 2H), 2.38 (dd, 1H, *J* = 8.0, 12.7), 3.43 (d, 2H, *J* = 4.7), 3.94 (d, 1H, *J* = 13.9), 4.13-4.20 (m, 1H), 7.22-7.49 (m, 8H) 7.61-7.68 (m, 2H); ^{13}C NMR: δ 30.1, 35.6, 38.1, 39.4, 40.8, 43.0, 54.5, 69.7, 70.4, 79.7, 127.2, 128.1, 128.2, 128.4, 128.6, 135.4, 135.7, 136.9, 137.6, 139.3, 155.1; HRMS (ESI) calcd for [C$_{24}$H$_{32}$N$_2$O$_4$ + Na]$^+$: 435.2260, found: 435.2282.
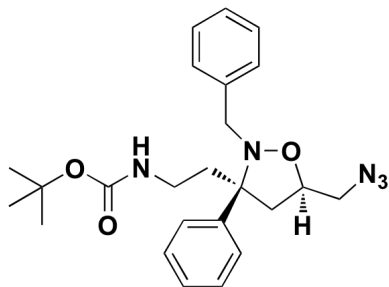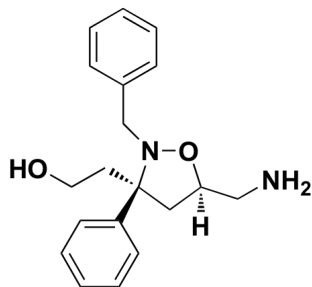
(*tert*-butyl (2-((3*S*,5*R*)-5-(azidomethyl)-2-benzyl-3-phenylisoxazolidin-3-yl)ethyl)carbamate) (64): Azide **64** was prepared as previously described for **51**. Purification by flash chromatography provided 31 mg of **64** in 84% yield. ^{1}H NMR: δ 1.45 (s, 9H), 1.58-1.63 (m, 2H), 1.70-1.78 (m, 2H), 1.92-2.01 (m, 1H), 2.06-2.11 (m, 1H), 2.14-2.20 (m, 2H), 2.38-2.44 (m, 2H), 3.24-3.31 (m, 1H), 3.90 (m, 1H), 7.22-7.49 (m, 8H) 7.61-7.68 (m, 2H); ^{13}C NMR: δ 30.1, 35.6, 38.1, 39.4, 40.8, 43.0, 45.7, 54.5, 70.4, 79.7, 127.2, 128.1, 128.2, 128.4, 128.6, 135.4, 135.7, 136.9, 137.6, 139.3, 155.1; HRMS (ESI) calcd for $[C_{24}H_{31}N_5O_3 + Na]^+$: 460.2325, found: 460.2332.
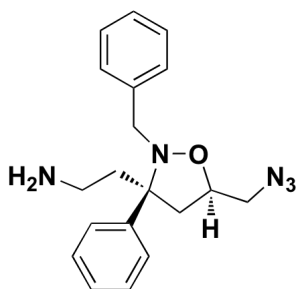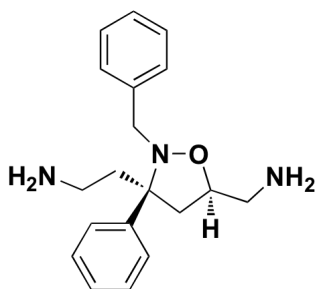

2-((3*S*,5*R*)-5-(azidomethyl)-2-benzyl-3-phenylisoxazolidin-3-yl)ethanamine (65): **64** (30 mg, 0.069 mmol) was dissolved in TFA/CH_2Cl_2/H_2O (2 mL, 1:1:0.1) and stirred at rt for 30 min. Acid, base workup yielded 20 mg of **65** in 86% yield as a clear oil. ^{1}H NMR: δ 1.66-1.73 (m, 3H), 1.91-2.01 (m, 1H), 2.06 (dd, 1H, *J* = 8.1, 12.7), 2.12-2.21 (m, 4H), 3.78-3.93 (m, 2H), 5.02-5.09 (bs, 2H), 7.21-7.49 (m, 8H) 7.60-7.69 (m, 2H); ^{13}C NMR: δ, 35.6, 36.7, 40.8, 41.6, 43.0, 69.7, 70.4, 127.2, 128.4, 128.6, 135.4, 135.7, 136.9, 137.6, 139.3; HRMS (ESI) calcd for $[C_{19}H_{23}N_5O + Na]^+$: 360.1800, found: 360.1808.

(2-((3*S*,5*R*)-5-(aminomethyl)-2-benzyl-3-phenylisoxazolidin-3-yl)ethanol)

(66): Azide **59** was reduced as described previously for **12** (PPh$_3$, THF/H$_2$O, reflux). Acid, base workup provided 4.5 mg of amine **66** in 87% percent yield as a waxy oil. ^{1}H NMR (CD$_3$OD): δ 1.70-1.79 (m, 3H), 1.91-2.01 (m, 1H), 2.06 (dd, 1H, *J* = 8.1, 12.7), 3.68-3.89 (m, 5H), 3.93-3.98 (m, 2H), 5.00-5.11 (bs, 2H), 7.21-7.49 (m, 8H) 7.60-7.69 (m, 2H); ^{13}C NMR: δ 36.6, 36.9, 40.4, 43.2, 55.4, 69.7, 70.4, 127.1, 128.2, 128.6, 135.4, 135.7, 136.9, 137.6, 139.3; HRMS (ESI) calcd for [C$_{19}$H$_{24}$NO$_2$ + Na]$^+$: 335.1735, found: 335.1744.


2-((3*S*,5*R*)-5-(aminomethyl)-2-benzyl-3-phenylisoxazolidin-3-yl)ethanamine

(67): To a solution of **65** (10 mg, 0.03 mmol, 1.0 eq) in THF/H$_2$O (2 mL, 1:1) was added PPh$_3$ (23 mg, 0.089 mmol, 3.0 eq). The reaction was heated to 80°C for 4h then cooled to rt. Acid, base, workup give 5.3 mg of **67** as a waxy oil in 62% yield. ^{1}H NMR (CD$_3$OD): δ 1.70-1.79 (m, 3H), 1.91-2.01 (m, 1H), 2.06 (dd, 1H, *J* = 8.1, 12.7), 2.20-2.34 (m, 4H), 3.78-3.93 (m, 2H), 5.02-5.13 (bs, 4H), 7.21-7.49 (m, 8H) 7.60-7.69 (m, 2H); ^{13}C NMR: δ, 35.6, 36.7, 36.9, 40.8, 43.0, 69.7, 70.4, 127.2, 128.4, 128.6, 135.4, 135.7, 136.9, 137.6, 139.3; HRMS (ESI) calcd for [C$_{19}$H$_{25}$N$_3$O + Na]$^+$: 334.1895, found: 334.1904.
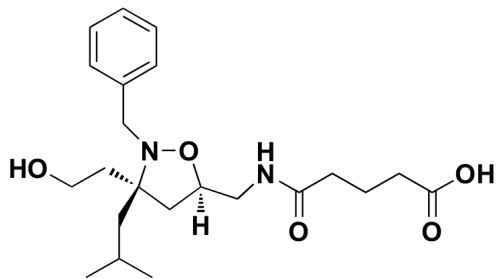
(5-(((((3S,5R)-2-benzyl-3-(2-hydroxyethyl)-3-isobutylisoxazolidin-5-yl)methyl)amino)-5-oxopentanoic acid) (68): To a solution of **18** (20 mg, 49 μmol, 1.0 eq) in CH₂Cl₂ (5 mL) was added DMAP (1.2 mg, 10 μmol, 0.2 eq) and Et₃N (27 μL, 196 μmol, 4.0 eq). The reaction mixture was cooled in an ice-water bath and glutaric anhydride (12 mg, 99 μmol, 2.0 eq) was added. The reaction stirred for 8h while warming to rt. Aqueous acetic acid (2 mL 1:1) was added and the biphasic reaction was allowed to stir for 20 minutes at rt. Acid, base, workup yielded crude product which was purified by flash chromatography (8.5:1:0.5 EtOAc/Hex/AcOH) providing 17 mg of **68** in 83% yield. ¹H NMR: δ 0.97 (s, 3H), 1.00 (d, 3H, J = 6.8), 1.39 (dd, 1H, J = 6.1, 14.4), 1.62 (dd, 1H, J = 5.4, 14.2), 1.68-1.74 (m, 2H), 1.80-1.90 (m, 2H), 1.95 (dd, 1H, J = 6.3, 12.6), 2.37-2.42 (m, 1H), 2.44 (dd, 1H, J = 8.8, 12.7), 2.51-2.57 (m, 2H), 2.85 (s, 2H), 2.98 (s, 2H), 3.28 (dd, 1H, J = 6.3, 13.7), 3.33 (dd, 1H, J = 4.9, 13.7), 3.80-3.90 (m, 3H), 4.10-4.15 (m, 1H), 7.18-7.37 (m, 5H); HRMS (ESI) calcd for [C₂₂H₃₄N₂O₅ + Na]⁺: 429.2365, found: 429.2372.
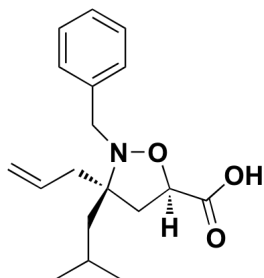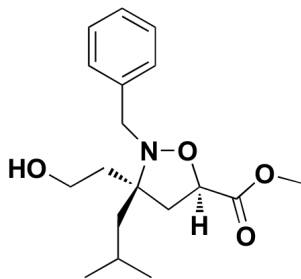

((3S,5R)-3-allyl-2-benzyl-3-isobutylisoxazolidine-5-carboxylic acid) (41): To a solution of **40** (50 mg, 0.17 mmol, 1.0 eq) in acetone (1.7 mL) cooled in an ice-water bath was added Jones reagent (105 μL) and the reaction was stirred for 4h while coming to rt. Isopropanol (2 mL) was added until the color of the solution changed

from dark orange to light green. The solvent was removed *in vacuo* and the residue was suspended in methanol. The product was isolated by flash chromatography (90:9:1 EtOAc/MeOH/AcOH) providing 32 mg of **41** in 62% yield. IR: 3388, 2956, 2930, 2870, 1699, 1445, 1346 cm^{-1}; ^{1}H NMR: δ 0.89 (d, 3H, J = 6.3), 0.95 (d, 3H, J = 6.6), 1.70-1.76 (m, 2H), 1.82-1.86 (m, 1H), 2.18-2.32 (dd, 2H, J = 12.0, 8.8), 2.48-2.53 (m, 1H), 2.60-2.64 (m, 1H), 4.69 (t, 1H, J = 7.7), 3.28 (dd, 1H, J = 6.3, 13.7), 3.33 (dd, 1H, J = 4.9, 13.7), 4.96-5.05 (m, 2H), 5.48-5.61 (m, 1H), 7.18-7.37 (m, 5H); ^{13}C NMR: δ 23.9, 24.0, 24.6, 45.0, 46.5, 65.1, 67.1, 74.7, 117.8, 126.67 128.0, 128.1, 134.9, 138.6, 155.8; HRMS (ESI) calcd for [C$_{18}$H$_{25}$NO$_3$ + Na]$^+$: 326.1732, found: 326.1740.
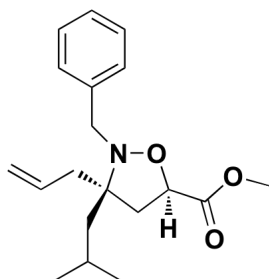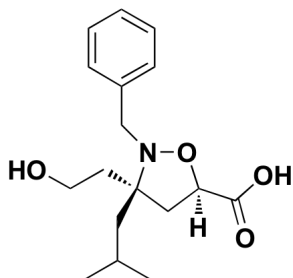

((3*S*,5*R*)-methyl 3-allyl-2-benzyl-3-isobutylisoxazolidine-5-carboxylate) (42):
To a solution of **41** (20 mg, 66 μmol, 1.0 eq) in THF (10 mL) and K$_2$CO$_3$ (45.6 mg, 330 μmol, 5.0 eq) was added. The heterogeneous mixture stirred for 30 minutes then iodomethane (4.1 μL, 66 μmol, 1.0 eq) was added. The reaction mixture stirred at rt for 2h. Water (10 mL) was added and the aqueous layer was extracted with Et$_2$O (3 x 10 mL) and the combined organic extracts were dried over MgSO$_4$ and the solvent removed *in vacuo*. The residue was dissolved in CH$_2$Cl$_2$ and the product isolated by flash chromatography (8:2 Hex/EtOAc) to give 18.6 mg of **42** in 89% yield. IR: 3388, 2956, 2930, 2870, 1699, 1346 cm^{-1}; ^{1}H NMR: δ 0.89 (d, 3H, J = 6.3), 0.95 (d, 3H, J = 6.6), 1.70-1.76 (m, 2H), 1.82-1.86 (m, 1H), 2.18-2.32 (dd, 2H, J = 12.0, 8.8), 2.48-2.53 (m, 1H), 2.60-2.64 (m, 1H), 3.61 (s, 3H), 4.69 (m, 1H), 3.28-3.34 (m, 2H), 4.96-5.05 (m, 2H), 5.48-5.61 (m, 1H), 7.18-7.37 (m, 5H); ^{13}C NMR: δ 23.9, 24.0, 24.6, 45.0, 46.5, 51.1, 65.1, 67.1, 74.7, 117.8, 126.67 128.0, 128.1, 134.9, 138.6, 155.8; HRMS (ESI) calcd for [C$_{19}$H$_{27}$NO$_3$ + Na]$^+$: 340.1889, found: 340.1894.
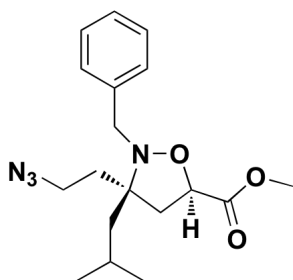
((3*S*,5*R*)-methyl 2-benzyl-3-(2-hydroxyethyl)-3-isobutylisoxazolidine-5-carboxylate) (43): To a solution of **42** (150 mg, .47 mmol, 1.0 eq) and NMO (83 mg, .071 mmol, 1.5 eq) in *t*BuOH/THF/H$_2$O (11 mL, 4:1:0.5) cooled in an ice-water bath was added OsO$_4$ (480 μL of a 2.5% wt solution in 2-propanol, 0.047 mmol, 0.1 eq) dropwise over 5 minutes and the reaction was allowed to come to rt with stirring for 12h. To quench the reaction, saturated aqueous Na$_2$S$_2$O$_4$ (2 mL) was added and the mixture stirred at rt for 1h. Sat. NH$_4$Cl (2 mL) was added and the aqueous layer was extracted with EtOAc (3 x 20 mL) and the combined organic extracts were washed with brine (20 mL) and dried over MgSO$_4$. The solvent was removed *in vacuo* and the crude diol was dissolved in ACN/H$_2$O (20 mL, 1:1) and NaIO$_4$ (302 mg, 1.41 mmol, 3.0 eq) was added. The reaction was stirred at rt for 4h at which point water (20 mL) was added and the aqueous layer was extracted with Et$_2$O (3 x 20 mL) and the combined organic extracts were dried over MgSO$_4$ and the solvent removed *in vacuo*. The crude aldehyde was dissolved in MeOH (20 mL) and NaBH$_4$ (21 mg, .564 mmol, 1.2 eq) was added. The reaction stirred at rt for 1h at which point TLC analysis indicated the reaction was complete. Water (20 mL) was added to the reaction and the reaction mixture was extracted with Et$_2$O (3 x 20 mL). The organic extracts were dried over MgSO$_4$ and the solvent removed *in vacuo*. The product was isolated by flash chromatography (7:3 Hex/EtOAc) providing 130 mg of **43** in 86% yield as a clear oil. IR: 3388, 2956, 2930, 2870, 2100, 1699, 1456, 1346 1045 cm^{-1}; ^{1}H NMR: δ 0.89 (d, 3H, J = 6.3), 0.95 (d, 3H, J = 6.6), 1.70-1.76 (m, 2H), 1.82-1.86 (m, 1H), 2.18-2.32 (dd, 2H, J = 12.0, 8.8), 2.48-2.53 (m, 1H), 2.60-2.64 (m, 1H), 2.06 (dd, 1H, *J* = 8.1, 12.7), 2.36 (dd, 1H, *J* = 8.0, 12.7), 3.41 (d, 2H, *J* = 4.7), 3.61 (s, 3H), 4.69 (m, 1H), 7.18-7.37 (m, 5H); ^{13}C NMR: δ 23.9, 24.0, 24.6, 40.1, 45.0, 46.5,

51.1, 65.1, 67.1, 74.7, 128.0, 128.1, 134.9, 138.6, 155.8; HRMS (ESI) calcd for [$C_{18}H_{27}NO_4$ + Na]$^+$: 344.1838, found: 344.1848.
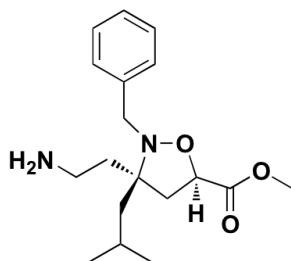

((3*S*,5*R*)-2-benzyl-3-(2-hydroxyethyl)-3-isobutylisoxazolidine-5-carboxylic acid) (44): To a solution of **43** (50 mg, .155 mmol, 1.0 eq) in THF/H_2O (5 mL, 1:1) was added LiOH (37 mg, 1.55 mmol, 10 eq). The reaction was heated to 80°C for 2h at which point TLC analysis indicated the reaction was complete. Acid, base, workup yielded crude product that was further purified by flash chromatography (90:9:1 EtOAc/MeOH/AcOH) providing 46 mg of **44** in 96% yield. IR: 3388, 2956, 2930, 2870, 1699, 1448, 1442, 1346 cm^{-1}; ^{1}H NMR: δ 0.89 (d, 3H, J = 6.3), 0.95 (d, 3H, J = 6.6), 1.70-1.76 (m, 2H), 1.82-1.86 (m, 1H), 2.18-2.32 (dd, 2H, J = 12.0, 8.8), 2.45-2.51 (m, 1H), 2.60-2.64 (m, 1H), 2.03 (dd, 1H, *J* = 8.1, 12.7), 2.33 (dd, 1H, *J* = 8.0, 12.7), 3.47 (d, 2H, *J* = 4.7), 4.75 (m, 1H), 7.18-7.37 (m, 5H); ^{13}C NMR: δ 23.9, 24.0, 24.6, 40.0, 45.0, 46.5, 65.3, 67.0, 74.9, 128.0, 128.1, 134.9, 138.6, 155.8; HRMS (ESI) calcd for [$C_{17}H_{25}NO_4$ + Na]$^+$: 330.1681, found: 330.1689.
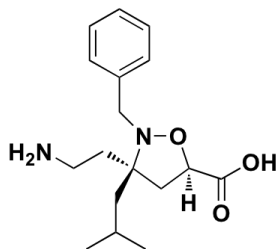

(3*S*,5*R*)-methyl 3-(2-azidoethyl)-2-benzyl-3-isobutylisoxazolidine-5-carboxylate (45): To a solution of **44** (100 mg, .311 mmol, 1.0 eq) in THF (5 mL) was added dry PPh$_3$ (245 mg, .933 mmol, 3.0 eq) followed by DEAD (408 μL of a

40% wt solution in THF, .933 mmol, 3.0 eq) dropwise. The reaction was cooled in an ice-water bath and DPPA (201 μL, .933 mmol, 3.0 eq) was added dropwise over 10 minutes. The reaction was allowed to warm to rt over 2h at which point water (5 mL) was added to the reaction mixture. The aqueous layer was extracted with Et_2O (3 x 10 mL) and the combined organic extracts were dried over $MgSO_4$ and the solvent removed *in vacuo*. The crude product was dissolved in EtOAc and purified by flash chromatography (1:1 Hex/EtOAc) providing 99 mg of **45** in 92% yield. ^1H NMR: δ 0.89 (d, 3H, J = 6.3), 0.95 (d, 3H, J = 6.6), 1.62 (d, 2H, *J* = 4.7), 1.70-1.76 (m, 2H), 1.82-1.86 (m, 1H), 2.06 (dd, 1H, *J* = 8.1, 12.7), 2.18-2.32 (dd, 2H, J = 12.0, 8.8), 2.36 (dd, 1H, *J* = 8.0, 12.7), 2.40-2.45 (m, 1H), 2.58-2.63 (m, 1H), 3.61 (s, 3H), 4.69 (m, 1H), 7.18-7.37 (m, 5H); ^{13}C NMR: δ 23.9, 24.0, 24.6, 34.7, 45.0, 46.5, 51.1, 58.2, 67.1, 74.7, 128.0, 128.1, 134.9, 138.6, 155.8; HRMS (ESI) calcd for $[C_{18}H_{26}N_4O_3 + Na]^+$: 369.1903, found: 369.1909.

((3*S*,5*R*)-methyl 3-(2-aminoethyl)-2-benzyl-3-isobutylisoxazolidine-5-carboxylate) (46): To a solution of **45** (20 mg, .058 mmol, 1.0 eq) in THF/H_2O (4 mL, 1:1) was added PPh_3 (45 mg, .173 mmol, 3.0 eq). The reaction mixture was heated to 80°C for 2h and cooled to rt. Acid, base, workup provided 16 mg of **46** in 88% yield. ^1H NMR (CD_3OD): δ 0.89 (d, 3H, J = 6.3), 0.95 (d, 3H, J = 6.6), 1.70-1.76 (m, 2H), 1.82-1.86 (m, 1H), 2.06 (dd, 1H, *J* = 8.1, 12.7), 2.18-2.32 (dd, 2H, J = 12.0, 8.8), 2.36 (dd, 1H, *J* = 8.0, 12.7), 2.40-2.45 (m, 1H), 2.58-2.63 (m, 1H), 2.72 (d, 2H, *J* = 4.7), 3.61 (s, 3H), 4.69 (m, 1H), 5.14 (bs, 2H), 7.18-7.37 (m, 5H); ^{13}C NMR: δ 23.9, 24.0, 24.6, 32.9, 45.0, 45.5, 51.1, 58.2, 67.1, 74.7, 128.1, 128.2, 135.0, 138.7, 154.9; HRMS (ESI) calcd for $[C_{18}H_{28}N_2O_3 + Na]^+$: 343.1998, found: 343.1999.
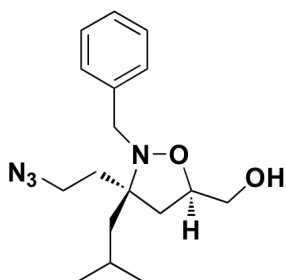
((3*S*,5*R*)-3-(2-aminoethyl)-2-benzyl-3-isobutylisoxazolidine-5-carboxylic acid) (47): To a solution of **46** (5 mg, .016 mmol, 1.0 eq) in THF/H_2O (2 mL, 1:1) was added LiOH (4 mg, .156 mmol, 10.0 eq). The reaction was heated to 80°C for 2h then the solvent was removed *in vacuo*. The residue was suspended in ACN/0.1% TFA, filtered and purified by reverse phase HPLC to give 2.9 mg of **47** as the TFA salt in 62% yield. ^{1}H NMR (CD$_3$OD): δ 0.89 (m, 3H), 0.95 (m, 3H), 1.70-1.76 (m, 2H), 1.82-1.86 (m, 1H), 2.06 (dd, 1H, *J* = 8.1, 12.7), 2.18-2.34 (m, 2H), 2.35 (dd, 1H, *J* = 8.0, 12.7), 2.40-2.45 (m, 1H), 2.58-2.63 (m, 1H), 2.72 (d, 2H, *J* = 4.7), 4.64 (m, 1H), 5.15 (bs, 2H), 7.18-7.37 (m, 5H); ^{13}C NMR: δ 23.9, 24.0, 24.6, 32.9, 45.0, 45.5, 58.2, 67.1, 74.7, 128.1, 128.2, 135.0, 138.7, 156.9; HRMS (ESI) calcd for [$C_{17}H_{26}N_2O_3$ + Na]$^+$: 329.1841, found: 329.1848.
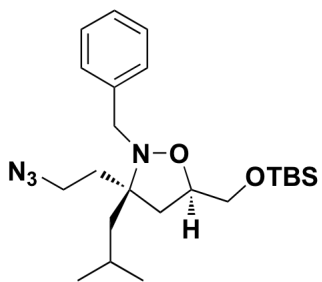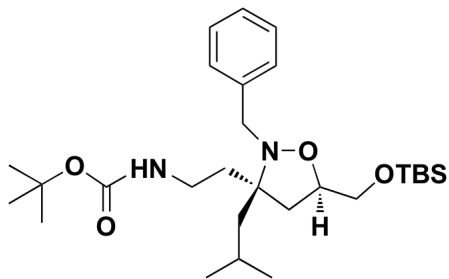

((3*S*,5*R*)-3-(2-azidoethyl)-2-benzyl-5-(((*tert*-butyldimethylsilyl)oxy)methyl)-3-isobutylisoxazolidine) (69): To a solution of **32** (75 mg, 0.18 mmol, 1.0 eq) and PPh$_3$ (145 mg, 0.55 mmol, 3.0 eq) in THF (10 mL) cooled in an ice-water bath was added DEAD (96 mg, 0.55 mmol, 3.0 eq) dropwise followed by dropwise addition of DPPA (240 μL of a 40% wt solution in THF, 0.55 mmol, 3.0 eq). The reaction was allowed to warm to rt and was stirred for 4 h. Water (20 mL) and EtOAc (20 mL) was added and the aqueous layer was extracted with EtOAc (3 x 20 mL). Combined

143

organic extracts were washed with brine (20 mL). Purification by flash chromatography (9:1-8:2 Hex/EtOAc) afforded 47 mg of **69** as a clear yellow oil in 60% yield. IR: 2952, 2855, 1454, 1360, 1253, 1119, 835 cm^{-1}; ^{1}H NMR: δ 0.09 (s, 6H), 0.90 (s, 9H), 1.00 (s, 3H), 1.02 (s, 3H), 1.50-1.60 (m, 1H), 1.64-1.95 (m, 5H), 2.06 (dd, 1H, *J* = 8.1, 12.7), 2.36 (dd, 1H, *J* = 8.0, 12.7), 3.38 (d, 2H, *J* = 4.7), 3.65-3.82 (m, 2H), 4.01 (d, 1H, *J* = 13.9), 4.20-4.30 (m, 1H), 7.22-7.37 (m, 5H); ^{13}C NMR: -5.5, -5.4, 18.2, 24.1, 24.5, 25.1, 25.8, 38.8, 39.5, 40.2, 43.5, 53.6, 62.4, 76.4, 126.6, 128.1, 128.3, 135.4, 139.3; HRMS (ESI) calcd for [C$_{23}$H$_{40}$N$_4$O$_2$Si + H]$^+$: 433.2999, found 433.3010.
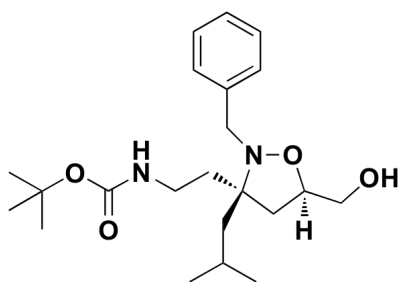

(((3*S*,5*R*)-3-(2-azidoethyl)-2-benzyl-3-isobutylisoxazolidin-5-yl)methanol) (70): To a solution of **69** (20 mg, .046 mmol, 1.0 eq) in THF (10 mL) cooled in an ice-water bath was added TBAF (185 µL, .185 mmol, 4.0 eq) drop wise and the mixture was stirred for 2 h. Sat. aq. NH$_4$Cl (3 mL) was added followed by aqueous workup. Purification by flash chromatography (1:1 EtOAc/Hex) gave 14 mg of **70** in 97% yield as a clear, light yellow oil. IR: 3352, 2952, 2855, 1454, 1360, 1253, 1119, 835 cm^{-1}; ^{1}H NMR: δ 1.01 (s, 3H), 1.04 (s, 3H), 1.50-1.60 (m, 1H), 1.64-1.95 (m, 5H), 2.06 (dd, 1H, *J* = 8.1, 12.7), 2.34-2.38 (m, 1H), 3.35 (d, 2H, *J* = 4.7), 3.79-3.91 (m, 2H), 4.12 (d, 1H, *J* = 13.9), 4.22-4.28 (m, 1H), 7.22-7.37 (m, 5H); ^{13}C NMR; 18.2, 24.1, 24.5, 25.1, 39.5, 40.2, 43.5, 53.6, 62.4, 76.4, 126.6, 126.8, 128.3, 128.4, 139.3; HRMS (ESI) calcd for [C$_{17}$H$_{26}$N$_4$O$_2$ + H]$^+$: 319.2134, found: 319.2122.
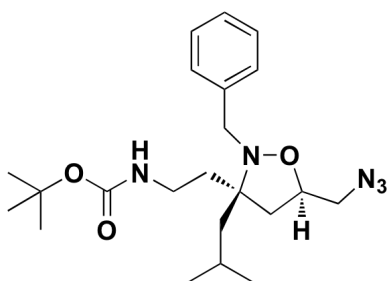
(**_tert_-butyl (2-((3_S_,5_R_)-2-benzyl-5-(((_tert_-butyldimethylsilyl)oxy)methyl)-3-isobutylisoxazolidin-3-yl)ethyl)carbamate) (71)**: A solution of **69** (55 mg, 0.12 mmol, 1.0 eq) and PPh₃ (97 mg, 0.37 mmol, 3.0 eq) in THF/H₂O (5 mL, 1:1) was heated at 80°C for 4 h. Acid, base workup yielded the crude amine which was carried on to the next step without further purification. Towards this, the amine was dissolved in MeOH (1.2 mL) and Et₃N (17 μL, 0.12 mmol, 2.0 eq) and Boc₂O (26.2 mg, 0.12 mmol, 2.0 eq) were added. The reaction stirred at rt for 6 h. Water (3 mL) and Et₂O (5 mL) were added. The aqueous layer was extracted with Et₂O (3 x 10 mL), the combined organic extracts were washed with brine (10 mL). Flash chromatography (95:5 Hex/EtOAc) afforded **71** in 80% as 19 mg of a clear light yellow oil. ¹H NMR: δ 0.06 (s, 6H), 0.98 (s, 9H), 1.00 (d, 3H, J = 6.6), 1.02 (d, 3H, J = 6.3), 1.36-1.60 (m, 10H), 1.65-1.90 (m, 6H), 2.05-2.12 (m, 2H), 2.24-2.32 (m, 2H), 2.68-2.74 (m, 2H), 2.89-2.93 (m, 2H), 7.22-7.42 (m, 5H); ¹³C NMR: δ -5.6, -5.5, 24.3, 24.9, 25.2, 25.8, 28.3, 30.1, 35.4, 38.1, 39.5, 40.8, 43.0, 53.7, 54.5, 65.3, 70.4, 80.1, 127.2, 128.4, 128.6, 137.6, 159.9; HRMS (ESI) calcd for [C₂₈H₅₀N₂O₄Si + Na]⁺: 529.3438, found: 529.3447.
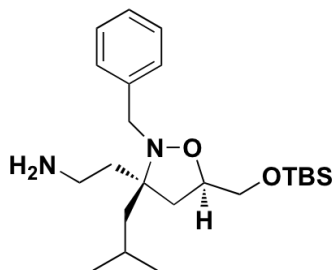

(**_tert_-butyl (2-((3_S_,5_R_)-2-benzyl-5-(hydroxymethyl)-3-isobutylisoxazolidin-3-yl)ethyl)carbamate) (35)**: To a solution of **71** (19 mg, .037 mmol, 1.0 eq) in THF (3
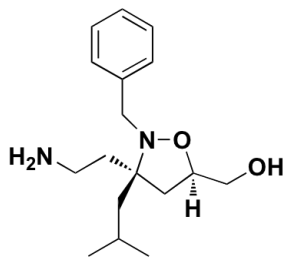
mL) cooled in an ice-water bath was added TBAF (150 μL of a 1.0M solution in THF, .15 mmol, 4.0 eq) drop wise and the reaction was allowed to warm to rt. After 2 h, sat. aq. NH$_4$Cl (1 mL) was added, followed by aqueous workup. Flash chromatography (9:1 Hex/EtOAc) provided 14 mg of **35** in 96% yield. ^{1}H NMR: δ 1.00 (d, 3H, J = 6.3), 1.02 (d, 3H, J = 6.6), 1.39-1.57 (m, 10H), 1.62-1.90 (m, 6H), 2.05-2.12 (m, 2H), 2.24-2.32 (m, 2H), 2.68-2.74 (m, 2H), 2.89-2.93 (m, 2H), 7.22-7.42 (m, 5H); ^{13}C NMR: δ 24.3, 24.9, 25.2, 28.3, 34.9, 40.8, 43.0, 53.7, 54.5, 65.3, 70.4, 80.1, 127.2, 128.4, 128.6, 137.6, 159.9; HRMS (ESI) calcd for [C$_{22}$H$_{36}$N$_2$O$_4$ + Na]$^+$: 415.2573, found: 415.2586.

(***tert*-butyl (2-((3*S*,5*R*)-5-(azidomethyl)-2-benzyl-3-isobutylisoxazolidin-3-yl)ethyl)carbamate) (37)**: To a solution of **35** (28.8 mg, 73 μmol, 1.0 eq) and Et$_3$N (11 μL, 77 μmol, 1.05 eq) in CH$_2$Cl$_2$ (1 mL) cooled in an ice-water bath was added Methanesulfonyl chloride (6 μL, 77 μmol, 1.05 eq) and the reaction was allowed to warm to rt. An aqueous workup was conducted after 2 h and the crude product was dissolved in DMSO (3.5 mL). NaN$_3$ (45 mg, 0.68 mmol, 10.0 eq) was added and the reaction was heated at 100°C for 2 h. Aqueous workup followed by flash chromatography (95:5 Hex/EtOAc) gave 24 mg of **35** in 86% yield as a clear yellow oil. ^{1}H NMR: δ 1.00 (d, 3H, J = 6.3), 1.02 (d, 3H, J = 6.6), 1.39-1.57 (m, 12H), 1.62-1.69 (m, 1H), 1.71-1.96 (m, 1H), 2.05-2.16 (m, 1H), 2.22-2.34 (m, 1H), 3.22-2.39 (m, 2H), 3.58-3.72 (m, 2H), 3.80-3.95 (m, 2H), 4.16-4.19 (m, 1H), 7.21-7.42 (m, 5H); ^{13}C NMR: δ 24.3, 24.9, 25.2, 28.3, 34.9, 35.6, 40.8, 43.0, 53.7, 54.5, 70.4, 80.1, 127.2, 128.4, 128.6, 137.6, 159.9; HRMS (ESI) calcd for [C$_{22}$H$_{35}$N$_5$O$_3$ + Na]$^+$: 440.2638, found: 440.2645.

(2-((3*S*,5*R*)-2-benzyl-5-(((*tert*-butyldimethylsilyl)oxy)methyl)-3-isobutylisoxazolidin-3-yl)ethanamine) (33): To a solution of **71** (20 mg, 0.046 mmol, 1.0 eq) in THF/H_2O (4 mL, 1:1) was added PPh_3 (36 mg, .139 mmol, 3.0 eq). The reaction was heated to 80°C for 4h then cooled to rt. The solvent was removed *in vacuo* and the product was isolated by flash chromatography (9:1:1 EtOAc/MeOH/ET3N) to give 16 mg of **33** in 84% yield. ^{1}H NMR: δ 0.09 (s, 6H), 0.90 (s, 9H), 1.00 (d, 3H, J = 6.3), 1.02 (d, 3H, J = 6.6), 1.50-1.60 (m, 1H), 1.64-1.95 (m, 5H), 2.06 (dd, 1H, *J* = 8.1, 12.7), 2.36 (dd, 1H, *J* = 8.0, 12.7), 2.49-2.66 (m, 4H), 4.05-4.15 (m, 3H), 5.08 (bs, 4H), 7.20-7.39 (m, 5H); ^{13}C NMR: -5.5, -5.4, 18.2, 24.1, 24.5, 25.1, 25.8, 38.8, 39.5, 40.2, 43.5, 45.9, 53.6, 76.4, 126.6, 128.1, 128.3, 135.4, 139.3;HRMS (ESI) calcd for $[C_{23}H_{42}N_2O_2Si + Na]^+$: 429.2913, found: 429.2902.

((3*S*,5*R*)-3-(2-aminoethyl)-2-benzyl-3-isobutylisoxazolidin-5-yl)methanol (36): **35** (10 mg, .024 mmol, 1.0 eq) was dissolved in THF (1 mL) and cooled in an ice-water bath. TBAF (98 μL of a 1.0M solution in THF, .098 mmol, 4.0 eq) was added drop wise and the reaction was allowed to warm to rt. After 4h, acid, base workup gave 4 mg of **36** in 61% yield. ^{1}H NMR (CD_3OD): δ 1.00 (s, 3H), 1.02 (s, 3H), 1.50-1.60 (m, 1H), 1.64-1.95 (m, 5H), 2.06 (dd, 1H, *J* = 8.1, 12.7), 2.36 (dd, 1H, *J* = 8.0, 12.7), 2.49-2.56 (m, 2H), 3.65-3.82 (m, 2H), 4.05 (d, 1H, *J* = 13.9), 4.21-4.30 (m, 1H),

5.10 (bs, 2H), 7.24-7.39 (m, 5H); ^{13}C NMR: 18.2, 24.1, 24.4, 25.7, 39.4, 43.4, 46.7, 53.7, 68.2, 76.4, 117.5, 126.7, 128.1, 128.2, 135.3, 138.9; HRMS (ESI) calcd for [$C_{17}H_{28}N_2O_2$ + Na]$^+$: 315.2048, found: 315.2040.
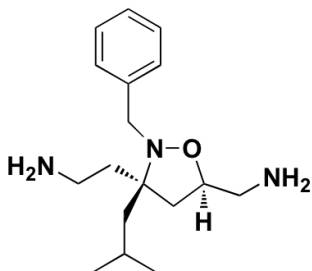

(2-((3S,5R)-5-(aminomethyl)-2-benzyl-3-isobutylisoxazolidin-3-yl) ethanamine) (39): To a solution of **37** (20 mg, .048 mmol, 1.0 eq) in THF/H_2O (5 mL, 1:1) was added PPh$_3$ (38 mg, .145 mmol, 3.0 eq). The reaction was heated to 80°C for 4h and allowed to cool to rt. Acid, base, workup yielded the crude amine which was dissolved in TFA:TIPS:H_2O (2 mL, 95:2.5:2.5) and stirred at rt for 1h. The Solvent was blown off with N_2 and the residue was dissolved in ACN/H_2O (1 mL, 1:1) and the product isolated by reverse phase HPLC to provide 6 mg of **39** in 41% yield. ^{1}H NMR (CD$_3$OD): δ 0.94 (d, 3H, J = 6.6), 0.94 (d, 3H, J = 6.6), 1.31-1.35 (m, 1H), 1.59 (m, 1H), 1.81-1.94 (m, 2H), 1.90-1.96 (m, 1H), 2.20 (dd, 1H, J = 12.0, 8.8), 2.22-2.47 (m, 2H), 2.82-2.95 (m, 4H), 3.79-3.85 (m, 2H), 5.12 (bs, 4H), 7.15-7.40 (m, 5H); ^{13}C NMR: 18.2, 24.1, 24.6, 25.8, 34.7, 39.4, 43.4, 45.9, 68.2, 76.4, 117.5, 126.7, 128.1, 128.2, 135.4, 139.3; HRMS (ESI) calcd for [$C_{17}H_{29}N_3O$ + Na]$^+$: 314.2208, found: 314.2212.

J. Appendix of Selected ¹H NMR Spectra and HPLC Traces

151
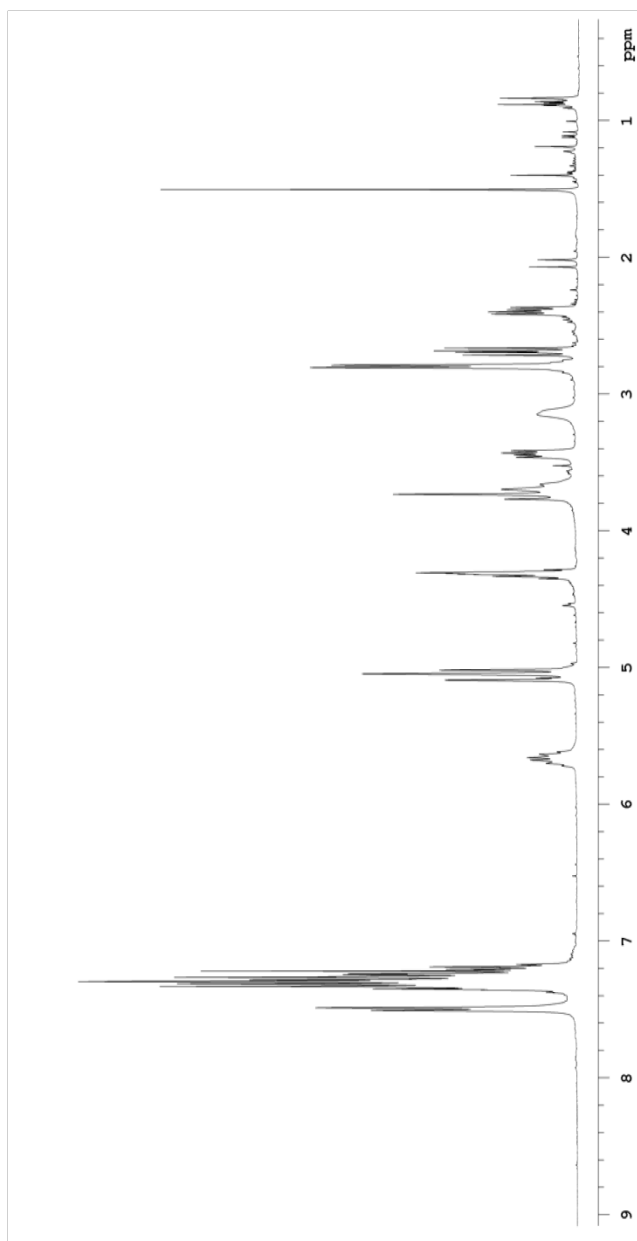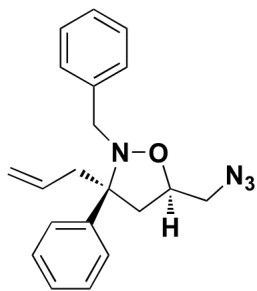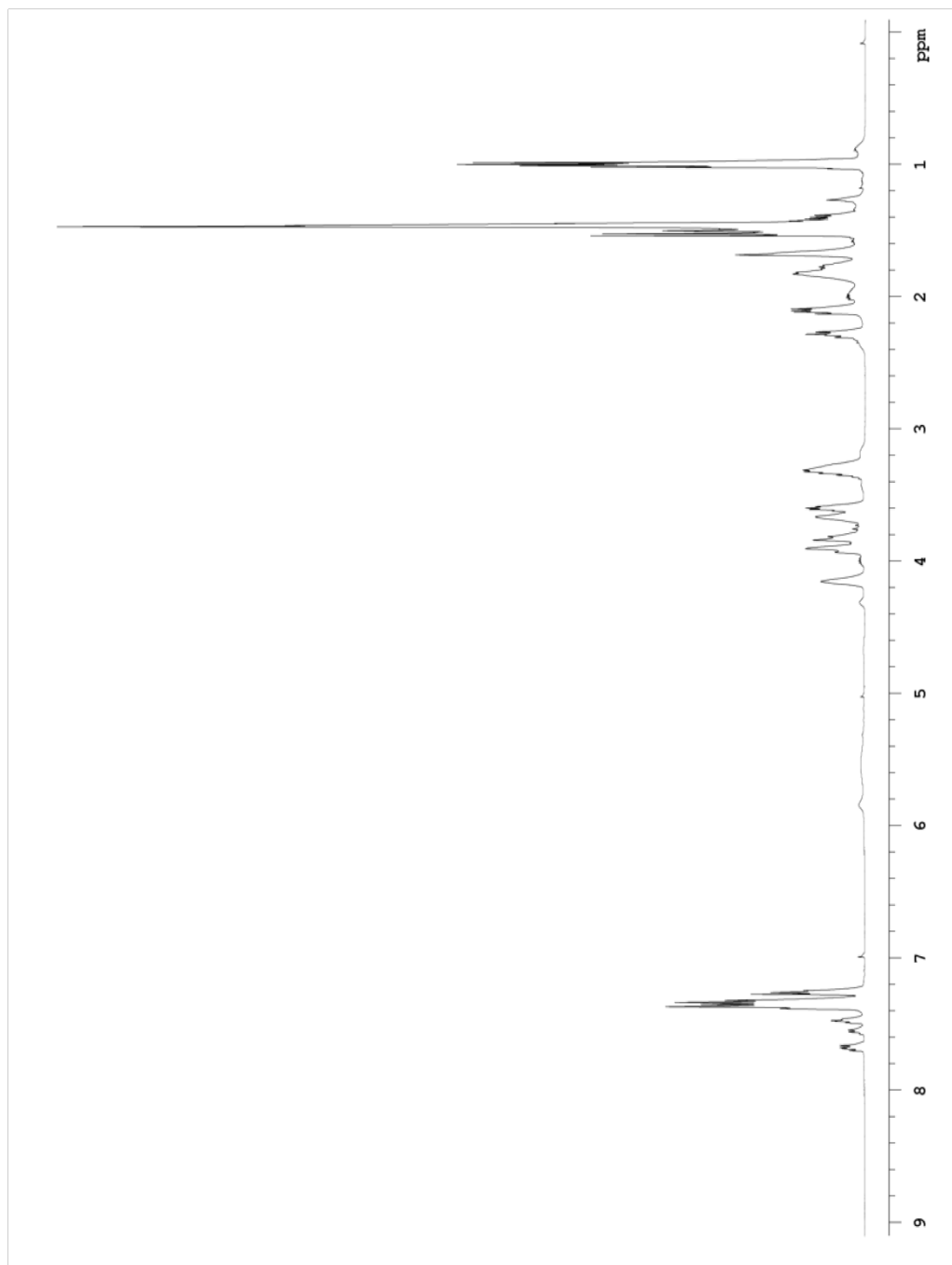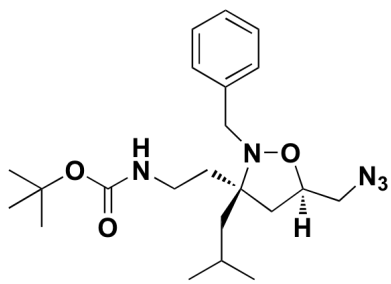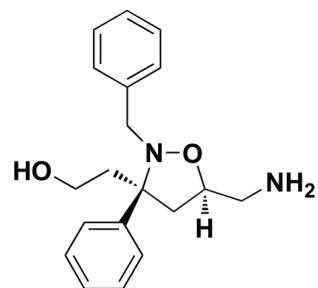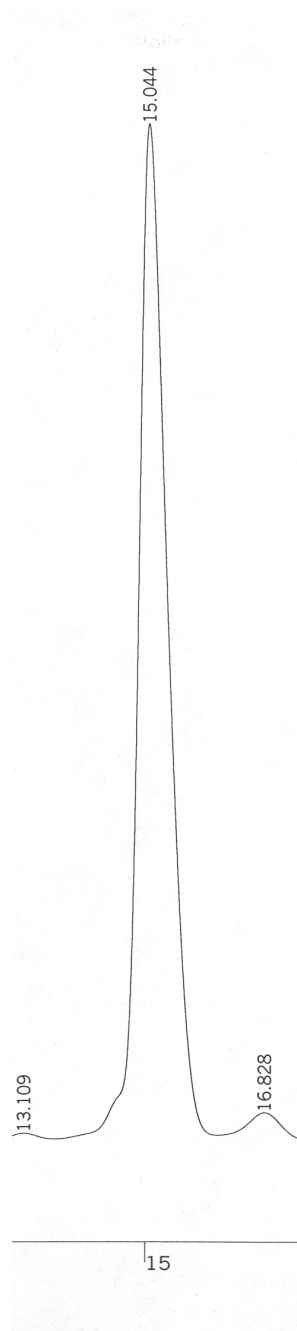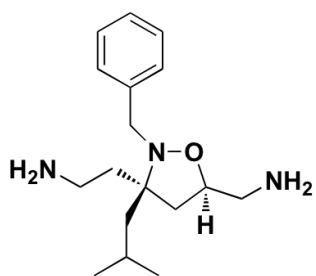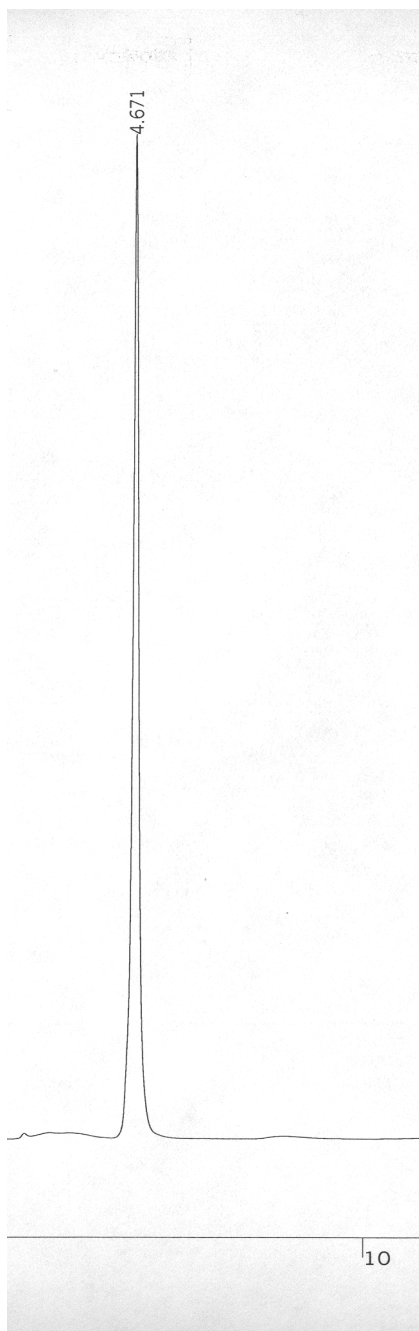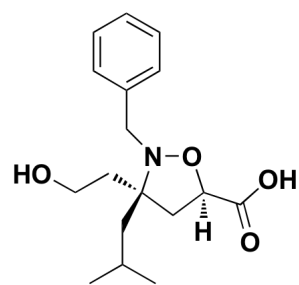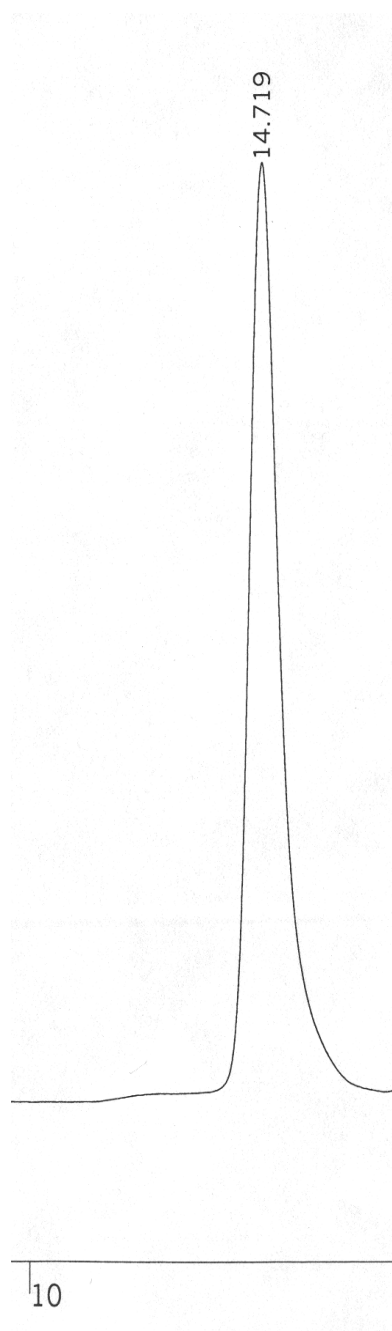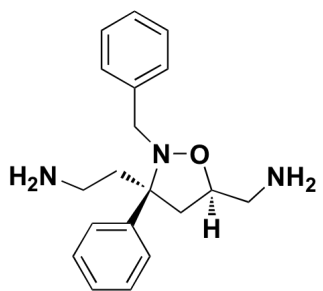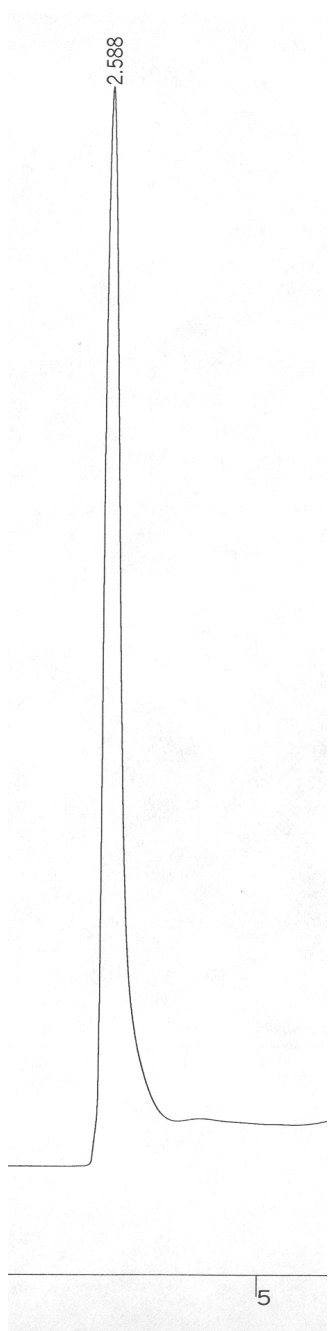
K. References

1.   Cochran, A. G., Antagonists of protein-protein interactions. *Chemistry & Biology* **2000,** *7* (4), R85-R94.

2.   DeLano, W. L.; Ultsch, M. H.; de Vos, A. M.; Wells, J. A., Convergent solutions to binding at a protein-protein interface. *Science* **2000,** *287* (5456), 1279-1283.

3.   Berg, T., Modulation of protein-protein interactions with small organic molecules. *Angewandte Chemie-International Edition* **2003,** *42* (22), 2462-2481.

4.   Arkin, M. R.; Wells, J. A., Small-molecule inhibitors of protein-protein interactions: Progressing towards the dream. *Nature Reviews Drug Discovery* **2004,** *3* (4), 301-317.

5.   Pagliaro, L.; Felding, J.; Audouze, K.; Nielsen, S. J.; Terry, R. B.; Krog-Jensen, C.; Butcher, S., Emerging classes of protein-protein interaction inhibitors and new tools for their development. *Current Opinion in Chemical Biology* **2004,** *8* (4), 442-449.

6.   Stockwell, B. R., Exploring biology with small organic molecules. *Nature* **2004,** *432* (7019), 846-854.

7.   Arkin, M., Protein-protein interactions and cancer: small molecules going in for the kill. *Current Opinion in Chemical Biology* **2005,** *9* (3), 317-324.

8.   Fletcher, S.; Hamilton, A. D., Protein surface recognition and proteomimetics: mimics of protein surface structure and function. *Curr Opin Chem Biol* **2005,** *9* (6), 632-8.

9.   Yin, H.; Hamilton, A. D., Strategies for targeting protein-protein interactions with synthetic agents. *Angew Chem Int Ed Engl* **2005,** *44* (27), 4130-63.

10.   Yin, H.; Lee, G. I.; Sedey, K. A.; Kutzki, O.; Park, H. S.; Omer, B. P.; Ernst, J. T.; Wang, H. G.; Sebti, S. M.; Hamilton, A. D., Terphenyl-based bak BH3 alpha-helical proteomimetics as low-molecular-weight antagonists of Bcl-X-L. *J Am Chem Soc* **2005,** *127* (29), 10191-10196.

11.   Fletcher, S.; Hamilton, A. D., Targeting protein-protein interactions by rational design: mimicry of protein surfaces. *J R Soc Interface* **2006,** *3* (7), 215-33.

12.   Murray, J. K.; Gellman, S. H., Targeting protein-protein interactions: Lessons from p53/MDM2. *Biopolymers* **2007,** *88* (5), 657-686.

13.   Vassilev, L. T., MDM2 inhibitors for cancer therapy. *Trends Mol Med* **2007,** *13* (1), 23-31.

14.   Lee, G. M.; Craik, C. S., Trapping Moving Targets with Small Molecules. *Science* **2009,** *324* (5924), 213-215.

15.   Vassilev, L. T.; Vu, B. T.; Graves, B.; Carvajal, D.; Podlaski, F.; Filipovic, Z.; Kong, N.; Kammlott, U.; Lukacs, C.; Klein, C.; Fotouhi, N.; Liu, E. A., In vivo activation of the p53 pathway by small-molecule antagonists of MDM2. *Science* **2004,** *303* (5659), 844-8.

16.   Oltersdorf, T.; Elmore, S. W.; Shoemaker, A. R.; Armstrong, R. C.; Augeri, D. J.; Belli, B. A.; Bruncko, M.; Deckwerth, T. L.; Dinges, J.; Hajduk, P. J.; Joseph, M. K.; Kitada, S.; Korsmeyer, S. J.; Kunzer, A. R.; Letai, A.; Li, C.; Mitten, M. J.; Nettesheim, D. G.; Ng, S.; Nimmer, P. M.; O'Connor, J. M.; Oleksijew, A.; Petros, A. M.; Reed, J. C.; Shen, W.; Tahir, S. K.; Thompson, C. B.; Tomaselli, K. J.; Wang, B.; Wendt, M. D.; Zhang, H.; Fesik, S. W.; Rosenberg, S. H., An inhibitor of Bcl-2 family proteins induces regression of solid tumours. *Nature* **2005,** *435* (7042), 677-81.

17.   Kussie, P. H.; Gorina, S.; Marechal, V.; Elenbaas, B.; Moreau, J.; Levine, A. J.; Pavletich, N. P., Structure of the MDM2 oncoprotein bound to the p53 tumor suppressor transactivation domain. *Science* **1996,** *274* (5289), 948-953.

18.   Vogelstein, B.; Lane, D.; Levine, A. J., Surfing the p53 network. *Nature* **2000,** *408* (6810), 307-10.

19.   Malkin, D., The role of p53 in human cancer. *J Neurooncol* **2001,** *51* (3), 231-43.

20.   Walensky, L. D.; Kung, A. L.; Escher, I.; Malia, T. J.; Barbuto, S.; Wright, R. D.; Wagner, G.; Verdine, G. L.; Korsmeyer, S. J., Activation of apoptosis in vivo by a hydrocarbon-stapled BH3 helix. *Science* **2004,** *305* (5689), 1466-70.

21.   Walensky, L. D.; Pitter, K.; Morash, J.; Oh, K. J.; Barbuto, S.; Fisher, J.; Smith, E.; Verdine, G. L.; Korsmeyer, S. J., A stapled BID BH3 helix directly binds and activates BAX. *Mol Cell* **2006,** *24* (2), 199-210.

22.   Verdine, G. L.; Walensky, L. D., The challenge of drugging undruggable targets in cancer: lessons learned from targeting BCL-2 family members. *Clin Cancer Res* **2007,** *13* (24), 7264-70.

23.   Green, M.; Ishino, M.; Loewenstein, P. M., Mutational analysis of HIV-1 Tat minimal domain peptides: identification of trans-dominant mutants that suppress HIV-LTR-driven gene expression. *Cell* **1989,** *58* (1), 215-23.

24.   Song, C. Z.; Loewenstein, P. M.; Green, M., Transcriptional activation in vitro by the human immunodeficiency virus type 1 Tat protein: evidence for specific interaction with a coactivator(s). *Proc Natl Acad Sci U S A* **1994,** *91* (20), 9357-61.

25.   Verhoef, K.; Koper, M.; Berkhout, B., Determination of the minimal amount of Tat activity required for human immunodeficiency virus type 1 replication. *Virology* **1997,** *237* (2), 228-36.

26.   Deng, L.; Ammosova, T.; Pumfery, A.; Kashanchi, F.; Nekhai, S., HIV-1 Tat interaction with RNA polymerase II C-terminal domain (CTD) and a dynamic association with CDK2 induce CTD phosphorylation and transcription from HIV-1 promoter. *J Biol Chem* **2002,** *277* (37), 33922-9.

27.   Goren, I.; Semmes, O. J.; Jeang, K. T.; Moelling, K., The amino terminus of Tax is required for interaction with the cyclic AMP response element binding protein. *J Virol* **1995,** *69* (9), 5806-11.

28.   Semmes, O. J.; Jeang, K. T., Definition of a minimal activation domain in human T-cell leukemia virus type I Tax. *J Virol* **1995,** *69* (3), 1827-33.

29.   Georges, S. A.; Giebler, H. A.; Cole, P. A.; Luger, K.; Laybourn, P. J.; Nyborg, J. K., Tax recruitment of CBP/p300, via the KIX domain, reveals a potent requirement for acetyltransferase activity that is chromatin dependent and histone tail independent. *Mol Cell Biol* **2003,** *23* (10), 3392-404.

30.   Negrini, M.; Cuneo, A.; Nakamura, T.; Baffa, R.; Sabbioni, S.; Alder, H.; Castoldi, G.; Croce, C. M., A Novel T(9-11)(P22-Q23) with All-1 Gene Rearrangement Associated with Progression of a Myeloproliferative Disorder to Acute Myeloid-Leukemia. *Cancer Genetics and Cytogenetics* **1995,** *83* (1), 65-70.

31.   Karin, M.; Liu, Z. G.; Zandi, E., AP-1 function and regulation. *Current Opinion in Cell Biology* **1997,** *9* (2), 240-246.

32.   Hanson, R. D.; Yu, B. D.; Hess, J.; Korsmeyer, S. J., The mixed lineage leukemia gene (MLL), a mammalian homologue of Trithorax, functions to maintain Hox expression and regulate both homeosis and segmentation. *Blood* **1997,** *90* (10), 184-184.

33.   Yu, B. D.; Hanson, R. D.; Hess, J. L.; Horning, S. E.; Korsmeyer, S. J., MLL, a mammalian trithorax-group gene, functions as a transcriptional maintenance factor in morphogenesis. *P Natl Acad Sci USA* **1998,** *95* (18), 10632-10636.

34.   Milne, T.; Briggs, S.; Brock, H.; Gibbs, D.; Allis, C. D.; Hess, J. L., The mixed lineage leukemia protein (MLL) targets SET domain methyltransferase activity to Hox gene promoters. *Blood* **2002,** *100* (11), 137A-137A.

35.   Milne, T. A.; Briggs, S. D.; Brock, H. W.; Martin, M. E.; Gibbs, D.; Allis, C. D.; Hess, J. L., MLL targets SET domain methyltransferase activity to Hox gene promoters. *Mol Cell* **2002,** *10* (5), 1107-1117.

36.   Ayton, P. M.; Cleary, M. L., Transformation of myeloid progenitors by MLL oncoproteins is dependent on Hoxa7 and Hoxa9. *Gene Dev* **2003,** *17* (18), 2298-2307.

37.   Zeisig, B. B.; Milne, T.; Garcia-Cuellar, M. P.; Schreiner, S.; Martin, M. E.; Fuchs, U.; Borkhardt, A.; Chanda, S. K.; Walker, J.; Soden, R.; Hess, J. L.; Slany, R. K., Hoxa9 and Mei7 are key targets for MLL-ENL-mediated cellular immortalization. *Mol Cell Biol* **2004,** *24* (2), 617-628.

38.   Milne, T. A.; Dou, Y. L.; Martin, M. E.; Brock, H. W.; Roeder, R. G.; Hess, J. L., MLL associates specifically with a subset of transcriptionally active target genes. *P Natl Acad Sci USA* **2005,** *102* (41), 14765-14770.

39.   Schraets, D.; Lehmann, T.; Dingermann, T.; Marschalek, R., MLL-mediated transcriptional gene regulation investigated by gene expression profiling. *Oncogene* **2003,** *22* (23), 3655-3668.

40.   Li, Z. Y.; Liu, D. P.; Liang, C. C., New insight into the molecular mechanisms of MLL-associated leukemia. *Leukemia* **2005,** *19* (2), 183-190.

41.   O'neil, J.; Look, A. T., Mechanisms of transcription factor deregulation in lymphoid cell transformation. *Oncogene* **2007,** *26* (47), 6838-6849.

42.   Li, Z.; Luo, R. T.; Mi, S.; Sun, M.; Chen, P.; Bao, J.; Neilly, M. B.; Jayathilaka, N.; Johnson, D. S.; Wang, L.; Lavau, C.; Zhang, Y.; Tseng, C.; Zhang, X.; Wang, J.; Yu, J.; Yang, H.; Wang, S. M.; Rowley, J. D.; Chen, J.; Thirman, M. J., Consistent deregulation of gene expression between human and murine MLL rearrangement leukemias. *Cancer Res* **2009,** *69* (3), 1109-16.

43.   Ernst, P.; Wang, J.; Huang, M.; Goodman, R. H.; Korsmeyer, S. J., MLL and CREB bind cooperatively to the nuclear coactivator CREB-binding protein. *Mol Cell Biol* **2001,** *21* (7), 2249-2258.

44.   Goto, N. K.; Zor, T.; Martinez-Yamout, M.; Dyson, H. J.; Wright, P. E., Cooperativity in transcription factor binding to the coactivator CREB-binding protein (CBP). The mixed lineage leukemia protein (MLL) activation domain binds to an allosteric site on the KIX domain. *J Biol Chem* **2002,** *277* (45), 43168-74.

45.   Vendel, A. C.; Lumb, K. J., NMR mapping of the HIV-1 Tat interaction surface of the KIX domain of the human coactivator CBP. *Biochemistry-Us* **2004,** *43* (4), 904-8.

46.   Ramirez, J. A.; Nyborg, J. K., Molecular characterization of HTLV-1 Tax interaction with the KIX domain of CBP/p300. *J Mol Biol* **2007,** *372* (4), 958-69.

47.   Vendel, A. C.; McBryant, S. J.; Lumb, K. J., KIX-mediated assembly of the CBP-CREB-HTLV-1 tax coactivator-activator complex. *Biochemistry-Us* **2003,** *42* (43), 12481-7.

48.	Alefantis, T.; Mostoller, K.; Jain, P.; Harhaj, E.; Grant, C.; Wigdahl, B., Secretion of the human T cell leukemia virus type I transactivator protein Tax. *J Biol Chem* **2005,** *280* (17), 17353-17362.

49.	Timothy R. Geiger, N. S., Young-Mi Kim, Jennifer K. Nyborg, The Human T-Cell Leukemia Virus Type 1 Tax Protein Confers CBP/p300 Recruitment and Transcriptional Activation Properties to Phosphorylated CREB. *Mol Cell Biol* **2008,** *28* (4), 10.

50.	Bannister, A. J.; Oehler, T.; Wilhelm, D.; Angel, P.; Kouzarides, T., Stimulation of c-Jun activity by CBP: c-Jun residues Ser63/73 are required for CBP induced stimulation in vivo and CBP binding in vitro. *Oncogene* **1995,** *11* (12), 2509-2514.

51.	Wisdom, R., AP-1: One switch for many signals. *Experimental Cell Research* **1999,** *253* (1), 180-185.

52.	Grondin, B.; Lefrancois, M.; Tremblay, M.; Saint-Denis, M.; Haman, A.; Waga, K.; Bedard, A.; Tenen, D. G.; Hoang, T., c-Jun homodimers can function as a context-specific coactivator. *Mol Cell Biol* **2007,** *27* (8), 2919-2933.

53.	Tsai, L. N.; Ku, T. K. S.; Salib, N. K.; Crowe, D. L., Extracellular signals regulate rapid coactivator recruitment at AP-1 sites by altered phosphorylation of both CREB binding protein and c-jun. *Mol Cell Biol* **2008,** *28* (13), 4240-4250.

54.	Daschner, P. J.; Ciolino, H. P.; Plouzek, C. A.; Yeh, G. C., Increased AP-1 activity in drug resistant human breast cancer MCF-7 cells. *Breast Cancer Research and Treatment* **1999,** *53* (3), 229-240.

55.	Schreiber, M.; Kolbus, A.; Piu, F.; Szabowski, A.; Mohle-Steinlein, U.; Tian, J. M.; Karin, M.; Angel, P.; Wagner, E. F., Control of cell cycle progression by c-Jun is p53 dependent. *Gene Dev* **1999,** *13* (5), 607-619.

56.	Smith, L. M.; Wise, S. C.; Hendricks, D. T.; Sabichi, A. L.; Bos, T.; Reddy, P.; Brown, P. H.; Birrer, M. J., cJun overexpression in MCF-7 breast cancer cells produces a tumorigenic, invasive and hormone resistant phenotype. *Oncogene* **1999,** *18* (44), 6063-6070.

57.	Wisdom, R.; Johnson, R. S.; Moore, C., c-Jun regulates cell cycle progression and apoptosis by distinct mechanisms. *Embo J* **1999,** *18* (1), 188-197.

58.	Bakiri, L.; Lallemand, D.; Bossy-Wetzel, E.; Yaniv, M., Cell cycle-dependent variations in c-Jun and JunB phosphorylation: a role in the control of cyclin D1 expression. *Embo J* **2000,** *19* (9), 2056-2068.

59.	Zhang, Y.; Pu, X. Y.; Shi, M.; Chen, L. Y.; Song, Y. H.; Qian, L.; Yuan, G. G.; Zhang, H.; Yu, M.; Hu, M. R.; Shen, B. F.; Guo, N., Critical role of c-Jun overexpression in liver metastasis of human breast cancer xenograft model. *Bmc Cancer* **2007,** *7*, -.

60.   Albanese, C.; D'Amico, M.; Reutens, A. T.; Fu, M.; Watanabe, G.; Lee, R. J.; Kitsis, R. N.; Henglein, B.; Avantaggiati, M.; Somasundaram, K.; Thimmapaya, B.; Pestell, R. G., Activation of the cyclin D1 gene by the E1A-associated protein p300 through AP-1 inhibits cellular apoptosis. *J Biol Chem* **1999,** *274* (48), 34186-95.

61.   Siegert, J. L.; Rushton, J. J.; Sellers, W. R.; Kaelin, W. G., Jr.; Robbins, P. D., Cyclin D1 suppresses retinoblastoma protein-mediated inhibition of TAFII250 kinase activity. *Oncogene* **2000,** *19* (50), 5703-11.

62.   Kim, J. K.; Diehl, J. A., Nuclear cyclin D1: an oncogenic driver in human cancer. *J Cell Physiol* **2009,** *220* (2), 292-6.

63.   Coller, H. A., What's taking so long? S-phase entry from quiescence versus proliferation. *Nat Rev Mol Cell Biol* **2007,** *8* (8), 667-70.

64.   Buhrlage, S. J.; Brennan, B. B.; Minter, A. R.; Mapp, A. K., Stereochemical promiscuity in artificial transcriptional activators. *J Am Chem Soc* **2005,** *127* (36), 12456-12457.

65.   Hall, D. B.; Struhl, K., The VP16 activation domain interacts with multiple transcriptional components as determined by protein-protein cross-linking in vivo. *J Biol Chem* **2002,** *277* (48), 46043-46050.

66.   Fishburn, J.; Mohibullah, N.; Hahn, S., Function of a eukaryotic transcription activator during the transcription cycle. *Mol Cell* **2005,** *18* (3), 369-378.

67.   Reeves, W. M.; Hahn, S., Targets of the Gal4 transcription activator in functional transcription complexes. *Mol Cell Biol* **2005,** *25* (20), 9092-102.

68.   Radhakrishnan, I.; Perez-Alvarado, G. C.; Parker, D.; Dyson, H. J.; Montminy, M. R.; Wright, P. E., Solution structure of the KIX domain of CBP bound to the transactivation domain of CREB: a model for activator:coactivator interactions. *Cell* **1997,** *91* (6), 741-52.

69.   Campbell, K. M.; Lumb, K. J., Structurally distinct modes of recognition of the KIX domain of CBP by Jun and CREB. *Biochemistry-Us* **2002,** *41* (47), 13956-64.

70.   Minter, A. R.; Brennan, B. B.; Mapp, A. K., A small molecule transcriptional activation domain. *J Am Chem Soc* **2004,** *126* (34), 10504-10505.

71.   Casey, R. J.; Desaulniers, J. P.; Hojfeldt, J. W.; Mapp, A. K., Expanding the repertoire of small molecule transcriptional activation domains. *Bioorgan Med Chem* **2009,** *17* (3), 1034-1043.

72.   Kanemasa, S.; Nishiuchi, M.; Kamimura, A.; Hori, K., 1st Successful Metal Coordination Control in 1,3-Dipolar Cycloadditions - High-Rate Acceleration and Regiocontrol and Stereocontrol of Nitrile Oxide Cycloadditions to the Magnesium

Alkoxides of Allylic and Homoallylic Alcohols. *J Am Chem Soc* **1994,** *116* (6), 2324-2339.

73.   Bode, J. W.; Fraefel, N.; Muri, D.; Carreira, E. M., A general solution to the modular synthesis of polyketide building blocks by Kanemasa hydroxy-directed nitrile oxide cycloadditions. *Angewandte Chemie-International Edition* **2001,** *40* (11), 2082-2085.

74.   Cress, W. D.; Triezenberg, S. J., Critical Structural Elements of the Vp16 Transcriptional Activation Domain. *Science* **1991,** *251* (4989), 87-90.

75.   Ingles, C. J.; Shales, M.; Cress, W. D.; Triezenberg, S. J.; Greenblatt, J., Reduced Binding of Tfiid to Transcriptionally Compromised Mutants of Vp16. *Nature* **1991,** *351* (6327), 588-590.

76.   Triezenberg, S. J.; Cress, W. D.; Regier, J. L., Critical Role for Specific Hydrophobic Amino-Acids within the Acidic Transcriptional Activation Domain of Vp16. *Faseb J* **1991,** *5* (4), A784-A784.

77.   Regier, J. L.; Shen, F.; Triezenberg, S. J., Pattern of Aromatic and Hydrophobic Amino-Acids Critical for One of 2 Subdomains of the Vp16 Transcriptional Activator. *P Natl Acad Sci USA* **1993,** *90* (3), 883-887.

78.   Hassell, J. A.; Triezenberg, S. J.; Brinton, B.; Desjardins, P., Common Structural Elements in the Vp16 Activation Domain Mediate Interaction with Tbp and Rpa. *Journal of Cellular Biochemistry* **1994**, 31-31.

79.   Shen, F.; Triezenberg, S. J.; Hensley, P.; Porter, D.; Knutson, J. R., Critical amino acids in the transcriptional activation domain of the herpesvirus protein VP16 are solvent-exposed in highly mobile protein segments - An intrinsic fluorescence study. *J Biol Chem* **1996,** *271* (9), 4819-4826.

80.   Sullivan, S. M.; Horn, P. J.; Olson, V. A.; Koop, A. H.; Niu, W.; Ebright, R. H.; Triezenberg, S. J., Mutational analysis of a transcriptional activation region of the VP16 protein of herpes simplex virus (vol 26, pg 4487, 1998). *Nucleic Acids Research* **1998,** *26* (23), U9-U10.

81.   Drysdale, C. M.; Duenas, E.; Jackson, B. M.; Reusser, U.; Braus, G. H.; Hinnebusch, A. G., The Transcriptional Activator Gcn4 Contains Multiple Activation Domains That Are Critically Dependent on Hydrophobic Amino-Acids. *Mol Cell Biol* **1995,** *15* (3), 1220-1233.

82.   Jackson, B. M.; Drysdale, C. M.; Natarajan, K.; Hinnebusch, A. G., Identification of seven hydrophobic clusters in GCN4 making redundant contributions to transcriptional activation. *Mol Cell Biol* **1996,** *16* (10), 5557-5571.

83.   Almlof, T.; Gustafsson, J. A.; Wright, A. P. H., Role of hydrophobic amino acid clusters in the transactivation activity of the human glucocorticoid receptor. *Mol Cell Biol* **1997,** *17* (2), 934-945.

84.   IniguezLluhi, J. A.; Lou, D. Y.; Yamamoto, K. R., Three amino acid substitutions selectively disrupt the activation but not the repression function of the glucocorticoid receptor N terminus. *J Biol Chem* **1997,** *272* (7), 4149-4156.

85.   Almlof, T.; Wallberg, A. E.; Gustafsson, J. A.; Wright, A. P. H., Role of important hydrophobic amino acids in the interaction between the glucocorticoid receptor tau 1-core activation domain and target factors. *Biochemistry-Us* **1998,** *37* (26), 9586-9594.

86.   Kamei, Y.; Xu, L.; Heinzel, T.; Torchia, J.; Kurokawa, R.; Gloss, B.; Lin, S. C.; Heyman, R. A.; Rose, D. W.; Glass, C. K.; Rosenfeld, M. G., A CBP integrator complex mediates transcriptional activation and AP-1 inhibition by nuclear receptors. *Cell* **1996,** *85* (3), 403-414.

87.   Horvai, A. E.; Xu, L.; Korzus, E.; Brard, G.; Kalafus, D.; Mullen, T. M.; Rose, D. W.; Rosenfeld, M. G.; Glass, C. K., Nuclear integration of JAK/STAT and Ras/AP-1 signaling by CBP and p300. *P Natl Acad Sci USA* **1997,** *94* (4), 1074-1079.

88.   Goodman, R. H.; Smolik, S., CBP/p300 in cell growth, transformation, and development. *Genes Dev* **2000,** *14* (13), 1553-77.

89.   Chan, H. M.; La Thangue, N. B., p300/CBP proteins: HATs for transcriptional bridges and scaffolds. *Journal of Cell Science* **2001,** *114* (13), 2363-2373.

90.   Pangborn, A. B.; Giardello, M. A.; Grubbs, R. H.; Rosen, R. K.; Timmers, F. J., Safe and convenient procedure for solvent purification. *Organometallics* **1996,** *15* (5), 1518-1520.

91.   Still, W. C.; Kahn, M.; Mitra, A., Rapid Chromatographic Technique for Preparative Separations with Moderate Resolution. *J Org Chem* **1978,** *43* (14), 2923-2925.

92.   Liu, B.; Alluri, P. G.; Yu, P.; Kodadek, T., A potent transactivation domain mimic with activity in living cells. *J Am Chem Soc* **2005,** *127* (23), 8254-8255.

Chapter IV

Conclusions and Future Directions

A. Conclusions

My doctoral work focused on gaining mechanistic insight into the function of a small molecule transcriptional activation domain, iTAD **1**. Specifically, the goal was to identify key protein targets that are responsible for iTAD **1**-mediated activation, and to determine whether overlapping binding sites between small molecules and endogenous TADs affect transcriptional output. When my doctoral work began, iTAD **1** had been shown to activate transcription in HeLa cells, but there was no mechanistic information about the cellular targets of iTAD **1** responsible for this activation. Consequently, the work presented here has shown that iTAD **1** functions in a manner similar to that of natural transcriptional activators by binding the KIX domain of CBP. Furthermore, in-cell inhibition experiments and Western blotting have shown that iTAD **1** and several related molecules, block the binding of the endogenous TADs MLL and Jun to the KIX domain of CBP, resulting in decreased transcription of a Jun target gene, cyclin D1. iTAD **1** thus provides a means to block specific activator·coactivator interactions and decrease transcriptional output. Furthermore, iTAD **1**-DBD functions as a small molecule handle for recruiting CBP to other transcription factors such as the nuclear receptor family. Bifunctional constructs that feature a GR-binding terminus at one end and iTAD **1** at the other may modulate GR function in a way that is unique from existing ligands that bind GR alone.

B. Future Directions

1) Identification of Additional iTAD 1 Binding Partners *in vitro*

CBP was identified as an important target of iTAD **1**-driven gene expression through *in vitro* crosslinking experiments and in cellulo knockdown and competitive inhibition experiments. However, the crosslinking data show additional protein binding partners of iTAD-BpA, and the knockdown and competition studies decreased iTAD **1** activity, but did not result in complete abrogation of transcriptional activation. These suggest that there are other binding parters of iTAD **1** that play a role in the initiation of transcription. Furthermore, these proteins may play indirect roles in iTAD **1**-mediated activation through aiding in cellular transport or localization.

Exploration of these binding partners could be continued by performing additional in vitro crosslinking experiments, followed by purification, digestion, and mass spectral analysis. There has been success in identifying binding regions of the natural activators Gcn4, Gal4, and VP2 with the coactivator Med15 using traditional LC-MS and MALDI-TOF techniques.[1] There are also advanced proteomics techniques available such as MudPIT (Multidimensional Protein Identification Technology). This technology uses two liquid chromatography systems, strong cation exchange followed by reverse phase HPLC, to separate peptides from a digested protein sample. This methodology has also proven successful at identifying proteins from both *in vitro* and *in cellulo* crosslinking experiments.[2, 3]

2) Crosslinking In Cells

To further understand the mechanism of iTAD **1**-driven gene expression, it would advantageous to elucidate the cellular binding partners that are directly contacted by iTAD **1** during transcriptional activation. Three compounds designed for *in cellulo* crosslinking experiments were synthesized and tested for activity, but unfortunately, none were able to upregulate transcription in a dose-dependent manner (Figure IV-1a-b). Each molecule contains a GR ligand (for localization to

DNA) in red, an affinity handle (for purification) in blue, a photocrosslinking group in yellow, and iTAD **1** in green.
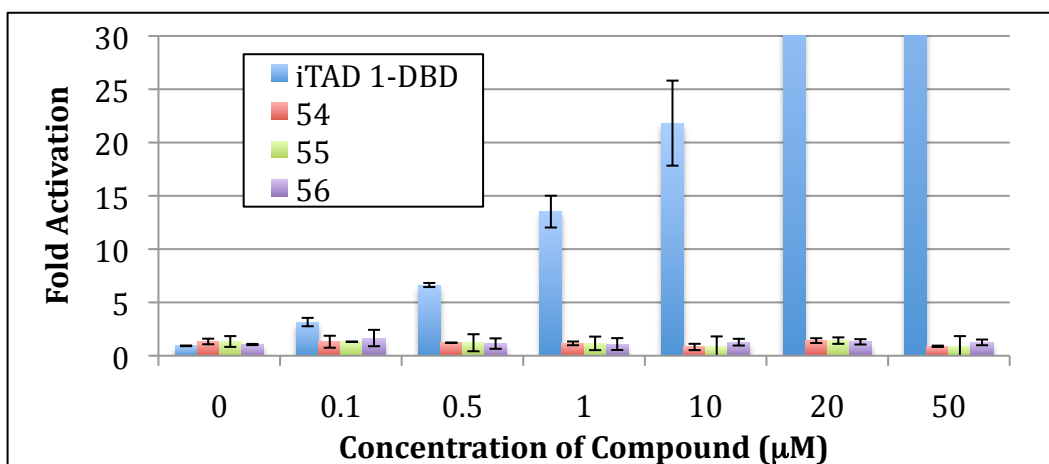
a)
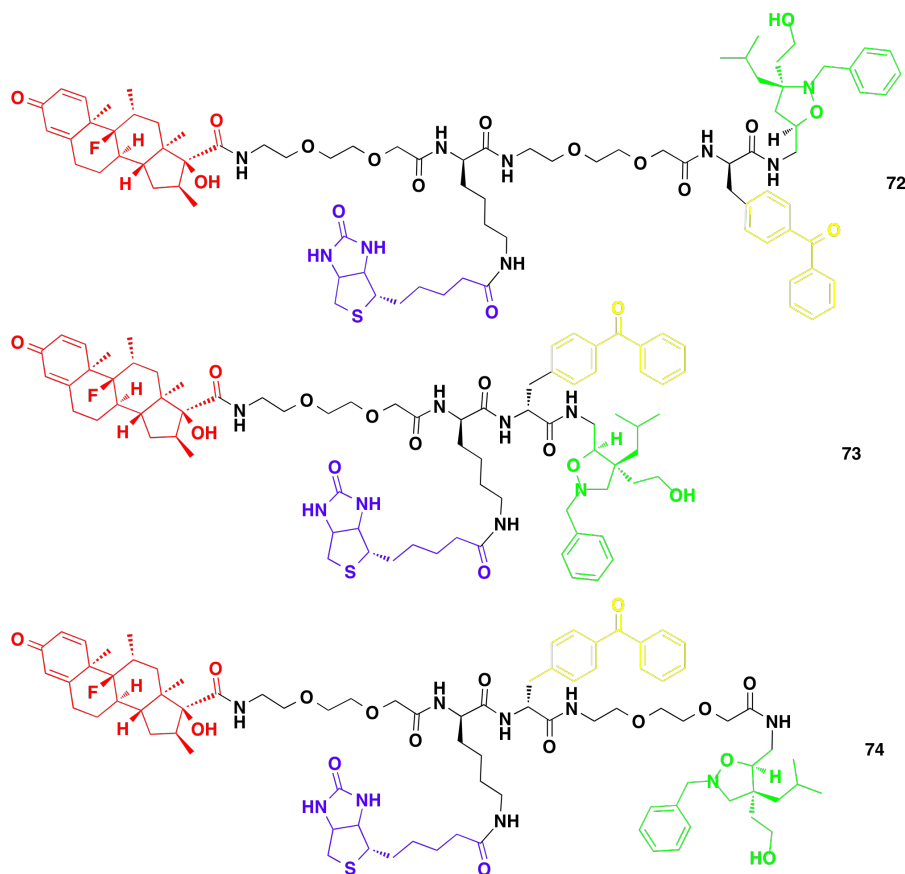
b)

Figure IV-1. Activity of *celluo* crosslinking compounds in cell culture. a) Structure of three compounds tested for activation. b) Activation of reporter gene transcription. Transfection and activity experiments were performed as previously described.

This could be due to several factors, including decreased cellular permeability of the larger construct and decreased proximity of iTAD **1** to DNA with the longer linker. Further investigation is therefore necessary to generate an iTAD conjugate with a crosslinking functionality that retains the ability to upregulate gene expression. One strategy would be to use a fully synthetic transcriptional activator consisting of iTAD **1** tethered to a polyamide DBD (Figure IV-2).
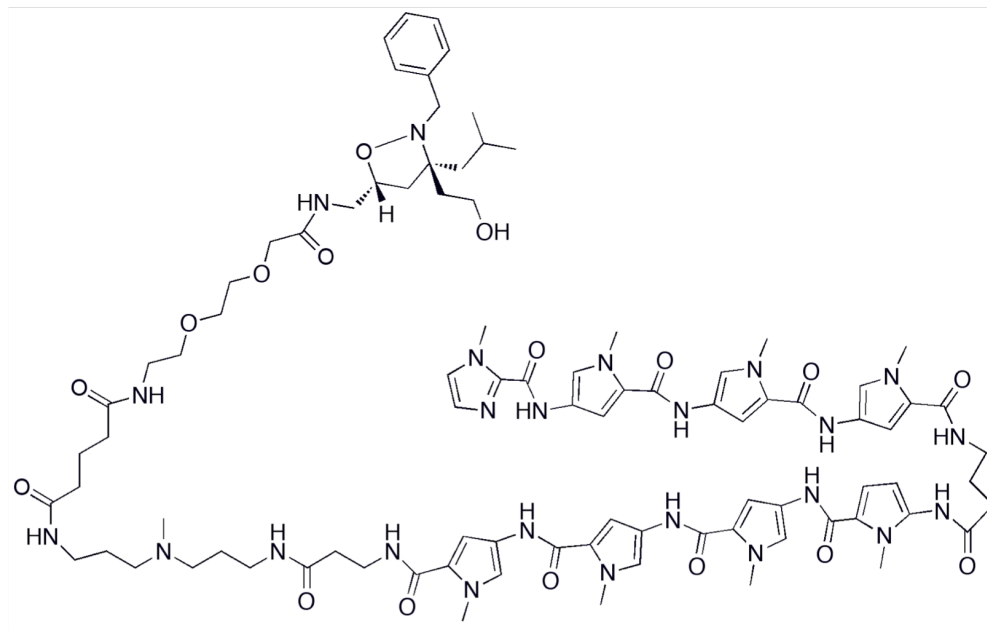

Figure IV-2. Small molecule transcriptional activator. BpA would be inserted in the linker region between iTAD **1** and the polyamide DBD.

Another crosslinking method uses formaldehyde to nonspecifically crosslink proteins and DNA; these complexes are then purified, the crosslinks are reversed, and the proteins identified. In the case of formaldehyde crosslinking, antibodies against a particular protein may be used to pull out proteins and protein complexes. This would provide a means to examine changes in CBP recruitment during transcriptional activation with a suite of both active and non-active small molecules (iTAD **1**, Santonin-RO, alkene iTAD **11**). This would provide information about which proteins and protein complexes are present at a particular promoter, but not about the connectivity of the binding interactions. These crosslinking methods, in combination, would identify proteins that directly contact iTAD **1**, in addition to

protein complexes recruited during iTAD **1**-driven gene expression. Furthermore, these crosslinking experiments could be performed at different time points during the activation of transcription providing a valuable timeline for the arrival and dismissal of different coactivators from the promoter.[4, 5] Time-resolved crosslinking would answer the questions: what proteins are necessary for iTAD **1**-driven transcription? In what order do these proteins and complexes arrive and how long do they remain at the promoter? These answers would enable more in-depth understanding of the combinatorial control of gene expression by recruitment of different coactivators and coactivator complexes at different times during the initiation of transcription by a small molecule.

3) Identification of Other Small Molecule Transcription Inhibitors

The iTAD compounds tested for inhibition of MLL- and Jun-driven luciferase expression were successful at obtaining >50% inhibition at 50 µM; however, these compounds are not particularly potent inhibitors. Additional potency may be achieved through multimerization of iTAD compounds, for example bis- and tris-isoxazolidines, though the synthesis and functionalization of such compounds is quite lengthy. To identify other, perhaps more potent, inhibitors of KIX-binding TADs, a screen was performed at the Center for Chemical Genomics at the University of Michigan Life Sciences Center. 67,000 compounds and natural product extracts were screened for their ability to inhibit the interaction between the KIX domain and a fluorescein-tagged variant of MLL-19 in a fluorescence polarization assay (compounds tested at 22 µM). There were no hits from the compound library and 22 hits from the natural products collection (Z score = 0.8).[2] Further studies with these natural product extracts are currently underway in collaboration with Dr. David Sherman's laboratory. By purifying these extracts and characterizing the compounds present, the specific molecule(s) responsible for the inhibition of the MLL·KIX interaction may be identified. This would provide additional information for the design and synthesis of small molecule transcriptional inhibitors.

4) KIX Contacts Necessary for iTAD 1 Function

As we have shown in Chapter II, the KIX domain of CBP is a critical binding partner for iTAD **1**-DBD-mediated transcription, and that iTAD **1** binds to the MLL/Jun/Tat/Tax site. It remains unclear, however, what specific residues are necessary for this interaction. By titrating CBP, with specific mutations in the KIX domain, into cells during iTAD activation experiments, these residues may be identified. The Chang lab used this strategy to identify the residues that were critical for SREBP binding of the CREB/Myb site on the KIX domain, and the Wright and Nyborg labs have identified the residues critical for MLL and Tax (respectively) binding as well.[6-8] These experiments would provide further insight into the mechanism by which iTAD **1** activates transcription through contacting the KIX domain of CBP, and may enable the design of more potent KIX-binding ligands.

5) Cooperative Recruitment of CBP

In Chapter II it was shown that iTAD **1** interacts with the KIX domain of CBP in a remarkably similar fashion to endogenous TADs that bind the MLL/Jun/Tat/Tax site of this domain. It has also been demonstrated that this interaction is critical for iTAD **1**-driven gene transcription. *In vitro* evidence supports the prevailing model that the two sites on the KIX domain are bound cooperatively; in fact, some promoters may require this synergistic interaction.[6, 9-11] Thus, a ternary complex of CREB·CBP·small molecule may provide a new strategy for the recruitment of CBP. Although preliminary binding experiments have shown that iTAD **1** is unable to potentiate KID (TAD of CREB) binding to the KIX domain, other iTAD structures such as iTAD dimers or trimers may provide the contacts necessary for cooperative interactions.

6) Kinetics of iTAD·KIX Interaction

A multitude of transient, low affinity interactions occur in biological systems. Traditionally, the affinity of a particular interaction has been correlated to its

importance. In transcription, however, several studies have shown that TAD binding affinity is not well correlated with activator potency. Studies currently underway in our laboratory with natural TADs suggest that the lifetime of a complex (k_{on}/k_{off}) between TADs and coactivators plays a significant role in the level of activation achieved by a particular activator. Stopped-flow kinetics and fluorescence polarization was used to dissect the interaction between Gal4, Gcn4 and VP16 with the coactivator Med15; similar studies could be performed with iTAD **1**.[12] This would provide another piece in the mechanistic puzzle of how small molecule transcriptional activation domains function.

7) Inhibition of CBP/p300 Interactions in Cancer Stem Cells

Recent studies have shown that certain cancer cells, termed cancer initiating (CI) cells, display self-renewal properties leading to metastasis and unresponsiveness to chemotherapy.[13] The pluripotency of embryonic stem cells (ESCs) is regulated in large part by three transcriptional activators: Sox2, Oct4, and Nanog. Nanog has emerged as the key player in regulating critical ESC genes, possibly through the recruitment of the coactivator p300, a homolog of CBP.[13-15] In murine ESCs, removal of p300 results in decreased expression of genes required for maintaining pluripotency, leading to differentiation.[16, 17] In Chapters II and III, I have shown that iTAD **1** binds to the KIX domain of CBP, and that this binding inhibits the interaction of certain natural TADs. Using a similar strategy, inhibitors of p300 binding interactions can be identified, their binding site specificity characterized, and their ability to decrease transcription of Nanog target genes assessed. Some preliminary results have been obtained in collaboration with the Pan lab at Ohio State University: treatment of a mixed cell population (CI and non-CI) from a tumorsphere with 30 μM iTAD **1** for 24 hours resulted in an 18.2% decrease in the CI cell population. Cis-platinum, however, reduced the non-CI cell population, and had no effect on the CI cells.[18] These results suggest that targeting p300 will be a promising approach to eliminating CI cells.

8) Small Molecule Transcription-Based Therapeutics

The recent advances in small molecule transcriptional modulators bring us ever closer to the realization of small molecule transcription-targeted therapeutics. These molecules could be designed to replace a malfunctioning endogenous TAD, localizing to the nucleus and upregulating expression of a specific gene. Additionally, as I have shown in Chapter III, certain small molecules are able to block activator·coactivator interactions, leading to a decrease in expression of a particular gene. Both types of molecules are highly sought after commodities due to the prevalence of misregulated transcription in disease, with the pathology of nearly 40 different cancers linked to malfunctions in transcription.[19-31] We now have additional strategies for the design of potential small molecule transcription-based therapeutics.

C. Experimental
Cell-based Activity Assay.

HeLa cells were purchased from the American Tissue Culture Center (ATCC) and plated onto treated polystyrene petri dishes (Corning) with 10 mL of D-MEM (+ 4.5 g/L d-glucose, + l-glutamine, - sodium pyruvate, + 10% FBS, + NEAA) (invitrogen). The cells were grown at 37°C 5% and 5% CO_2 to 80-90% confluence. Upon reaching the desired confluence, the D-MEM was removed and 4 mL 0.25% trypsin was added. The cells were incubated with the trypsin solution for 5 minutes at 37°C and 5% CO_2. Following the inubation, 10 mL of D-MEM were added and the resultant solution was pipetted up and down several times to ensure removal of all cells from the dish surface. The solution was centrifuged in a 15-mL Falcon tube at 1000 rpm for 2 minutes in a Fisher Centrific centrifuge. The supernatant was removed and the cell pellet was resuspended in 10 mL of D-MEM. The concentration of cells was calculated using a Hausser Scientific improved Neubauer phase counting chamber hemocytometer. Based on the determined concentration the cells were diluted to 100,000/mL in D-MEM. 100 μL of the cell solution was then added

to each well of a Microtest flat-bottom, low-evaporation-lid 96-well plates (Becton-Dickinson) and the plated cells were incubated overnight at 37°C and 5% CO_2. The media was removed from the plated cells and they were washed once with Opti-MEM (+ HEPES, + 2.4 g/L sodium bicarbonate, + l-glutamine) (Invitrogen) and then transfected.

The transfection procedure consisted of first mixing appropriate plasmids and Lipofectamine 2000® together in Opti-MEM® media for each well being transfected. After a 20 minute incubation at room temperature 100 μL of the solution was placed in the appropriate wells and the cells were incubated for 5 hours at 37°C and 5% CO_2. At the end of the 5-hour incubation, the transfection solution was removed and 100 μL fresh D-MEM was added to each well. To the media was added 1 μL of either DMSO or the appropriate concentration of a molecule being tested dissolved in DMSO (the final concentration of DMSO in all the wells was 1%). The cells were then incubated for 24 hours at 37°C and 5% CO_2.

Following the 24-hour incubation, the media was removed from each well and the cells were washed once with PBS buffer. 20 μL of passive lysis buffer (Promega) was added to each well and the cells were incubated for 20 minutes at room temperature on an orbital shaker. Subsequently, the total volume of each well was added to a cuvette along with 25 μL of Luciferase Assay Reagent II (Promega) and the luminescence was recorded. Then 25 μL Stop & Glo reagent was added and the Renilla luminescence was recorded again on a Berthold FB12 single cuvette luminometer.[32]

General procedure for cellular crosslinker synthesis.

Each compound contains the following elements: 1) OxDex, 2) AEEA linker units, 3) biotin affinity handle, 4) BpA photocrosslinking group, and 5) iTAD. Fmoc-BpA-OH was first coupled to Wang resin, as previously described, followed by addition of Fmoc-AEEA-OH (**54**, **56**) or Fmoc-Lys-MTT (**55**). Following deprotection, additional linker units and OxDex were coupled as described

169

previously. Once the core structure was complete, the beads were agitated for 1h at rt in a solution of 2% TFA in CH₂Cl₂ to affect removal of the MTT protecting group. Biotin was then coupled to the side chain of lysine, and the product was cleaved from the beads as previously described. The solvent was removed in vacuo and the crude acid was immediately coupled to **12A** to afford compounds **54-56**.
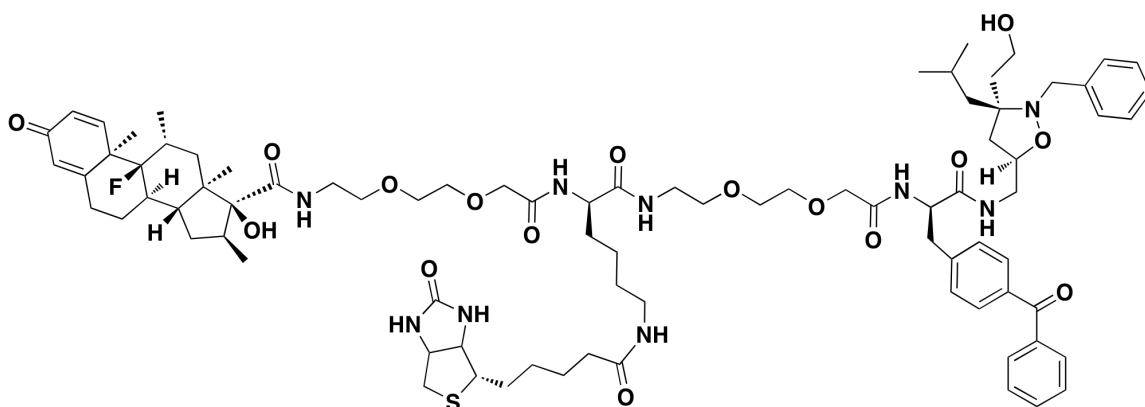
((8R,9S,10R,11R,13R,14R,16S,17S)-N-((4R,16R)-4-(4-benzoylbenzyl)-1-((3S,5R)-2-benzyl-3-(2-hydroxyethyl)-3-isobutylisoxazolidin-5-yl)-3,6,15,18-tetraoxo-16-(4-(5-((4S)-2-oxohexahydro-1H-thieno[3,4-d]imidazol-4-yl)pentanamido)butyl)-8,11,20,23-tetraoxa-2,5,14,17-tetraazapentacosan-25-yl)-9-fluoro-17-hydroxy-10,11,13,16-tetramethyl-3-oxo-6,7,8,9,10,11,12,13,14,15,16,17-dodecahydro-3H-cyclopenta[a]phenanthrene-17-carboxamide) (72): HRMS (ESI) calcd for $[C_{83}H_{116}FN_9O_{16}S + Na]^+$: 1568.8142, found 1568.8204.
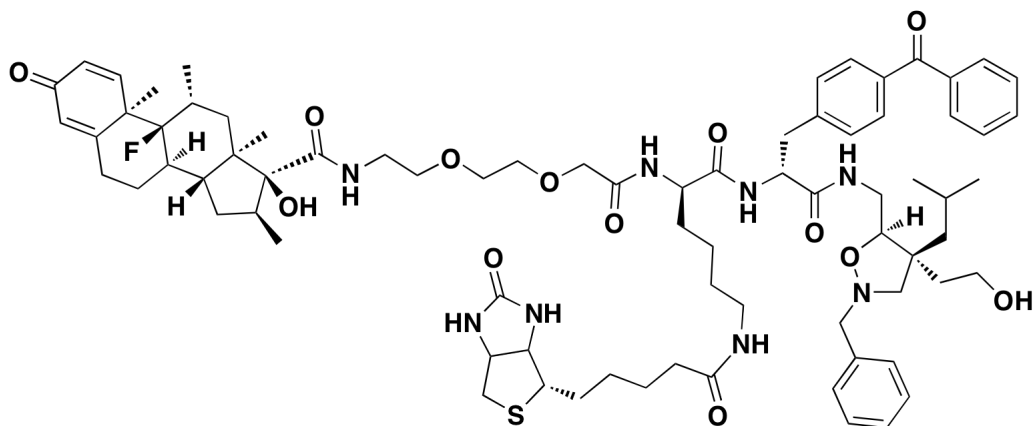
((8*R*,9*S*,10*R*,11*R*,13*R*,14*R*,16*S*,17*S*)-*N*-((4*R*,7*R*)-4-(4-benzoylbenzyl)-1-((4*R*,5*R*)-2-benzyl-4-(2-hydroxyethyl)-4-isobutylisoxazolidin-5-yl)-3,6,9-trioxo-7-(4-(5-((4*S*)-2-oxohexahydro-1*H*-thieno[3,4-*d*]imidazol-4-yl)pentanamido)butyl)-11,14-dioxa-2,5,8-triazahexadecan-16-yl)-9-fluoro-17-hydroxy-10,11,13,16-tetramethyl-3-oxo-6,7,8,9,10,11,12,13,14,15,16,17-dodecahydro-3*H*-cyclopenta[*a*]phenanthrene-17-carboxamide) (73): HRMS (ESI) calcd for [$C_{77}H_{105}FN_8O_{13}S$ + Na]$^+$: 1423.7404, found 1423.7431.
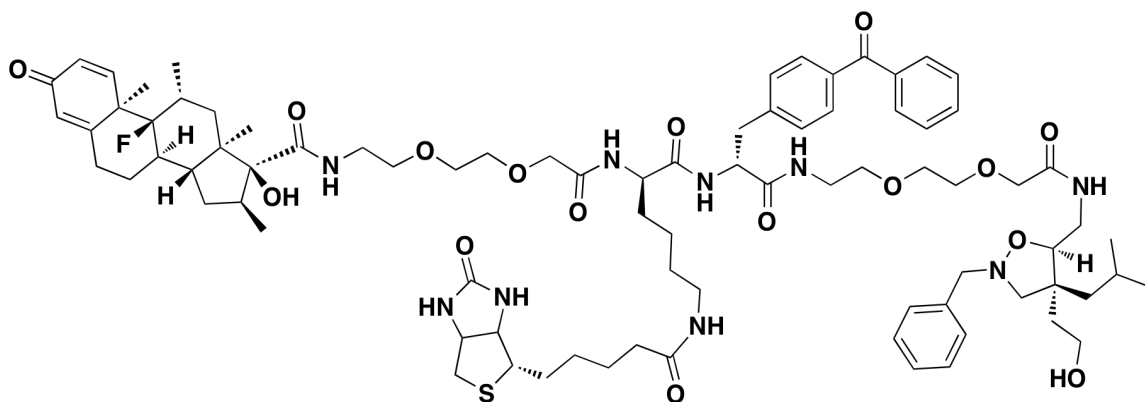
((8*R*,9*S*,10*R*,11*R*,13*R*,14*R*,16*S*,17*S*)-*N*-((13*R*,16*R*)-13-(4-benzoylbenzyl)-1-((4*R*,5*R*)-2-benzyl-4-(2-hydroxyethyl)-4-isobutylisoxazolidin-5-yl)-3,12,15,18-tetraoxo-16-(4-(5-((4*S*)-2-oxohexahydro-1*H*-thieno[3,4-*d*]imidazol-4-yl)pentanamido)butyl)-5,8,20,23-tetraoxa-2,11,14,17-tetraazapentacosan-25-yl)-9-fluoro-17-hydroxy-10,11,13,16-tetramethyl-3-oxo-6,7,8,9,10,11,12,13,14,15,16,17-dodecahydro-3*H*-cyclopenta[*a*]phenanthrene-

17-carboxamide) (74): HRMS (ESI) calcd for $[C_{83}H_{116}FN_9O_{16}S + Na]^+$: 1568.8142, found 1568.8275.

D. References

1.   Majmudar, C. Y.; Wang, B.; Lum, J. K.; Hakansson, K.; Mapp, A. K., A High-Resolution Interaction Map of Three Transcriptional Activation Domains with a Key Coactivator from Photo-Cross-Linking and Multiplexed Mass Spectrometry. *Angewandte Chemie-International Edition* **2009,** *48* (38), 7021-7024.

2.   Majmudar, C. Y., Unpublished results.

3.   Sieber, S. A.; Niessen, S.; Hoover, H. S.; Cravatt, B. F., Proteomic profiling of metalloprotease activities with cocktails of active-site probes. *Nat Chem Biol* **2006,** *2* (5), 274-281.

4.   Cosma, M. P.; Tanaka, T.; Nasmyth, K., Ordered recruitment of transcription and chromatin remodeling factors to a cell cycle- and developmentally regulated promoter. *Cell* **1999,** *97* (3), 299-311.

5.   Degenhardt, T.; Rybakova, K. N.; Tomaszewska, A.; Mone, M. J.; Westerhoff, H. V.; Bruggeman, F. J.; Carlberg, C., Population-Level Transcription Cycles Derive from Stochastic Timing of Single-Cell Transcription. *Cell* **2009,** *138* (3), 489-501.

6.   Goto, N. K.; Zor, T.; Martinez-Yamout, M.; Dyson, H. J.; Wright, P. E., Cooperativity in transcription factor binding to the coactivator CREB-binding protein (CBP). The mixed lineage leukemia protein (MLL) activation domain binds to an allosteric site on the KIX domain. *J Biol Chem* **2002,** *277* (45), 43168-74.

7.   Liu, Y. P.; Chang, C. W.; Chang, K. Y., Mutational analysis of the KIX domain of CBP reveals residues critical for SREBP binding. *FEBS Lett* **2003,** *554* (3), 403-9.

8.   Ramirez, J. A.; Nyborg, J. K., Molecular characterization of HTLV-1 Tax interaction with the KIX domain of CBP/p300. *J Mol Biol* **2007,** *372* (4), 958-69.

9.   Herzig, S.; Long, F.; Jhala, U. S.; Hedrick, S.; Quinn, R.; Bauer, A.; Rudolph, D.; Schutz, G.; Yoon, C.; Puigserver, P.; Spiegelman, B.; Montminy, M., CREB regulates hepatic gluconeogenesis through the coactivator PGC-1. *Nature* **2001,** *413* (6852), 179-83.

10.   Ptashne, M., Regulated recruitment and cooperativity in the design of biological regulatory systems. *Philosophical Transactions of the Royal Society of London Series a-Mathematical Physical and Engineering Sciences* **2003,** *361* (1807), 1223-1234.

11.   De Guzman, R. N.; Goto, N. K.; Dyson, H. J.; Wright, P. E., Structural basis for cooperative transcription factor binding to the CBP coactivator. *J Mol Biol* **2006,** *355* (5), 1005-13.

12.   Wands, A. M. W., N.; Lum, J.K.; Tsieh, J.H.; Fierke, C.; Mapp, A.K., Submitted.

13.   Clarke, M. F.; Fuller, M., Stem cells and cancer: Two faces of eve. *Cell* **2006,** *124* (6), 1111-1115.

14.   Chiou, S. H.; Yu, C. C.; Huang, C. Y.; Lin, S. C.; Liu, C. J.; Tsai, T. H.; Chou, S. H.; Chien, C. S.; Ku, H. H.; Lo, J. F., Positive correlations of Oct-4 and Nanog in oral cancer stem-like cells and high-grade oral squamous cell carcinoma. *Clin Cancer Res* **2008,** *14* (13), 4085-4095.

15.   You, J. S.; Kang, J. K.; Seo, D. W.; Park, J. H.; Park, J. W.; Lee, J. C.; Jeon, Y. J.; Cho, E. J.; Han, J. W., Depletion of Embryonic Stem Cell Signature by Histone Deacetylase Inhibitor in NCCIT Cells: Involvement of Nanog Suppression. *Cancer Res* **2009,** *69* (14), 5716-5725.

16.   Chen, X.; Xu, H.; Yuan, P.; Fang, F.; Huss, M.; Vega, V. B.; Wong, E.; Orlov, Y. L.; Zhang, W. W.; Jiang, J. M.; Loh, Y. H.; Yeo, H. C.; Yeo, Z. X.; Narang, V.; Govindarajan, K. R.; Leong, B.; Shahab, A.; Ruan, Y. J.; Bourque, G.; Sung, W. K.; Clarke, N. D.; Wei, C. L.; Ng, H. H., Integration of external signaling pathways with the core transcriptional network in embryonic stem cells. *Cell* **2008,** *133* (6), 1106-1117.

17.   Ji, J. F.; Werbowetski-Ogilvie, T. E.; Zhong, B. N.; Hong, S. H.; Bhatia, M., Pluripotent Transcription Factors Possess Distinct Roles in Normal versus Transformed Human Stem Cells. *Plos One* **2009,** *4* (11), -.

18.   Pan, Q., Unpublished results.

19.   Ansari, A. Z., Regulating gene expression: The design of synthetic transcriptional regulators. *Current Organic Chemistry* **2001,** *5* (8), 903-921.

20.   Malkin, D., The role of p53 in human cancer. *J Neurooncol* **2001,** *51* (3), 231-43.

21.   Pandolfi, P. P., Transcription therapy for cancer. *Oncogene* **2001,** *20* (24), 3116-27.

22.   Ansari, A. Z.; Mapp, A. K., Modular design of artificial transcription factors. *Current Opinion in Chemical Biology* **2002,** *6* (6), 765-772.

23.   Darnell, J. E., Jr., Transcription factors as targets for cancer therapy. *Nat Rev Cancer* **2002,** *2* (10), 740-9.

24.   Urnov, F. D.; Rebar, E. J., Designed transcription factors as tools for therapeutics and functional genomics. *Biochem Pharmacol* **2002,** *64* (5-6), 919-923.

25.   Mapp, A. K., Regulating transcription: a chemical perspective. *Organic & Biomolecular Chemistry* **2003,** *1* (13), 2217-2220.

26.   Kung, A. L.; Zabludoff, S. D.; France, D. S.; Freedman, S. J.; Tanner, E. A.; Vieira, A.; Cornell-Kennon, S.; Lee, J.; Wang, B.; Wang, J.; Memmert, K.; Naegeli, H. U.; Petersen, F.; Eck, M. J.; Bair, K. W.; Wood, A. W.; Livingston, D. M., Small molecule blockade of transcriptional coactivation of the hypoxia-inducible factor pathway. *Cancer Cell* **2004,** *6* (1), 33-43.

27.   Mapp, A. K., Finding their groove: Bifunctional molecules arrest growth of cancer cells. *Chemistry & Biology* **2004,** *11* (11), 1480-1482.

28.   Majmudar, C. Y.; Mapp, A. K., Chemical approaches to transcriptional regulation. *Current Opinion in Chemical Biology* **2005,** *9* (5), 467-474.

29.   Redell, M. S.; Tweardy, D. J., Targeting transcription factors for cancer therapy. *Current Pharmaceutical Design* **2005,** *11* (22), 2873-2887.

30.   Jung, D. J.; Choi, Y. M.; Uesugi, M., Small organic molecules that modulate gene transcription. *Drug Discovery Today* **2006,** *11* (9-10), 452-457.

31.   Mapp, A. K.; Ansari, A. Z., A TAD further: Exogenous control of gene activation. *Acs Chem Biol* **2007,** *2* (1), 62-75.

32.   Liu, B.; Alluri, P. G.; Yu, P.; Kodadek, T., A potent transactivation domain mimic with activity in living cells. *J Am Chem Soc* **2005,** *127* (23), 8254-8255.

Appendix

Investigation and Alteration of Glucocorticoid Receptor Function

A. Abstract

The glucocorticoid receptor (GR) is a transcriptional activator that binds the endogenous ligand cortisol, as well as several synthetic steroids such as dexamethasone. These steroids are important anti-inflammatory therapeutics, but unfortunately possess significant side effects, typically arising from off-target effects. There has been enormous effort to design GR ligands that dissociate these two properties. To better understand the mechanism by which GR regulates transcription, a series of GR ligands with photocrosslinking groups were synthesized. By identifying the direct coregulator binding partners of GR, we may gain insight into the design of ligands to selectively induce binding to specific targets, leading to desired downstream effects. As a first step towards modulating GR activity, a dexamethasone derivative (OxDex) was tagged with iTAD **1**, a small molecule TAD that interacts with the KIX domain of CBP. These molecules have shown differing abilities to drive luciferase expression from a number of endogenous GR-bound promoters, an important first step in developing dissociated GR ligands and for the application of this chemical technology to the study of other nuclear receptors.

B. Introduction

The glucocorticoid receptor (GR) is one of a number of ligand-gated transcriptional activators in the nuclear hormone receptor family (NR). GR is involved in lipid and carbohydrate metabolism, bone remodeling, immunomodulation, and was initially identified as a receptor for the endogenous steroid cortisol.[1-5] Depending on the promoter context and the coregulators bound, GR may positively or negatively affect transcription.[3, 6-10] These receptors typically exist in the cytosol as part of large multiprotein chaperone complexes. Upon ligand binding, the receptor dissociates from these chaperones and into the nucleus where it binds to glucocorticoid response elements (GRE) as a dimer (Figure 1).[1, 3, 5, 7, 11]
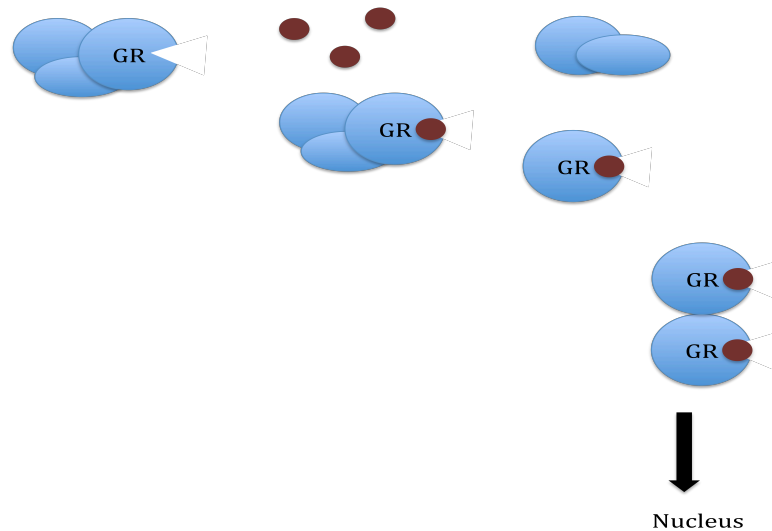
Figure 1. Schematic of glucocorticoid receptor function. Upon ligand binding, the chaperone·GR complex dissociates and GR enters the nucleus and binds glucocorticoid response elements (GREs) as a dimer.

GR contains an N-terminal TAD (AF-1), a C-terminal TAD (AF-2), a DBD, and a ligand-binding domain (LBD, contains AF-2), responsible for binding small molecule ligands (Figure 2).[11]

| NTD (AF-1) | DBD | | LBD (AF-2) |

Figure 2. The glucocorticoid receptor. GR contains two activations domains; AF-1 at the N-terminus, and AF-2, part of the ligand-binding domain (LBD).

Due to the remarkable anti-inflammatory effects of cortisol, this steroidal template has been the subject of extensive derivatization to deliver compounds with enhanced potency and receptor selectivity. However, most of these molecules cause significant side effects such as immunosuppression and weight gain (Figure 3). The design of dissociated GR ligands is meant to circumvent this problem by producing molecules that will selectively induce the desired effects. These ligands are not simply pure agonists or antagonists, but rather compounds that specifically induce particular therapeutic outcomes.[4, 5, 8, 9, 11-14]

Dexamethasone Agonist	OxDex Agonist	Cortisol Agonist	Mifepristone Antagonist	Prednisone Agonist
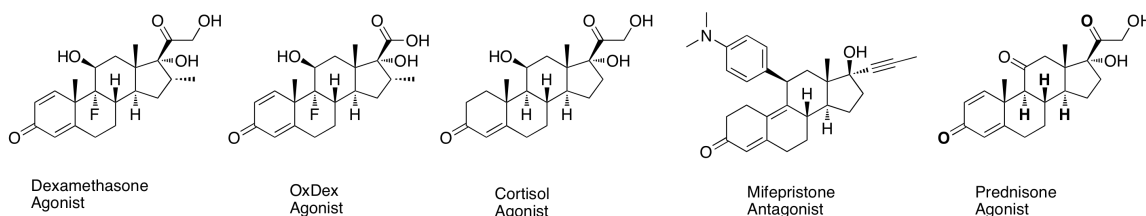
Figure 3. Glucocorticoid receptor ligands.

Similar to amphipathic TADs, GR exerts its transcriptional effects through binding coactivator (or corepressor) proteins and recruiting them to the promoter. Many binding partners of both GR and other NRs (such as the androgen and estrogen receptors) have been characterized *in vitro* and in cells; however, much of this information was gleaned from artificial reporter systems.[10, 11, 15] The Yamamoto group recently showed the importance of GRE sequence on GR-mediated transcription; it is thus crucial to determine GR binding partners in different endogenous promoter contexts and with different ligands bound.[16] To further elucidate the mechanism of GR-mediated activation and repression, OxDex was conjugated to a benzophenone photocrosslinking group and a biotin affinity handle. Identification of coactivators targeted by GR in different promoter contexts through

photocrosslinking may provide further insight into how to modulate downstream effects of GR through recruitment (or blocking) of specific coregulators.

C. Photoactive GR Ligands

The first step in generating a photoactive GR ligand was to create a functional handle on the ligand itself; in this case, dexamethasone was oxidized to create a carboxylic acid handle at C20 (OxDex). The compounds generated contain a GR ligand (OxDex) to facilitate receptor binding, a photoreactive group (benzophenone) to form covalent adducts with coregulator targets, and a biotin affinity handle to facilitate purification of crosslinked adducts. The first series of crosslinking compounds were synthesized with an alkyne handle that was to be used to capture an azide-functionalized biotin affinity label through copper-catalyzed "click" chemistry. Towards this end, propargylamine was coupled to Boc-protected BpA (**75**) using PyBrOP. After removal of the Boc group with 85% percent aqueous phosphoric acid, amine **76** was coupled to a linker then OxDex (**77**), or directly to OxDex (**78**), again using PyBrOP. The affinity handle synthesis began with 1-chloropropylamine hydrochloride, which was converted to 3-azidopropylamine (**79**) by treatment with sodium azide.[17] Biotin was treated with freshly distilled thionyl chloride; after removal of unreacted $SOCl_2$, **79** was added to yield biotin azide **80**.
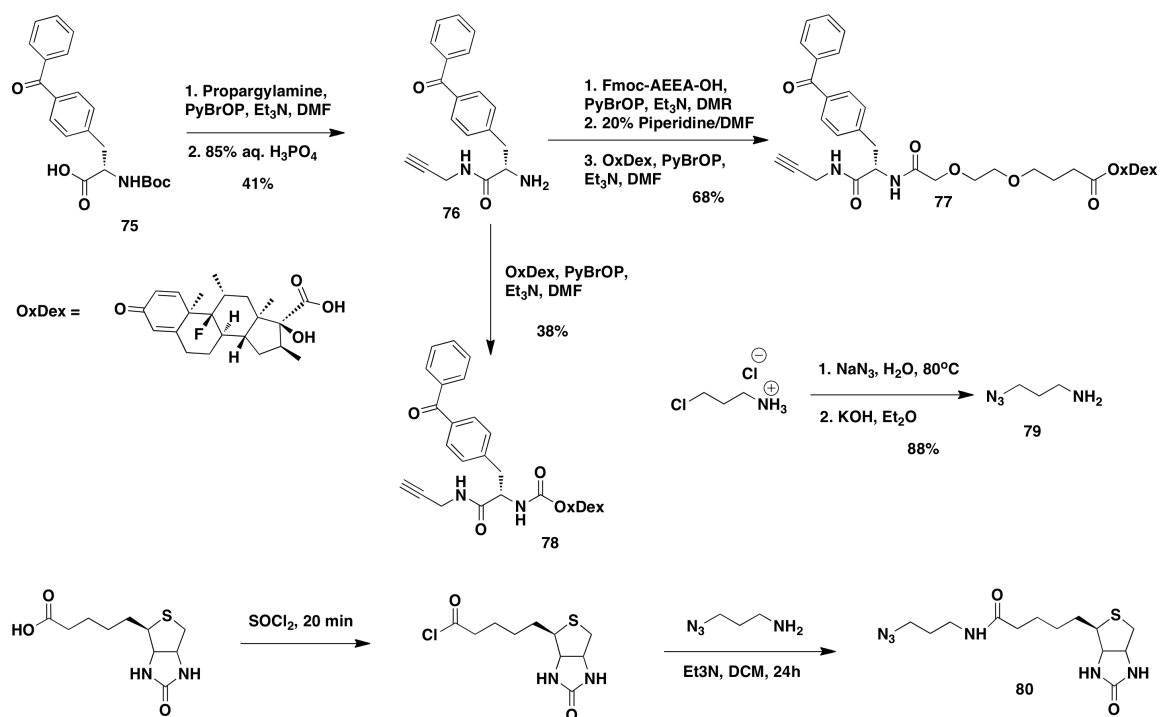
Scheme 1. Synthesis of azide/alkyne GR photocrosslinking compounds.

Both OxDex conjugates **77** and **78** bound to GR; however **78**, lacking a linker bound significantly less well based on dose-response data (Figure 4). When these compounds were used in cells, however, the copper (I) mediated click chemistry was unsuccessful at capturing protein adducts. Generally the copper concentrations needed for catalysis were high enough to precipitate protein from solution.
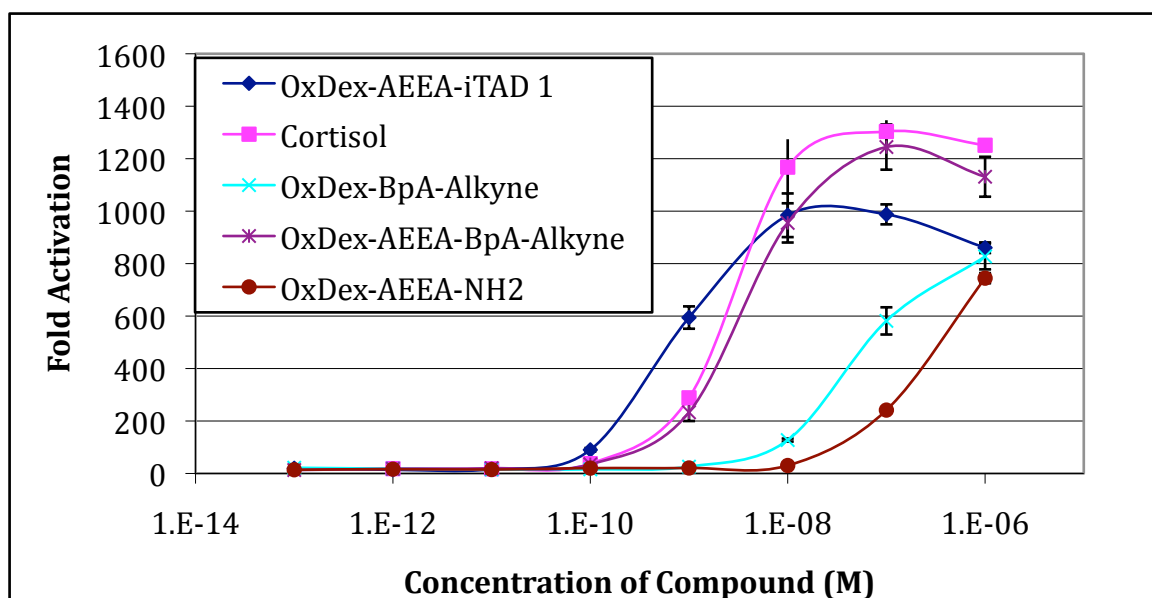
Figure 4. Dose response curve for glucocorticoid receptor compounds. Measured by endogenous GR-driven luciferase activity.

This was a disappointing, but not insurmountable, setback; the next series of compounds incorporated the affinity handle directly onto the molecule. Since each reaction was an amide bond coupling, this synthesis was performed on solid phase using Wang resin. Initially, Fmoc-protected BpA was coupled to the beads, followed by deprotection and subsequent addition of either one or two AEEA linker units. Once the linker was deprotected, OxDex was coupled to the amine and the molecule is cleaved from the resin with a solution of 95% TFA, 2.5% TIPS, and 2.5% H_2O. The crude product (**85**) was purified by reverse phase HPLC and coupled to the biotin-amine (**84**) derivative using standard peptide coupling conditions to provide the complete probe (**86**). The biotin amine was synthesized from biotin and *tert*-butyl (3-aminopropyl) carbamate under standard peptide coupling conditions, followed by removal of the Boc group.[18]
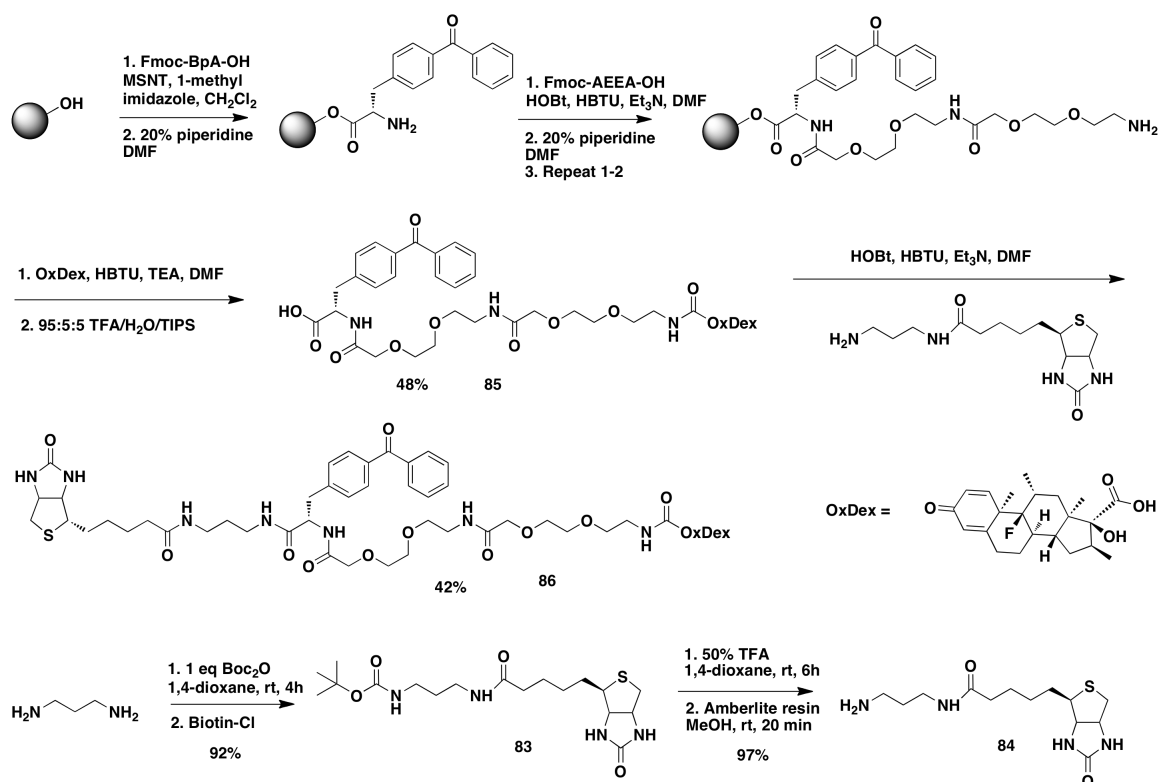
Scheme 2. Synthesis of second generation glucocorticoid photocrosslinking compounds.

Figure 5 shows these ligands with the crosslinking functionality in yellow, the GR ligand in blue, and the biotin affinity handle in red. These ligands will be used to capture GR·coregulator interactions at different GRE-containing promoters.
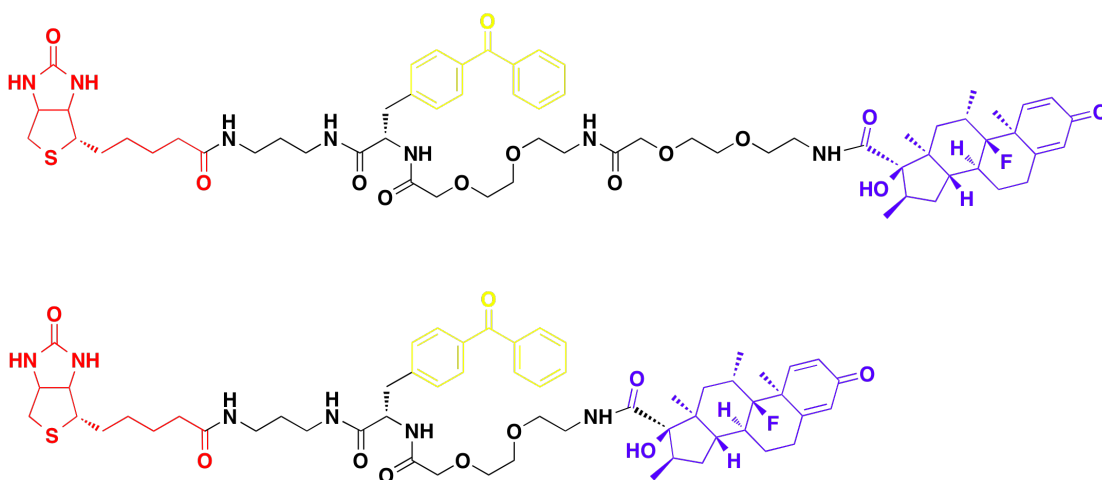
Figure 5. Glucocorticoid receptor photocrosslinking compounds.

By painting a detailed picture of these binding interactions we may begin to parse out specific contacts necessary to achieve a desired therapeutic endpoint, for example, significant reduction of inflammation without immunosuppression.

D. Modulators of GR Activity

In addition to deepening the understanding of GR·coregulator interactions with corticosteroid ligands, we are investigating the ability of small molecules tethered to GR ligands to alter the number or types of coregulators recruited to a particular promoter. Towards this end, OxDex was attached to iTAD **1** and **22** through two AEEA linker units, and these compounds are being tested for their ability to modulate GR function at different promoters. These compounds were synthesized on solid phase as described for photoprobe **86** and shown in the scheme below.
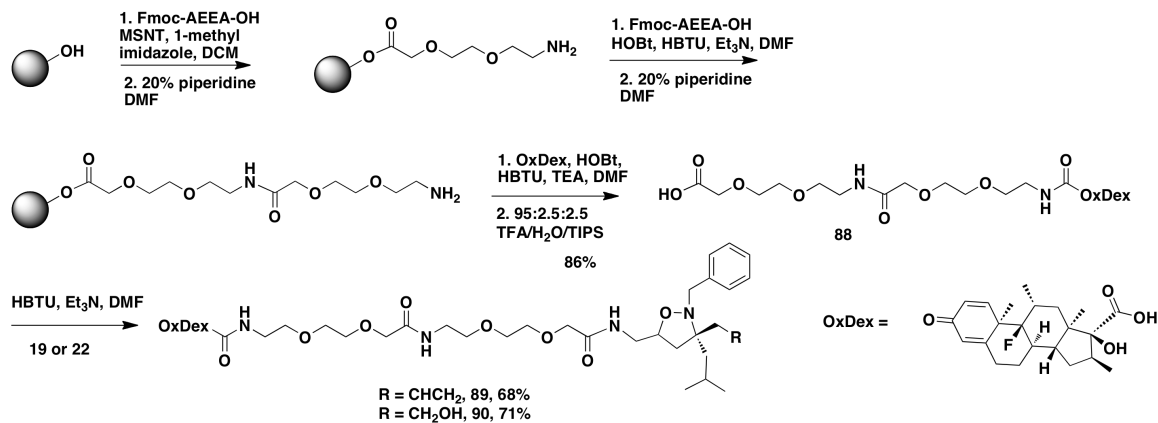
Scheme 3. Synthesis of glucocorticoid receptor modulators.
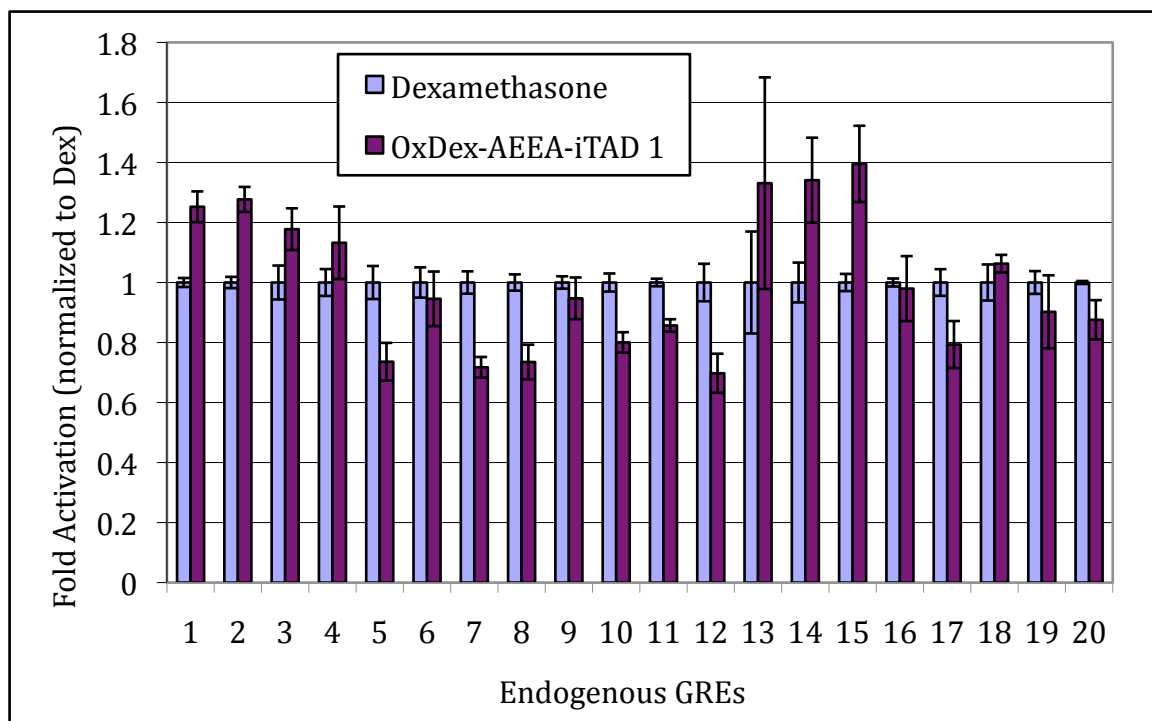
Figure 6. Effect of a GR modulator at endogenous GREs. Effect of iTAD **1**-DBD on GR driven-luciferase expression from 20 different endogenous GREs. Values are normalized to dexamethasone activity. HEK 293-T cells were transfected with plasmids containing 20 different endogenous GREs upstream of a luciferase reporter gene (one plasmid per experiment). Compound was added to cells 4 h after transfection (Dexamethasone 1 μM, iTAD **1**-AEEA-OxDex, 20 μM), compounds were added in DMSO to a final DMSO concentration of 1% (vol/vol). Activity data was calculated as previously described and normalized to dexamethasone.

The graph above shows the level of luciferase gene expression from several different endogenous GREs relative to a dexamethasone control. These data clearly demonstrate the difference in activity between these compounds at different promoters; for example, iTAD **1**-DBD is more active than dexamethasone at 14-15, but less active at 7-8. These distinct differences are promising initial results for the ability of small molecule-GR ligand conjugates to alter the transcriptional output of GR-driven promoters.[3-7, 9-13, 15, 19, 20]

E. Conclusions

Two classes of compounds, GR ligand photocrosslinkers and modulators of GR activity have provided a chemical platform for the elucidation of GR binding

partners at different promoters and for investigation of altering the GR binding profile with bifunctional ligands. In addition, this method is applicable for other GR ligands (both agonists and antagonists) and other members of the nuclear hormone receptor family. This information would provide valuable insight into the molecular recognition events responsible for GR-mediated regulation of transcription and facilitate the design of better dissociated GR ligands based on specific GR·coregulator interactions.

F. Experimental

General.

Unless otherwise noted, starting materials were obtained from commercial suppliers and used without further purification. Toluene, CH_2Cl_2, THF, and Et_2O were dried by passage through activated alumina columns. All reactions involving air- or moisture-sensitive compounds were performed under a dry N_2 atmosphere.[21] Unless otherwise noted, organic extracts were dried over Na_2SO_4, filtered, and concentrated under reduced pressure on a rotary evaporator. $BF_3 \cdot OEt_2$ and Et_3N were distilled from CaH_2. DMF was distilled under reduced pressure from P_2O_5. NBS was recrystallized from EtOH/water. Purification by column chromatography was carried out with E. Merck Silica Gel 60 (230-400 mesh) according to the procedure of Still, Kahn and Mitra.[22] Reverse-phase HPLC purification was performed on a Varian ProStar 210 equipped with Rainin Dynamix UV-D II detector using a C18 (8 x 100 mm) Radial PakTM cartridge using a gradient mixture of 0-80% 0.1% TFA/water and acetonitrile, unless otherwise specified. UV-Vis spectra were recorded in ethanol. In order to determine the concentrations of all OxDex conjugates, the characteristic UV-Vis absorption of dexamethasone at 242 nm with an extinction coefficient of 12,000 $M^{-1}cm^{-1}$ was used. Once concentration was determined, the sample was aliquoted, lyophilized, and stored at -80°C. ^1H and ^{13}C NMR spectra were recorded in $CDCl_3$ at 400 MHz and 125 MHz, respectively, unless otherwise specified. IR spectra were measured as thin films on NaCl plates using a

Perkin Elmer Spectrum 1000 FT-IR. High-resolution mass spectra were measured on a VG-250-S Micromass, Inc., mass spectrometer at the University of Michigan Mass Spectrometry Laboratory.

Small Molecule Synthesis and Characterization.
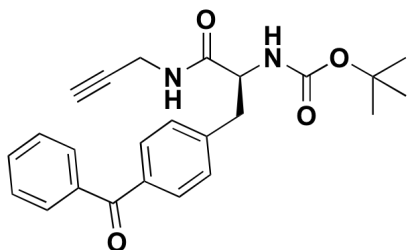
((S)-*tert*-butyl (3-(4-benzoylphenyl)-1-oxo-1-(prop-2-yn-1-ylamino)propan-2-yl)carbamate) (81): To a solution of Boc-benzoyl-L-phenylalanine (300 mg, 0.81 mmol, 1.0 eq) and Et$_3$N (230 μL, 1.62 mmol, 2.0 eq) in CH$_2$Cl$_2$ (20 mL) was added PyBOP (422 mg, 0.81 mmol, 1.0 eq) and the reaction mixture stirred for 30 min at rt. Propargylamine (80 μL, 1.22 mmol, 1.5 eq) was added dropwise and the reaction stirred at rt for 12 h. Water (10 mL) was added and the aq. layer was extracted with EtOAc (3 x 20 mL). Purification by flash chromatography (95:5 CH$_2$Cl$_2$/MeOH) yielded 224 mg of **81** in 68% yield as a light yellow solid. ^{1}H NMR (CD$_3$OD): δ 1.30 (s, 9H), 2.83-2.90 (m, 1H), 3.04-3.12 (m, 3H), 4.17-4.22 (m, 1H), 7.31-7.39 (m, 2H), 7.42-7.50 (m, 2H), 7.57-7.60 (m, 2H), 7.61-7.76 (m, 3H); ^{13}C NMR: δ 29.5, 30.0, 37.9, 57.6, 74.8, 80.0, 80.2, 127.4, 128.8, 130.0, 130.3, 130.4, 132.0, 135.9, 138.5, 140.6, 155.6, 172.1, 194.4; HRMS (ESI) calcd for : [C$_{24}$H$_{26}$N$_2$O$_4$ + Na]$^+$: 429.1790, found: 429.1807.
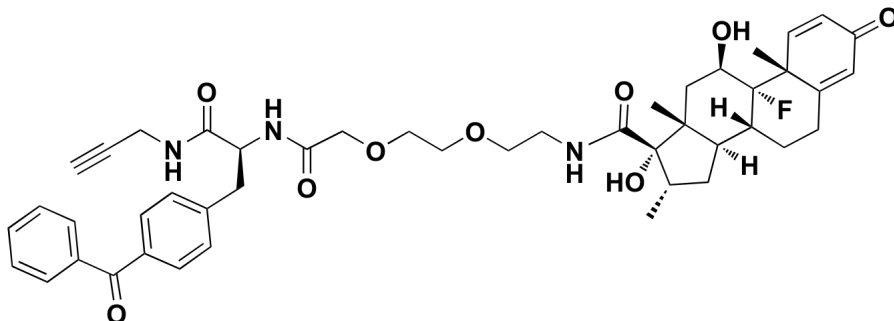
((8R,9S,10R,11R,13R,14R,16S,17S)-N-((S)-10-(4-benzoylbenzyl)-8,11-dioxo-3,6-dioxa-9,12-diazapentadec-14-yn-1-yl)-9-fluoro-17-hydroxy-10,11,13,16-tetramethyl-3-oxo-6,7,8,9,10,11,12,13,14,15,16,17-dodecahydro-3H-cyclopenta[a]phenanthrene-17-carboxamide) (77): **81** (500 mg, 1.23 mmol, 1.0 eq) was dissolved in 85% aq. phosphoric acid (2 mL, 24.6 mmol, 20 eq) and stirred at rt for 4 h. Acid, base workup afforded crude amine () in 60% yield, which was directly coupled to AEEA-OxDex. Towards this, OxDex-AEEA (969 mg, 1.85 mmol, 1.5 eq) and PyBrOP (863 mg, 1.85 mmol, 1.5 eq) were dissolved in DMF (10 mL) and stirred for 1 h. A solution of the crude amine (377 mg, 1.23 mmol, 1.0 eq) and Et$_3$N (260 µL, 1.85 mmol, 1.5 eq) in DMF (2 mL) was added dropwise and the reaction stirred for 12 h. The sample was concentrated and the product was purified by reverse-phase HPLC using a 0.1% TFA in H$_2$O/ACN gradient affording **77** in 68% yield as a white powder. HRMS (ESI) calcd for [C$_{46}$H$_{54}$FN$_3$O$_9$ + Na]$^+$: 834.3742, found: 834.3768.
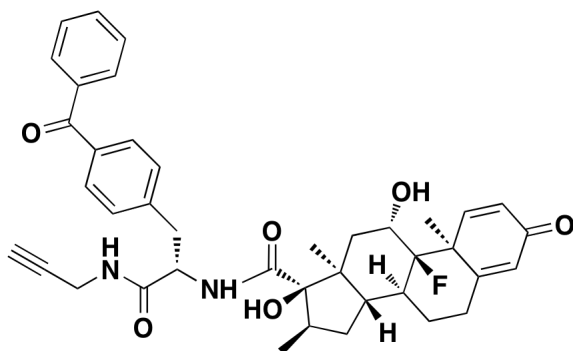
((8S,9R,10S,11S,13S,14S,16R,17R)-N-((S)-3-(4-benzoylphenyl)-1-oxo-1-(prop-2-yn-1-ylamino)propan-2-yl)-9-fluoro-11,17-dihydroxy-10,13,16-trimethyl-3-

oxo-6,7,8,9,10,11,12,13,14,15,16,17-dodecahydro-3*H*-cyclopenta[*a*]phenanthrene-17-carboxamide) (78): Synthesis of **78** proceeded as previously described for **77** by coupling with OxDex in 38% yield as a white powder. HRMS (ESI) calcd for $[C_{40}H_{43}FN_2O_6 + Na]^+$: 689.3003, found: 689.3019.
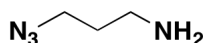

(3-azidopropan-1-amine) (79): Was synthesized in 88% yield from 3-chloropropylamine hydrochloride as previously described. Spectral data matched published values.[17]
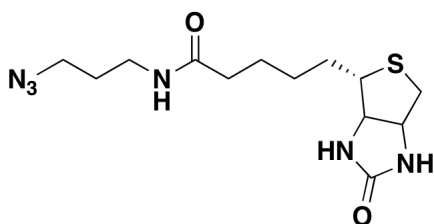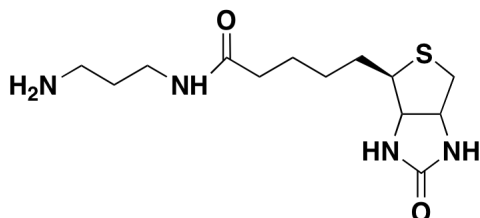

(*N*-(3-azidopropyl)-5-((4*R*)-2-oxohexahydro-1*H*-thieno[3,4-*d*]imidazol-4-yl)pentanamide) (80): To a solution of biotin (1.0 g, 4.1 mmol, 1.0 eq) in DMF (20 mL) was added HBTU (3.11 g, 8.2 mmol, 2.0 eq) and iPr$_2$NEt (1.5 mL, 8.2 mmol, 2.0 eq), and the reaction stirred at rt for 20 min. 3-azidopropylamine (821 mg, 8.2 mmol, 2.0 eq) in DMF (2 mL) was added dropwise and the reaction was stirred for 12 h. Sat. aq. NH$_4$Cl (10 mL) was added followed by water (30 mL) and the aqueous layer was extracted with EtOAc (3 x 30 mL). Product was purified by flash chromatography to provide **80** in 89% yield as a clear yellow waxy oil. ^{1}H NMR (CD$_3$OD) δ 1.66-1.60 (m, 2H), 1.97-1.75 (m, 6H), 2.38 (t, 2H, J = 7.2 Hz), 3.10 (dd, 1H, J = 5.2, 12.8 Hz), 3.38 (dd, 1H, J = 4.4, 8.4 Hz), 3.42 (t, 2H, J = 6.8 Hz), 3.52 (t, 2H, J = 6.8 Hz), 4.51-4.66 (m, 2H); ^{13}C NMR δ 26.9, 29.6, 29.9, 29.9, 36.9, 37.9, 41.2, 50.3, 57.1, 61.8, 63.6, 166.2,176.3; HRMS (ESI) calcd for $[C_{13}H_{22}O_2N_6S + Na]^+$: 349.1423, found: 349.1437.
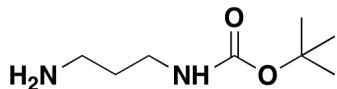
(*tert*-butyl (2-aminopropyl)carbamate) (82): Was synthesized in 97% yield from 1,3-diaminopropane as previously described. Spectral data matched published values.[18]
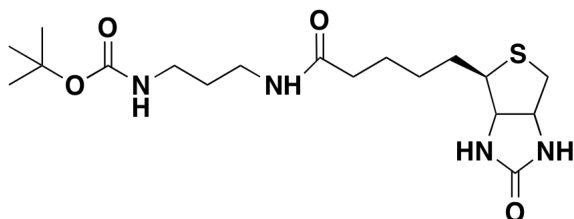

(*tert*-butyl (3-(5-((4*R*)-2-oxohexahydro-1*H*-thieno[3,4-*d*]imidazol-4-yl)pentanamido)propyl)carbamate) (83): To a solution of biotin (500mg, 2.05 mmol, 1.0 eq) in CH_2Cl_2 (20 mL) was added DIC (285 mg, 2.26 mmol, 354 µL) and HOBt (55 mg, 0.41 mmol, 0.2 eq) and stirred for 5 min at rt. *tert*-butyl (2-aminopropyl)carbamate (580 mg, 3.08 mmol, 1.5 eq) and Et_3N (207 mg, 2.05 mmol, 286 µL) in CH_2Cl_2 (5 mL) were added drop wise and the reaction stirred for 12 h at rt. Product was purified by flash chromatography (9:1 to 8:2 CH_2Cl_2/MeOH) to afford **83** in 92% yield. ^{1}H NMR (CD_3OD): δ 1.42 (s, 9H), 1.44-1.53 (m, 8H) 2.19 (t, 2H, *J* = 7.3), 2.69 (d, 1H, *J* = 12.7), 2.90 (dd, 1H, *J* = 5.0, 12.7), 3.02 (t, 2H, *J* = 6.5), 3.12-3.19 (m, 3H), 4.25 (dd, 1H, *J* = 4.5, 7.9), 4.42 (dd, 1H, *J* = 4.2, 7.9); ^{13}C NMR: δ 26.6, 27.3, 28.8, 29.5, 29.8, 29.9, 30.2, 37.3, 40.5, 41.5, 57.4, 62.1, 63.8, 80.3, 159.0, 166.6, 176.4; HRMS (ESI) calcd for $[C_{18}H_{32}N_4O_3S + Na]^+$: 423.2042, found: 423.2035.


(*N*-(3-aminopropyl)-5-((4*R*)-2-oxohexahydro-1*H*-thieno[3,4-*d*]imidazol-4-yl)pentanamide) (84): **83** (50 mg, .12 mmol, 1.0eq) was suspended in EtOAc (10

mL) and a solution of HCl in dioxane (10 mL, 4 M) was added dropwise. The mixture was stirred at rt for 1 h and the solvent was removed *in vacuo*. The crude product was recrystallized from MeOH/Et$_2$O to provide 37 mg of **84** in 97% yield as an off-white solid. ^{1}H NMR (CD$_3$OD): δ 1.43-1.53 (m, 4H), 1.57-1.85 (m, 6H), 2.28 (t, 2H, *J* = 7.4), 2.76 (d, 1H, *J* = 12.9), 2.95-3.05 (m, 1H), 3.23-3.30 (m, 3H), 4.43 (dd, 1H, *J* = 4.4, 7.9), 4.61 (dd, 1H, *J* = 4.7, 7.9), 4.95 (bs, 2H); ^{13}C NMR: δ 26.3, 27.3, 29.8, 30.2, 37.0, 40.2, 40.7, 41.2, 57.2, 63.1, 64.7, 166.2, 174.0; HRMS (ESI) calcd for [C$_{13}$H$_{24}$N$_4$O$_2$S + H]$^+$: 301.1698, found: 301.1714.
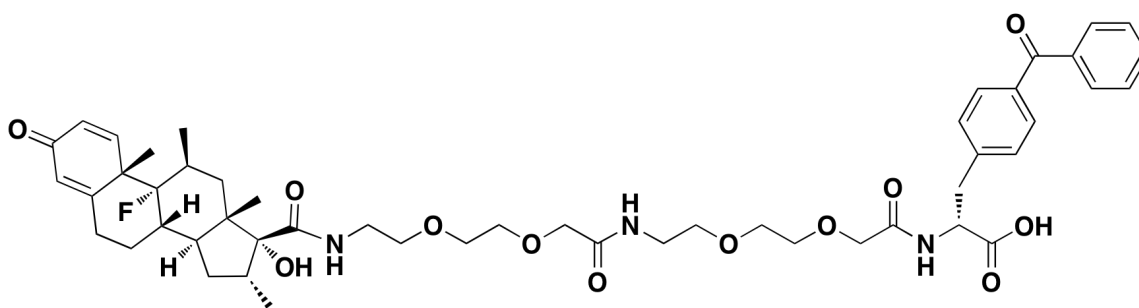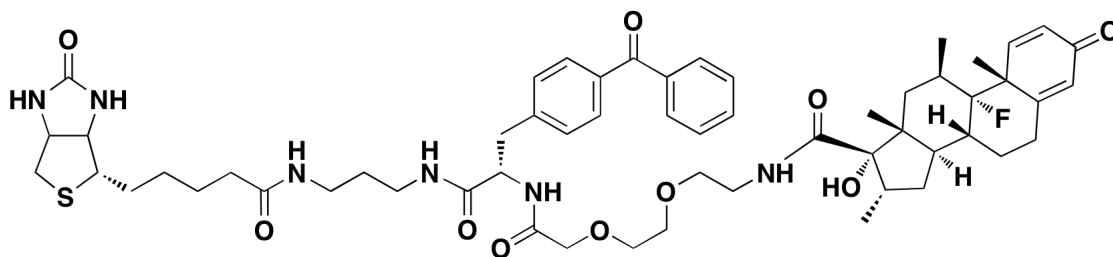

((*S*)-21-(4-benzoylbenzyl)-1-((8*R*,9*S*,10*R*,11*R*,13*R*,14*R*,16*S*,17*S*)-9-fluoro-17-hydroxy-10,11,13,16-tetramethyl-3-oxo-6,7,8,9,10,11,12,13,14,15,16,17-dodecahydro-3*H*-cyclopenta[*a*]phenanthren-17-yl)-1,10,19-trioxo-5,8,14,17-tetraoxa-2,11,20-triazadocosan-22-oic acid) (85): Wang Resin (100 mg, 0.11 mmol, 1.0 eq) was swelled in CH$_2$Cl$_2$ for 10 min. Fmoc-BpA-OH (270 mg, 0.55 mmol, 5.0 eq) was dissolved in 9:1 CH$_2$Cl$_2$/DMF and 1-methylimidazole (34 mg, 33 µL, .41 mmol, 3.75 eq) was added, followed by MSNT (163 mg, .55 mmol, 5.0 eq). The mixture agitated at rt for 5 min. The beads were washed once with CH$_2$Cl$_2$ and once with DMF and the reaction mixture was added. The reaction agitated at rt for 24 hours. The beads were washed with DMF (2 x 5 mL), MeOH (2 x 5 mL), and CH$_2$Cl$_2$ (2 x 5 mL), swelled in CH$_2$Cl$_2$ for 5 min at rt and incubated with 20% piperidine in DMF for 30 min at rt to remove the Fmoc group. The beads were then washed with 20% piperidine in DMF (2 x 5 mL), DMF (2 x 5 mL), and CH$_2$Cl$_2$ (2 x 5 mL). Fmoc-AEEA-OH (127 mg, .33 mmol, 3.0 eq), HBTU (125 mg, .33 mmol, 3.0 eq), HOBt (45 mg, .33 mmol, 3.0 eq), and Et$_3$N (46 µL, .33 mmol, 3.0 eq) were dissolved in DMF (6

mL) and incubated at rt for 10 minutes. The reaction mixture was agitated with the beads for 24 hours at rt. The washing and deprotection steps were repeated, followed by appending of another AEEA linker as described in the previous step. Following washing and deprotection, OxDex (125 mg, .33 mmol, 3.0 eq), HBTU (125 mg, .33 mmol, 3.0 eq), HOBt (45 mg, .33 mmol, 3.0 eq), and Et_3N (46 µL, .33 mmol, 3.0 eq) were added in DMF (5 mL) and the coupling and washing steps were repeated. The product was cleaved from the resin with a solution of 95:2.5:2.5 TFA/TIPS/H_2O (2 mL). Solvent was blown off under a stream f N_2 and the crude product was purified by reverse phase HPLC to afford **85** in 48% yield as a white powder. HRMS (ESI) calcd for $[C_{50}H_{64}FN_3O_{12} + Na]^+$: 940.4372, found: 940.4407.
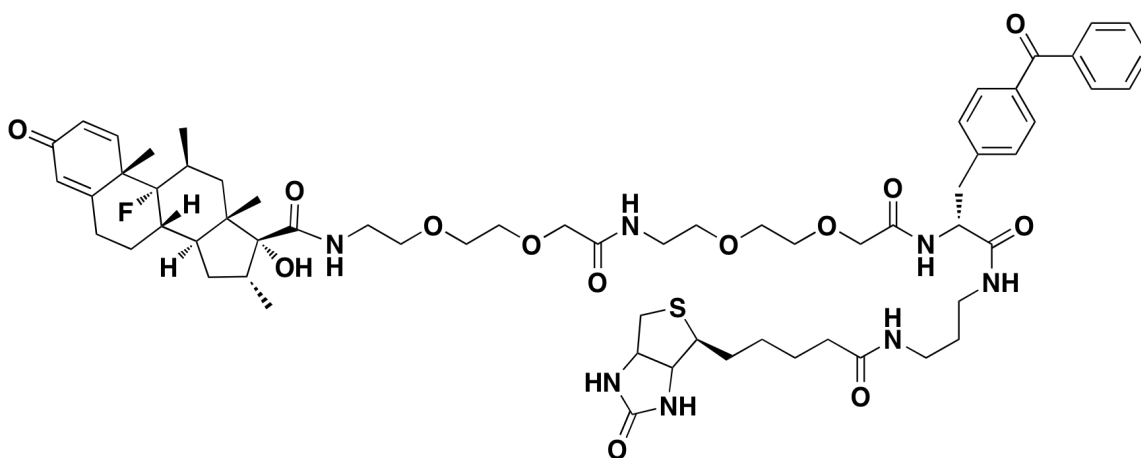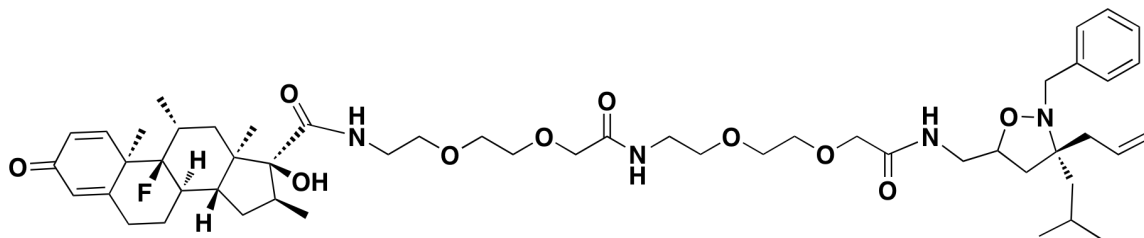

((8*R*,9*S*,10*R*,11*R*,13*R*,14*R*,16*S*,17*S*)-*N*-((19*S*)-19-(4-benzoylbenzyl)-8,17,20,26-tetraoxo-30-((4*S*)-2-oxohexahydro-1*H*-thieno[3,4-*d*]imidazol-4-yl)-3,6,12,15-tetraoxa-9,18,21,25-tetraazatriacontyl)-9-fluoro-17-hydroxy-10,11,13,16-tetramethyl-3-oxo-6,7,8,9,10,11,12,13,14,15,16,17-dodecahydro-3*H*-cyclopenta[*a*]phenanthrene-17-carboxamide) (86): Was synthesized in 42% yield as an off white powder from the coupling of **85** and **84** as described for compound **80**. Product was isolated by reverse phase HPLC. HRMS (ESI) calcd for $[C_{63}H_{86}FN_7O_{13}S + Na]^+$: 1222.5886, found 1222.5912.

((8R,9S,10R,11R,13R,14R,16S,17S)-N-((10S)-10-(4-benzoylbenzyl)-8,11,17-trioxo-21-((4S)-2-oxohexahydro-1H-thieno[3,4-d]imidazol-4-yl)-3,6-dioxa-9,12,16-triazahenicosyl)-9-fluoro-17-hydroxy-10,11,13,16-tetramethyl-3-oxo-6,7,8,9,10,11,12,13,14,15,16,17-dodecahydro-3H-cyclopenta[a]phenanthrene-17-carboxamide) (87): Was prepared in 56% yield as described previously for **86** by using one fewer AEEA units. HRMS (ESI) calc for $[C_{57}H_{75}FN_6O_{10}S + Na]^+$: 1077.5147, found 1077.5205.
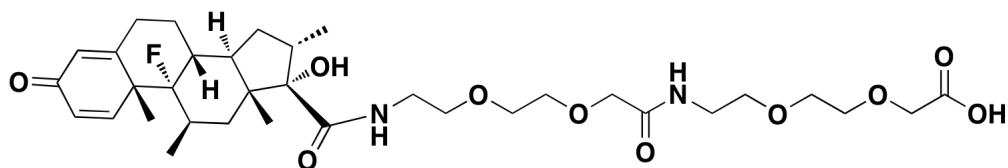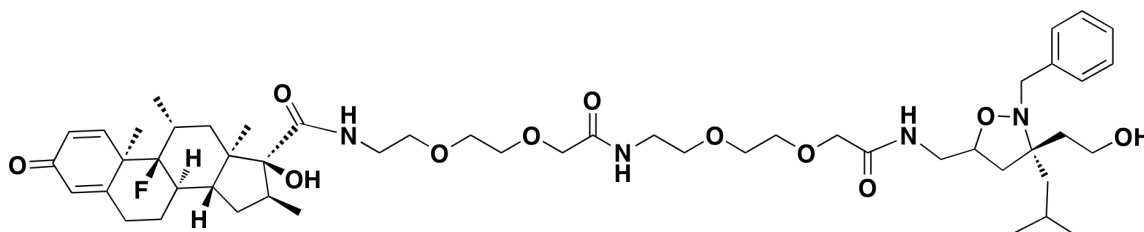

(1-((8R,9S,10R,11R,13R,14R,16S,17S)-9-fluoro-17-hydroxy-10,11,13,16-tetramethyl-3-oxo-6,7,8,9,10,11,12,13,14,15,16,17-dodecahydro-3H-cyclopenta[a]phenanthren-17-yl)-1,10-dioxo-5,8,14,17-tetraoxa-2,11-diazanonadecan-19-oic acid) (88): Was prepared in 86% yield on solid phase as previously described. HRMS (ESI) calc for $[C_{34}H_{51}FN_2O_{10} + Na]^+$: 689.3425, found 689.3445.


((8R,9S,10R,11R,13R,14R,16S,17S)-N-(1-((3S)-3-allyl-2-benzyl-3-isobutylisoxazolidin-5-yl)-3,12-dioxo-5,8,14,17-tetraoxa-2,11-

diazanonadecan-19-yl)-9-fluoro-17-hydroxy-10,11,13,16-tetramethyl-3-oxo-6,7,8,9,10,11,12,13,14,15,16,17-dodecahydro-3*H*-cyclopenta[*a*]phenanthrene-17-carboxamide) (89): Was prepared in 68% yield from coupling **22** and **88** as described for compound **85**. HRMS (ESI) calc for $[C_{52}H_{77}FN_4O_{10} + Na]^+$: 959.5521, found 959.5550.


((8*R*,9*S*,10*R*,11*R*,13*R*,14*R*,16*S*,17*S*)-*N*-(1-((3*S*)-2-benzyl-3-(2-hydroxyethyl)-3-isobutylisoxazolidin-5-yl)-3,12-dioxo-5,8,14,17-tetraoxa-2,11-diazanonadecan-19-yl)-9-fluoro-17-hydroxy-10,11,13,16-tetramethyl-3-oxo-6,7,8,9,10,11,12,13,14,15,16,17-dodecahydro-3*H*-cyclopenta[*a*]phenanthrene-17-carboxamide) (90): Was prepared in 71% yield from coupling **19** and **88** as described for compound **85**. HRMS (ESI) calc for $[C_{51}H_{77}FN_4O_{11} + Na]^+$: 963.5471, found 963.5493.

G. Appendix of Selected ¹H NMR Spectra and HPLC Traces

194

195

196
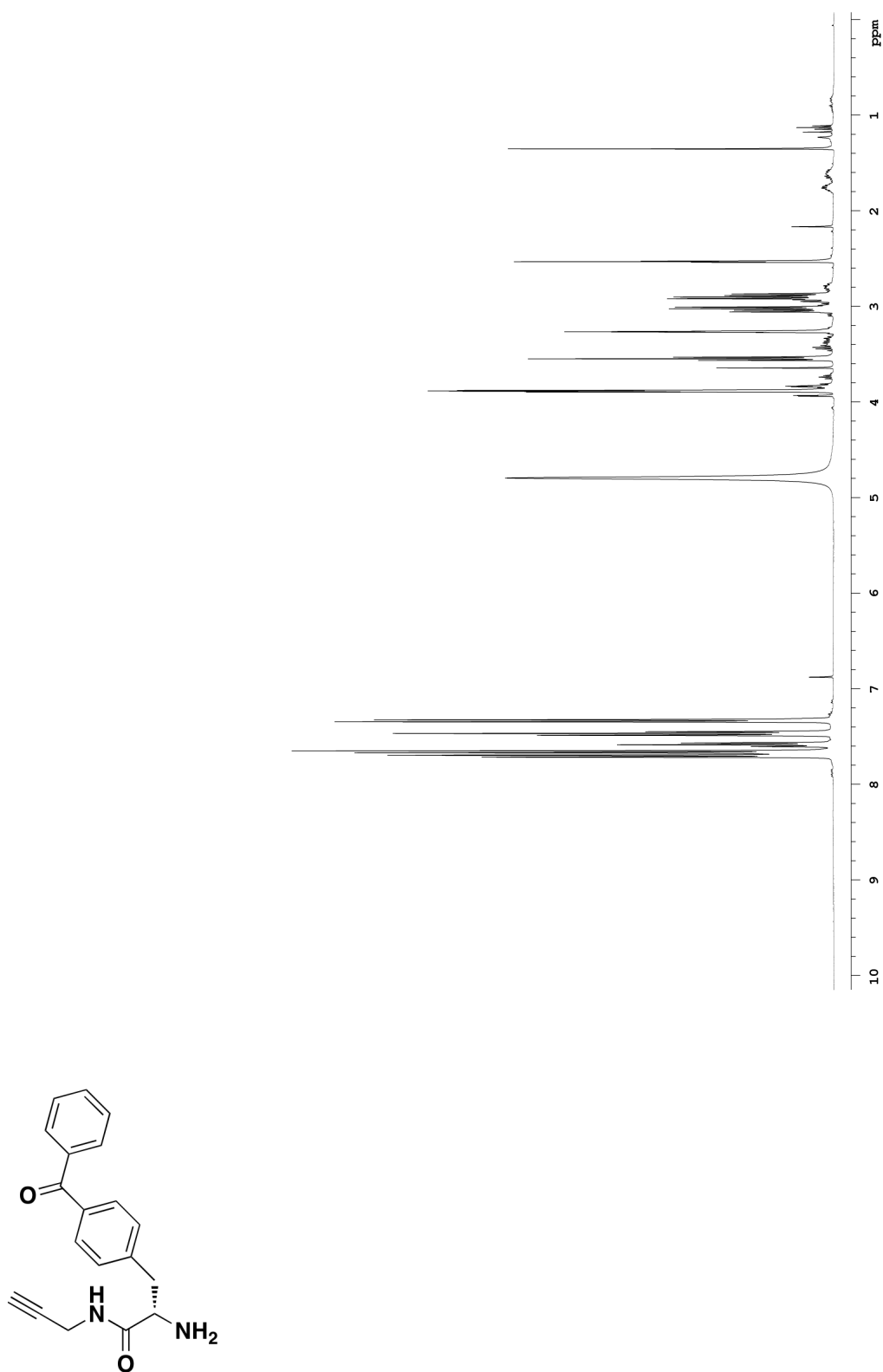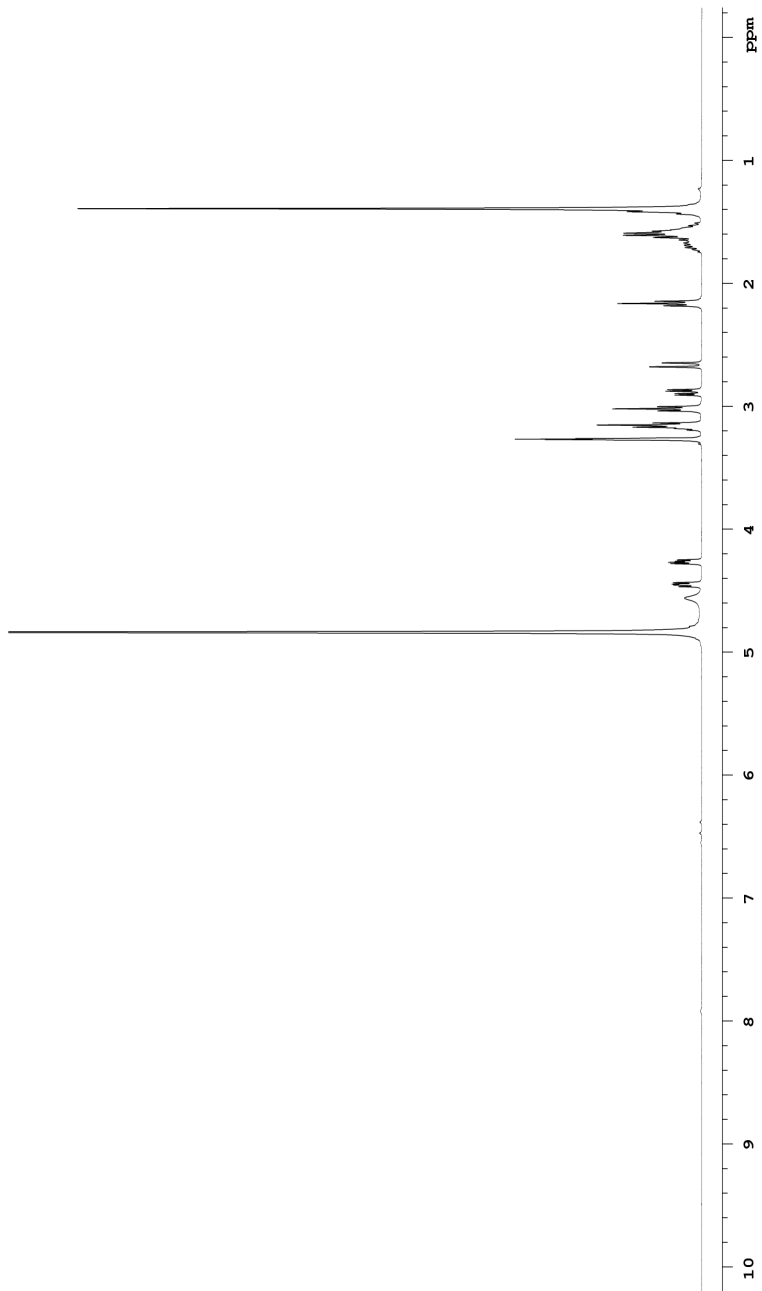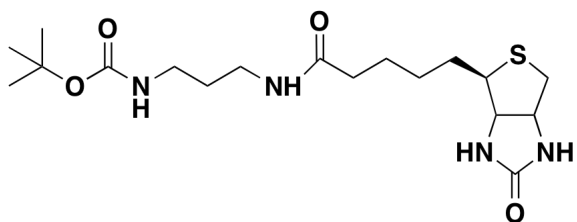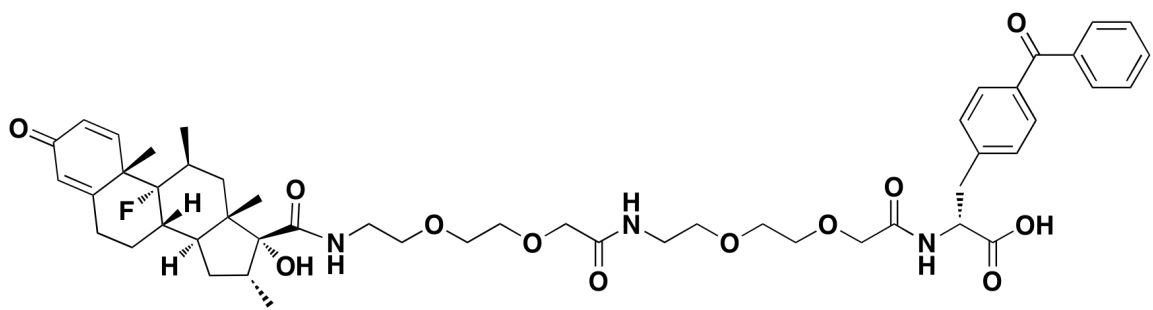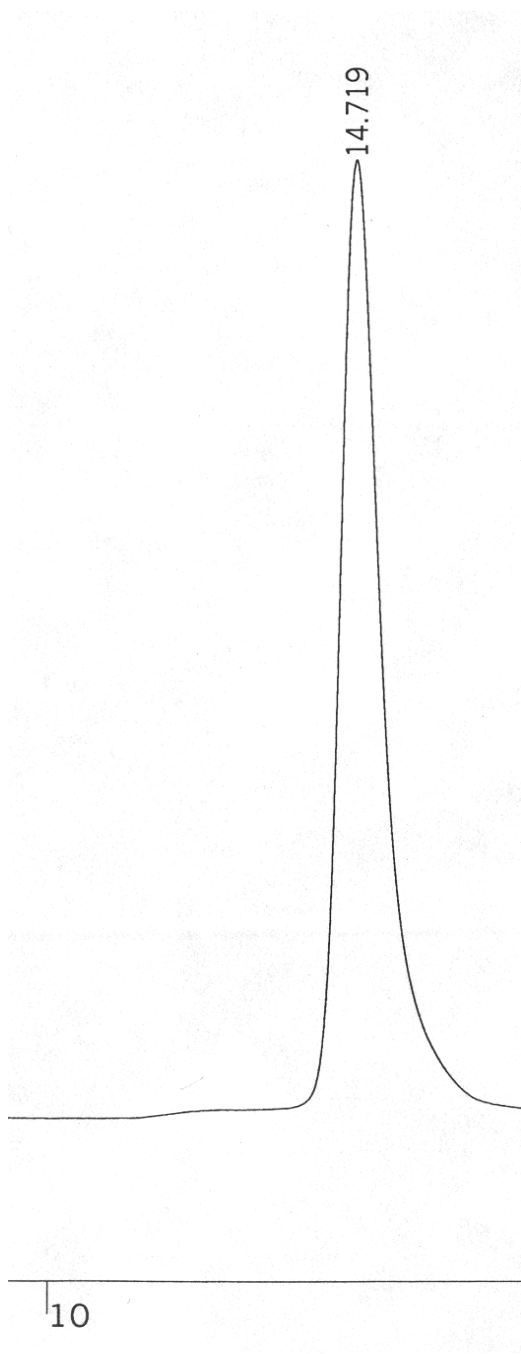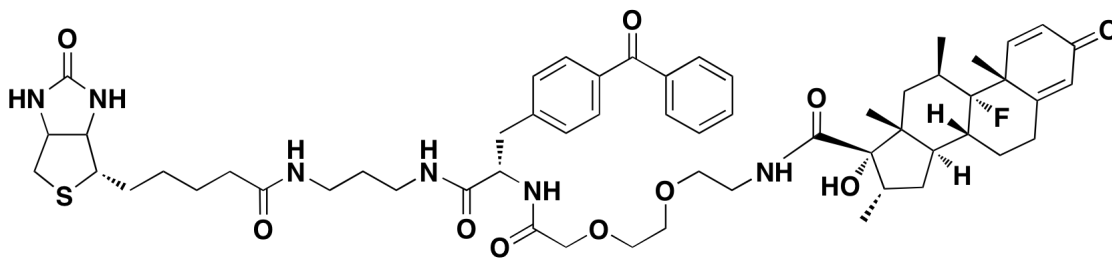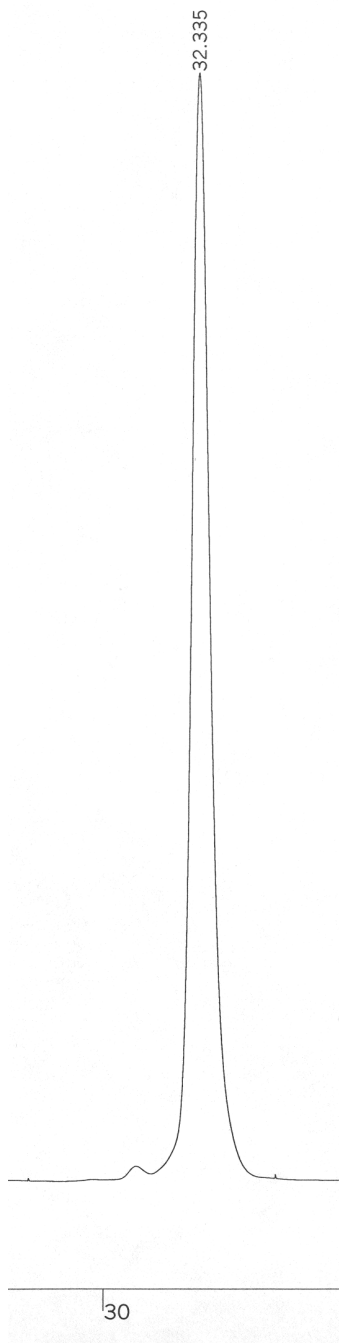
H. References

1.   Glass, C. K.; Rose, D. W.; Rosenfeld, M. G., Nuclear receptor coactivators. *Curr Opin Cell Biol* **1997,** *9* (2), 222-32.

2.   McKenna, N. J.; Lanz, R. B.; O'Malley, B. W., Nuclear receptor coregulators: cellular and molecular biology. *Endocr Rev* **1999,** *20* (3), 321-44.

3.   McKenna, N. J.; O'Malley, B. W., Combinatorial control of gene expression by nuclear receptors and coregulators. *Cell* **2002,** *108* (4), 465-74.

4.   Kumar, R.; Thompson, E. B., Gene regulation by the glucocorticoid receptor: structure:function relationship. *J Steroid Biochem Mol Biol* **2005,** *94* (5), 383-94.

5.   Biggins, J. B.; Koh, J. T., Chemical biology of steroid and nuclear hormone receptors. *Curr Opin Chem Biol* **2007,** *11* (1), 99-110.

6.   Hittelman, A. B.; Burakov, D.; Iniguez-Lluhi, J. A.; Freedman, L. P.; Garabedian, M. J., Differential regulation of glucocorticoid receptor transcriptional activation via AF-1-associated proteins. *Embo J* **1999,** *18* (19), 5380-8.

7.   McKenna, N. J.; Xu, J. M.; Nawaz, Z.; Tsai, S. Y.; Tsai, M. J.; O'Malley, B. W., Nuclear receptor coactivators: multiple enzymes, multiple complexes, multiple functions. *J Steroid Biochem* **1999,** *69* (1-6), 3-12.

8.   Kassel, O.; Herrlich, P., Crosstalk between the glucocorticoid receptor and other transcription factors: molecular aspects. *Mol Cell Endocrinol* **2007,** *275* (1-2), 13-29.

9.   De Bosscher, K.; Van Craenenbroeck, K.; Meijer, O. C.; Haegeman, G., Selective transrepression versus transactivation mechanisms by glucocorticoid receptor modulators in stress and immune systems. *Eur J Pharmacol* **2008,** *583* (2-3), 290-302.

10.   O'Malley, B. W.; Qin, J.; Lanz, R. B., Cracking the coregulator codes. *Curr Opin Cell Biol* **2008,** *20* (3), 310-5.

11.   Jenkins, B. D.; Pullen, C. B.; Darimont, B. D., Novel glucocorticoid receptor coactivator effector mechanisms. *Trends Endocrinol Metab* **2001,** *12* (3), 122-6.

12.   Lavery, D. N.; McEwan, I. J., Structure and function of steroid receptor AF1 transactivation domains: induction of active conformations. *Biochem J* **2005,** *391* (Pt 3), 449-64.

13.   Newton, R.; Holden, N. S., Separating transrepression and transactivation: a distressing divorce for the glucocorticoid receptor? *Mol Pharmacol* **2007,** *72* (4), 799-809.

14.   Chen, T., Nuclear receptor drug discovery. *Current Opinion in Chemical Biolgoy* **2008,** *12*, 9.

15.   Jung, S. Y.; Malovannaya, A.; Wei, J.; O'Malley, B. W.; Qin, J., Proteomic analysis of steady-state nuclear hormone receptor coactivator complexes. *Mol Endocrinol* **2005,** *19* (10), 2451-65.

16.   Meijsing, S. H.; Pufall, M. A.; So, A. Y.; Bates, D. L.; Chen, L.; Yamamoto, K. R., DNA binding site sequence directs glucocorticoid receptor structure and activity. *Science* **2009,** *324* (5925), 407-10.

17.   Carboni, B. B., A.; Vaultier, M., *J Org Chem* **1993,** *58*, 3736-3741.

18.   Elisa Dragoni, V. C., Marco Fragai, Rahul Jaiswal, Claudio Luchinat,* and Cristina Nativi, Biotin-Tagged Probes for MMP Expression and Activation: Design, Synthesis, and Binding Properties. *Bioconjugate Chem* **2009,** *20*, 719–727.

19.   Glass, C. K.; Rosenfeld, M. G., The coregulator exchange in transcriptional functions of nuclear receptors. *Gene Dev* **2000,** *14* (2), 121-141.

20.   Lonard, D. M.; O'Malley, B. W., Expanding functional diversity of the coactivators. *Trends Biochem Sci* **2005,** *30* (3), 126-32.

21.   Pangborn, A. B.; Giardello, M. A.; Grubbs, R. H.; Rosen, R. K.; Timmers, F. J., Safe and convenient procedure for solvent purification. *Organometallics* **1996,** *15* (5), 1518-1520.

22.   Still, W. C.; Kahn, M.; Mitra, A., Rapid Chromatographic Technique for Preparative Separations with Moderate Resolution. *J Org Chem* **1978,** *43* (14), 2923-2925.